Bioactive Materials 26 (2023) 24–51

Contents lists available at ScienceDirect

Bioactive Materials

journal homepage: www.keaipublishing.com/en/journals/bioactive-materials

Review article

Chemically revised conducting polymers with inflammation resistance for intimate bioelectronic electrocoupling

Sihao Qian [a,b,1], Hsing-An Lin [b,1], Qichao Pan [b], Shuhua Zhang [b], Yunhua Zhang [b], Zhi Geng [b], Qing Wu [b], Yong He [c,**], Bo Zhu [b,*]

[a] State Key Laboratory for Modification of Chemical Fibers and Polymer Materials, College of Materials Science and Engineering, Donghua University, Shanghai, 201620, China
[b] School of Materials Science and Engineering & Shanghai Engineering Research Center of Organ Repair, Shanghai University, Shanghai, 200444, China
[c] Innovation Center for Textile Science and Technology, Donghua University, Shanghai, 201620, China

ARTICLE INFO

Keywords:
Bioelectronic
Conducting polymer
Zwitterion
Antifouling
Inflammation resistance

ABSTRACT

Conducting polymers offer attractive mixed ionic-electronic conductivity, tunable interfacial barrier with metal, tissue matchable softness, and versatile chemical functionalization, making them robust to bridge the gap between brain tissue and electronic circuits. This review focuses on chemically revised conducting polymers, combined with their superior and controllable electrochemical performance, to fabricate long-term bioelectronic implants, addressing chronic immune responses, weak neuron attraction, and long-term electrocommunication instability challenges. Moreover, the promising progress of zwitterionic conducting polymers in bioelectronic implants (≥4 weeks stable implantation) is highlighted, followed by a comment on their current evolution toward selective neural coupling and reimplantable function. Finally, a critical forward look at the future of zwitterionic conducting polymers for in vivo bioelectronic devices is provided.

1. Introduction

Bioelectronic implants function as neural prostheses, brain-machine interfaces, and other biointegrated devices to detect and record biological signals [1,2]. Commercial implantable electrodes, made of metals or silicon, have been applied in auditory implants [3], visual implants [4], and other neuroprosthetic implants [5,6]. Owing to the stiff nature of these materials, the mechanical mismatch between electrodes and tissues induces interface stress due to electrode micromotion in brain tissues, leading to foreign body reactions and even malfunction of devices [7]. Thus, tissue-matching softness is critical for brain implants to reduce chronic immune responses. Besides, the surfaces of these electrode materials likely adsorb proteins through nonspecific interaction, triggering the first step for foreign body reaction [7–11]. The scar formation from inflammatory reactions would isolate implants from neural tissues, and increase the distance and electrical resistance between electrodes and neural cells/tissue, resulting in a low signal-to-noise ratio (SNR). In addition, the inertness of their surfaces makes it challenging to functionalize them with biomolecules for bridging a solid interaction with nerve cells/tissues.

Furthermore, with the progress in biomedical engineering, the demand for small-size and high multiplexity neural electrodes has vastly increased. These electrodes can deliver stimulating signals or record neural activities with a relatively high spatial resolution, even reaching a single-cell level [12,13]. Since the interfacial electrode impedance is inversely proportional to its active surface area, with a decrease in geometry size, the impedance of electrodes significantly increases, dramatically reducing the SNR. As conventional electrode materials are only electroconducting, charge transfer at their interfaces in an aqueous environment is conducted through electrochemical reactions and is thus heavily dependent on the limited interfacial area. Their relatively high impedance does not meet the requirement for a high multiplex electrode. The next generation of electrode material should have extremely low impedance, ensuring efficient electrical stimulation or sensitive monitoring of minute neural activity when serving as spatially resolved electrodes.

Peer review under responsibility of KeAi Communications Co., Ltd.
* Corresponding author.
** Corresponding author.
E-mail addresses: yhe@dhu.edu.cn (Y. He), bozhu@shu.edu.cn (B. Zhu).
[1] These authors contributed equally to this work.

https://doi.org/10.1016/j.bioactmat.2023.02.010
Received 26 July 2022; Received in revised form 26 January 2023; Accepted 10 February 2023

Conducting polymers (CPs) provide advantages over inorganic and metallic materials. The elastic modulus of CPs is much lower than that of inorganic and metal materials, which minimizes the mechanical mismatch and reduces the stress concentration at the device-tissue interface. Coating CPs onto electrodes dramatically improves the tissue-recording site electrocoupling in vitro and in vivo by significantly lowering the overall device impedance [14–16]. This is primarily due to their mixed ionic-electronic conductivity, yielding enormous volumetric capacitance [17–19]. In addition, CP electrodes provide high charge storage and injection capacity for safe stimulation due to their vast bulk capacitance [14,20]. Furthermore, incorporating biomolecules into CPs provides a feasible method to enhance the interfacial interaction with neurons and reduce the inflammatory response [21]. However, surface modification by biomolecules does not usually solve the nonspecific protein adsorption issue. This would increase the interfacial impedance [22,23], even triggering an immune response [24–26].

Most recently, zwitterionic CPs demonstrated excellent capabilities to reduce nonspecific cell/protein interactions, combined with efficient electrocommunication with cells/tissues at low impedance [27]. In addition to the mixed ionic-electronic conductivity of CPs, zwitterionic CPs possess enhanced ionic conductivity and close metal-CP electrocoupling strengthened by zwitterions, further facilitating charge transfer between electrodes and cells/tissues. Zwitterionic CPs also demonstrated their superiority in antifouling, aqueous stability, low inflammation, and electrochemical properties over other hydrophilic CPs [28–30], and have been extensively applied in in vivo and in vitro bioelectronic devices. Moreover, zwitterionic CPs provide spots for cell attachments through specific interactions from the grafted cell-recognized molecules. Given these exciting signs of progress, zwitterionic CPs potentially provide a feasible solution to the limitations mentioned above for CPs due to their impressive combination of softness, nonspecific interaction resistance, and cell-targeted electrocoupling, which provides the required biocompatibility and efficient electrical trade-offs for interfacing with cells/tissues.

In this review, we first argue the significance of CPs for bioelectronic implants, highlight their tunable softness and unique electrochemical properties, and discuss the underlying reasons for the low impedance of CP electrodes, which is crucial for bioelectronic implants. Then, we shift our focus to biomolecule-functionalized CPs and their impacts on their in vitro and in vivo neuron interactions and the chronic stability of implants. We discuss our primary concerns regarding the nonspecific interaction challenge and the higher impedance issue of these in vivo CP electrodes for long-term application. To solve these issues, we highlight the molecular design and synthesis of zwitterionic CPs, which have recently emerged as inflammation-resistant CP materials for bioelectronic implants. To clarify their structure-property relationship, we also compare their antifouling performances by concentrating on the zwitterion's hydration and the effects of solution pH, zwitterion spacer length, copolymer composition, and chemical structure. In addition, we discuss their surprisingly reduced impedance by investigating the inherent explanation of their zwitterion-enhanced ionic conductivity and CP-metal electrocoupling. Finally, we highlight the promising progress in zwitterionic CP electrodes for bioelectronic devices either in vitro or in vivo, referring to other zwitterionic neural probes, and provide a future perspective on zwitterionic CPs for implantable bioelectronic devices.

2. Conducting polymers for bioelectronic devices

To date, the electrode materials used for clinical devices are mostly made of metals and inorganic materials, such as gold [31,32], platinum (Pt) [32], indium tin oxide (ITO) [33–35], and iridium oxide (IrO_2) [36], as these materials are highly conductive corrosion resistant. However, these materials currently have several critical challenges when employed as neural electrodes. First, the elastic modulus of metals is much higher than that of neural tissues, resulting in the electrodes not fully conforming to the nerve tissues. Second, reducing the size of metal electrodes leads to a dramatic increase in impedance, leading to an increase in electrical noise [37]. In addition, the smaller size of metal electrodes causes a smaller charge injection window for safe neural stimulation [20]. Furthermore, the inert nature of these electrode surfaces makes it difficult to modify them for adequate interaction with neural tissues, either chemically or physically. Recently, CPs have been considered an attractive alternative for neural signal recording/stimulation in cochlear implants, neural probes bionic eyes, and brain-machine interfaces due to their softness, excellent quality electrochemical characteristics, and accessible surface biofunction modification [38]. Fig. 1 is the layout of a typical planar neural probe equipped with conducting polymer-coated electrodes as recording sites, where biomolecules are used to enhance biocompatibility.

It was frequently reported that the mechanical mismatch between the hard planar electronics and the soft biological tissues would lead to interfacial stress. Recently, to minimize the negative impact of this mechanical mismatch, some novel flexible bioelectronic devices were fabricated on soft elastomer substrates, whose Young's modulus could even reach 10 kPa level, being similar to that of nerve tissue [39–43]. However, in comparison to the amorphous SiO_2, their low permeability and long-term hermetic encapsulation have not been verified, and their long-term application in bioelectronic implants is very challenging. Moreover, those organic elastomers are normally solution-processed and are highly susceptible to damage from both organic solvents and ultraviolet light exposure, making them incompatible with photolithography processing. In addition, to establish intimate integration with the soft tissues of brains, it is highly demanded to develop wet adhesive and flexible substrates/encapsulation materials for bioelectronic implants. Its combination with CPs would offer a promising opportunity to fabricate long-term bioelectronic tools for diagnosing and treating diseases.

Besides the neuro-inflammatory response, several abiotic factors are considered crucial for the electrode and implant lifetime. The electrode mechanical damage occurring during the insertion and implantation could lead to implant failure. Normally, hard bioelectronic implants made of brittle materials were rarely mechanically damaged during insertion and implantation. In contrast, the implants equipped with soft CP electrodes likely suffered from electrode delamination and cracking issues [44]. Several approaches were developed to enhance the interfacial adhesion of CPs with underlying substrates. These include grafting carboxyl [45,46] and amine moieties onto CPs [47], optimizing electrochemistry conditions [48], and anchoring CPs onto metal surfaces by diazonium chemistry [49] or bioinspired dopamine polymer [50–52]. Moreover, the corrosion of electrical contacts and the degradation of passivation layers and insulating coatings were also frequently reported to be responsible for the failure of bioelectronic implants [53–55]. Therefore, a comprehensive effort on the stabilities of both electrodes and encapsulation materials should be carried out to extend the life span of bioelectronic implants.

As this review focuses on the chemically revised conducting polymers for long-term bioelectronic implants, this section only provides a brief discussion on the substrate/encapsulation materials, the wet adhesion to tissues, and abiotic factors to electrode/implant lifetime, and wishes to give readers a complete picture of the recent progress of long-term electronic implants. If readers are interested in additional details, please refer to some recent reviews on these topics [55,56].

2.1. Biocompatibility and softness of conducting polymers

The biocompatibility of electronic materials is one of the key factors for bioelectronic implants to function under complex biological conditions [57,58]. Cytotoxicity tests are often utilized to assess their biocompatibility before their in vivo implantation. Traditional electrode materials, consisting of Pt, Au, and IrOx, have been widely used in neural probes and found to be compatible with several cell lines by the

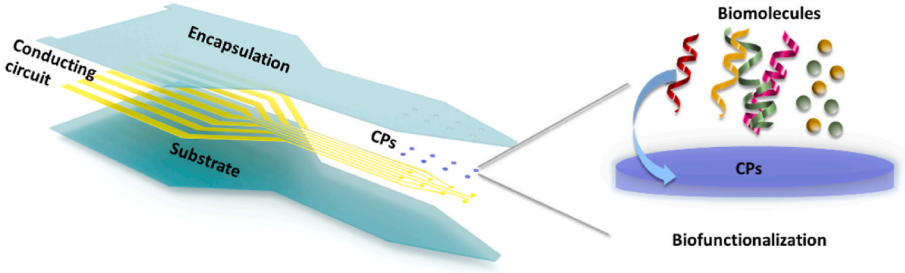

Fig. 1. Schematic representation of a neural electrode and biofunctionalization of CPs.

cytotoxicity test, as shown in Table 1. However, these electrode materials were frequently reported to suffer from severe tissue response, as they are susceptible to biofouling [57,59]. CPs were found to be compatible with neural cell lines, such as cortical cells [60,61], hippocampal neurons [14,62–64], PC12 cells [65–69], and motor neurons [70]. Furthermore, they were also recently demonstrated to have improved implanting biocompatibility, plausibly due to their much smaller elastic modulus [71–77].

The elastic modulus of the bioelectronic implant is a critical factor that is closely related to the foreign body response. The Young's modulus of brain tissues ranges from 0.1 to 16 kPa [78–81]. Traditional electrodes have a high Young's modulus, e.g., 140 GPa for Pt, 70 GPa for Au, and 300 GPa for IrOx [31,32,36]. In comparison, the mechanical properties of CPs are much closer to those of neural tissues. The Young's modulus of CPs, including polypyrrole (PPy), poly(3, 4-ethylenedioxythiophene) (PEDOT), and polyaniline (PANI), is much smaller (lower than 3 GPa) and varies over a wide range due to their flexible chemistry and processing methods [71–73]. To further reduce the Young's modulus of conductive biomaterials to kPa, researchers have put much effort into developing conductive polymer hydrogels [74–77]. Conductive polymer hydrogels (CPHs) combine the beneficial characteristics of hydrogels and CPs, endowing CPHs with attractive physical and biological properties, including tissue-like mechanical features, high water content, and excellent biocompatibility. For example, Hur et al. [74] developed a conductive hydrogel composed of PPy and agarose, of which Young's modulus (27–46 kPa) is close to that of human skin (5–100 kPa). Rinoldi et al. [75] designed a polythiophene-based hydrogel with a Young's modulus of 4.6 kPa, which well matched the mechanical properties of the brain slice. In a recent study by Wang et al. [77], an adhesive and ultrasoft brain-machine interface integrated with a dopamine methacrylate-hybridized PEDOT nanoparticle-incorporated hydrogel was successfully developed. The hydrogel exhibits robust adhesiveness to wet and soft biological tissues. Most importantly, the hydrogel has a modulus lower than 1 kPa, presenting ultrasoftness and excellent mechanical compliance to tissues. CP implants can significantly reduce the inflammatory tissue response compared to conventional electrode materials [82,83]. Since the implant tightly adheres to the tissues, soft CPs as coatings on implantable electrodes can act as a buffer layer between soft tissue and stiff metals, significantly reducing the interfacial mechanical stress of neural implants and dramatically improving the performance and lifetime of the implantable device. The Young's modulus and compatible cell lines of conducting materials are summarized in Table 1.

Table 1
Mechanical Properties of tissues and the conducting materials for bioelectronic implants and cell lines used to assess the biocompatibility of conducting materials.

Tissues/ materials	Young's modulus	Cells for biocompatibility test
Skin	5–100 kPa [84]	/
Brain	0.1–100 kPa [78–81]	/
Pt	~140 GPa [32]	SH-SY5Y cells [85], retina cells [86]
Au	~54–70 GPa [31, 32]	SH-SY5Y cells [87], rat primary cortical cells [88], retina cells [89]
IrOx	~300 GPa [36]	Rat primary cerebral cortex neurons [90], rat cortical neurons [91]
PEDOT	0.21 kPa-3Gpa [72,74–77,92,93]	SH-SY5Y cells [94], rat cortical cell [60], rat primary dorsal root ganglion (DRG) explants [95], PC12 cells [65,67], C2C12 [93], rat primary neurons and astrocyte [96], rat primary motor neurons [70], rat hippocampus neurons [14,63]
PPy	27kPa-2.9 GPa [31,71,74]	Rat cortical cells [61], rat primary DRG explants [97], rat and mouse neural stem cells [98], rat hippocampus neurons [99], PC12 cells [66,100]
PANI	7.9kPa-2.3 GPa [73,101]	SH-SY5Y cells [102], rat hippocampus neurons [62,64], PC12 cells [68,69]

2.2. Electrochemical properties of conducting polymers

2.2.1. Mixed ionic-electronic conductivity of CPs

CPs conduct both ionic and electronic charge carriers [17–19], leading to a relatively high ionic conductivity and capacitance for CPs. CPs feature a continuous channel of overlapping π-orbitals, allowing electrons or holes to move through the polymer backbone [103]. The hopping mechanism allows electrons to hop to the π-orbitals of neighboring chains, leading to interchain charge transfer. The delocalized π bond enlarges the range of π electron movement, reduces the bandgap, and increases the polymer conductivity. The ion transport of CPs is a more complex process. Ions exist in various forms, single valent or multivalent, and can form pairs and larger clusters. Furthermore, they are susceptible to solvents and solvation [104]. Of note, interactions between ions and conjugated polymer chains cause considerable changes in the local structure and stabilize or destabilize the electronic charge carriers, altering electronic transport. As a result, the ion transport in CPs cannot be examined individually; instead, the interaction between the ionic and electronic conduction should be investigated. The ionic-electronic coupling (doping) of CPs under a bias significantly reduces the charge carrier loss, distinctly enriches accessible hopping states, and dramatically improves the electrical conductivity of CPs [105]. If the CP's highest occupied molecular orbital (HOMO) is shallow enough, forming positive electronic charge carriers (in the form of holes) stabilized by anions is energetically favored, referred to as p-type doping. In contrast, if its lowest unoccupied molecular orbital (LUMO) is sufficiently deep, forming negative electronic charge carriers stabilized by cations, known as n-type doping, is energetically favored [17,106]. P-type CPs are usually more prevalent than n-type CPs for bioelectronic applications, as is also general for other organic electronic devices [107].

Due to its volumetric nature, this ionic-electronic coupling dramatically influences almost all electronic, physical, and chemical properties of CPs. This potential-dependent ionic-electronic coupling is the underlying mechanism for the transduction between electronic and ionic

signals, making CP electrodes superior to other materials in neural recording and stimulation. For bioelectronic devices, e.g., biosensors and neural electrodes, their frequency bandwidth and response time for electrical communication are determined by the interaction of the ionic-electronic coupling with ionic transport [108,109]. Furthermore, the interaction of the ionic–electronic coupling with electronic transport also dominates the amplification capability of organic electrochemical transistors [110,111].

During practical application, p-type CPs contact a metal electrode and an electrolyte. There are primarily four processes involved in the charge transport of bioelectronic devices: dopant ion transit at the interface of CP/electrolyte, electronic carrier (hole) stabilization/destabilization by a dopant ion (anion) in the interior of CPs, electronic carrier hopping, and charge transfer between the metal electrode and CPs. [17], In the charge transport process, the ionic and electronic conduction interaction plays a critical role in the operation of CP-based devices. Thus, a trade-off between electronic and ionic conductivity is usually necessary to optimize electronic device performance. For example, Rivnay et al. [18] discovered that the addition of cosolvents oppositely affected the ion and hole transport in PEDOT:PSS films; an optimized condition was available to reach the maximized device performance with a balance between ionic mobility and hole conductivity.

This section provides only a brief explanation of the ionic-electronic interactions and coupled transport properties of CPs to aid readers in understanding CP conductivity. It is a massive topic, and readers interested in additional details can refer to excellent reviews on this subject [17,104].

2.2.2. Low impedance of CPs

As described above, electrodes of both small size and low impedance are required to endow neural electrodes with both high SNR and high spatial resolution. Depositing CPs on neural electrodes is accepted as a great approach to ensure a large electrode capacitance and a low impedance for microelectrodes of smaller sizes [14–19].

The 1 kHz impedance is a critical characteristic of neural electrodes and is coherently related to the neuronal signal recording quality and electrical neural stimulation safety. Many studies have confirmed that CPs have a much lower electrochemical impedance at 1 kHz than traditional electrode materials, such as IrOx [112], platinum [113], gold [16], and ITO [15]. When CPs act as neural electrodes, their low impedance depresses electrical noise and reduces signal loss. For example, Nyberg et al. [15] reported that the impedance (5 kΩ) of a PEDOT-modified ITO microelectrode was markedly lower than that of an ITO electrode (270 kΩ) at 1 kHz. These PEDOT microelectrodes evoked a much more pronounced neural network response than ITO microelectrodes [15]. In another study by Kim et al., the PEDOT coating reduced the impedance of gold electrodes by approximately two orders of magnitude, enabling the electrodes to record the neural signal at a much higher SNR [16]. A recent investigation by Zhang et al. also indicated that the impedance of PEDOT-modified electrodes was much lower than that of the gold electrode in frequencies range from 1 Hz to 100 kHz [28]. Moreover, CP electrodes provided a wider charge injection window for safe neural stimulation. These PEDOT electrodes exhibited a lower voltage excursion, a higher charge injection limit (CIL), and a higher charge storage capacity (CSC) than the gold electrode [28], making CP electrodes more biocompatible for chronic stimulation.

The substantial reduction in impedance for CPs is primarily attributed to their unique mixed ionic-electronic conductivity, which facilitates electrocoupling between the electrode substrate and the electrolyte, promoting interface exchange of carriers, either ions or electrons [18,19]. In addition, the rough surface and porous structure of CPs were also reported to be crucial for their impedance. Cui et al. [114] studied the relationship between impedance and surface roughness, revealing that the impedance decreased sharply as the CP surface became rough. However, they found that the calculated electroactive interface area of the CP electrode at 1 kHz was 26 times that of the gold electrode, much larger than the value estimated using AFM topographic results. This clearly indicates that some minor accesses and pores exist inside the film, similar to a "branching tree" structure [114]. Ions can penetrate the porous membrane, forming a larger accessible electroactive interface area. The porous structure also leads to a vast capacitance of CPs, as it promotes volumetric electrocoupling between ionic and electron charges within a short time [115]. Rivnay et al. [111] demonstrated that the 130 nm thick PEDOT:PSS film had a capacitance of 39 F/cm^3, which is approximately 100 times larger than the double-layer capacitance of a flat metal electrode. This volumetric electrocoupling of ionic and electronic charges further gives a low impedance for CP materials, as impedance is inversely proportional to the capacitance.

2.2.3. Critical roles of metal-CP interfaces

In addition to their unique bulk properties, charge transfers at metal-CP and CP-liquid interfaces are crucial for communicating CP electrodes with cells/tissues. However, to the best of our knowledge, few review papers have concentrated on the critical roles of these two interfaces on the electro impedance besides that by Rubinson et al. [116].

The interface of CPs with metal is critical for CP electrodes, as it defines the contact of CP with metal as either ohmic or rectifying. Good ohmic contact between the metal and the semiconductor layer is essential for injecting high-density current across the interface and fabricating high-performance semiconductor devices [117]. The difference in the work function of the CP and metal establishes a thermodynamic equilibrium and an interfacial barrier (Schottky barrier) between them [118]. The interfacial barrier height determines the activation energy required for electrons to overcome this interfacial barrier and, thus, its contribution to the overall impedance. For implantable devices, high work function metals, such as Pt (5.7 eV) and Au (5.1) eV, are more favorable due to their stability [119]. The typical p-type CPs have a higher work function than n-type CPs [120]. When CPs contact metals, the interface's intrinsic asymmetry leads to charge transfer, polarization, or rearrangement of the electron cloud, inducing interfacial dipoles [121]. The interfacial dipoles between metals and p-type CPs favor decreasing the potential barrier between them [117,122]. Thus, p-type CPs can help achieve ohmic contacts with high work function metals [119,123]. It has also been observed that the total interface dipole can be tuned by adjusting the magnitude of the molecular dipole moments. Thus, it is possible that the interfacial barrier could be lowered by changing the chemical structure of CPs. However, with our limited knowledge, a systematic, either theoretical or experimental survey is still lacking concerning the impact of CP chemical structures on the interfacial barrier of CP electrodes. Further studies are needed to explore the nature of these zones and the underlying mechanisms.

Increasing the doping levels of p-type CPs further benefits the formation of good ohmic contact between CPs and metals. In this case, the charge accumulation/depletion region near the interface can be narrowed down [116,124], and charge carriers can be tunneled through the potential barrier higher than their thermal kinetic energy due to their wave nature [116,125].

Implanted bioelectronic devices typically work in aqueous environments. Many studies have demonstrated that the presence of water causes a substantial decrease in the work function of metals due to the complex structure of water in the vicinity of the metal surface [126]. Furthermore, the hydration of CPs was also found to significantly lower the work functions of CPs [123,127] This might be attributed to the rearrangements of their surface dipoles induced by polymer swelling and the increase in the dielectric constant with the incorporation of water. This induces dielectric screening of the thin film surface dipole (between subsurface $PEDOT^+$ and surface PSS^-) [127]. As described above, metals and CPs alter their working function when meeting water molecules. However, a thorough investigation and discussion of the effect of water on the CP/metal interface is still absent and deserves further research.

2.3. Biomolecular interaction with conducting polymers

The interaction of biomolecules with the CP surface is critical for the long-term application of bioelectronic implants, which normally involves van der Waals, hydrophobic, and electrostatic forces. Understanding the interaction between biomolecules and CPs would benefit the rational design of CPs for bioelectronic applications. The biomolecules, particularly proteins, often present an altered viscoelastic profile in their adsorption to the CP surface as they would experience specific molecular conformational rearrangement after adsorption. Molino et al. [128] discovered that the adsorption of (bovine serum albumin) BSA on the rough PPy film is divided into two stages: proteins arrive and are initially adsorbed on the polymer surface; the molecules rearrange into a more dehydrated and dense conformation, which facilitates further adsorption of proteins to the polymer interface.

The interaction of biomolecules with CPs is coherently related to the chemical structure, redox status, and dopants. The chemical structure of CPs has a critical impact on their interaction with biomolecules. Normally, all the unfunctionalized CPs, e.g., PEDOT, PANI, and PPy, present nonspecific interaction toward proteins, cells, and even bacteria [52,129–131]. The nonspecific interaction of CPs mainly arises from van der Waals, hydrophobic, and electrostatic forces between CPs and biomatter. In contrast, CPs with hydrophilic side groups, e.g., polyethylene glycol (PEG) and zwitterions, could resist the protein/cells binding well due to their strong hydrophilicity and/or neutral charge [28,29,52,129–132].

The CP redox also has a great effect on the interaction of biomolecules to the CP surface. Gumus et al. [133] investigated the interaction of fibronectin to a p-toluenesulfonate-doped PEDOT stripe under an applied bias. Biasing at ±1 V could form a potential gradient, thus inducing a location-dependent redox state along the polymer stripe. Marked differences were observed in the fibronectin adsorption as a function of the location along the polymer stripe. Fibronectins were found to adsorb preferentially on the reduced PEDOT instead of the oxidized one. However, in another research by Molino et al. [128], fibronectins were demonstrated to adsorb preferentially on the oxidized PPy. In this case, the fibronectins adsorbed on the oxidized PPy have greater flexibility and higher viscoelasticity than those on the reduced one. Chen et al. [30] also demonstrated that protein adsorption could be tuned by the redox state of zwitterionic CPs. It was found that when an oxidation potential was applied, the bovine serum albumin (BSA) adsorption of the phosphorylcholine functionalized PEDOT (PEDOT-PC) significantly increased, attributing to the electrostatic attraction between positively charged polymer films and negatively charged BSA. In contrast, when a reduced potential was applied, the BSA adsorption was almost completely suppressed. For the positively charged lysozyme, the lysozyme adsorption was found to be reduced and enhanced, respectively for the oxidized and reduced PEDOT-PC films. Gelmi et al. [134], using an electrochemical-atomic force microscopy (AFM) setup, verified that applying a positive bias to PPy could lead to a strong electrostatic attraction to the negatively charged protein domains, resulting in one order of magnitude higher adhesion force (approximately 1–2 nN) between them. This electrochemically induced adhesion is strong and non-specific but can be reversibly switched to a much smaller piconewton adhesion force by applying an opposite negative bias to the polymer. Zhang et al. [135] combined single-cell force spectroscopy with electrochemical AFM to quantify the adhesion between live single cells and CPs. The cell-CP adhesion was mainly due to the non-specific interaction between the glycocalyx molecules of cells and the sulfonate and dodecylbenzene groups of dopants, which rearrange their orientation during electrical switching. The cell-CP adhesion was found to be significantly strengthened when the CP film was electrochemically switched from an oxidized state to a fully reduced state, indicating a stronger cell binding to sulfonate groups as opposed to hydrophobic groups. These results indicated that the redox-switched electrostatic interaction plays a critical role in controlling cell-CP interaction.

CP Dopants were also found to influence the interaction between biomolecules and CPs [128,136]. It was found that the dextran sulfate-doped PPy adsorb much more fibronectins when doped at a high concentration of dextran sulfate [128]. Simultaneously, the viscoelasticity of the protein layer adsorbed on PPy also increases with the dextran sulfate concentration. Gelmi et al. [136] investigated the interaction of fibronectins with the glycosaminoglycan-doped PPy by the fibronectin-functionalized AFM tip at the molecular scale. They classified four main types of interactions between the FN and doped PPy films: non-specific adhesion (including electrostatic, hydrophobic, hydrogen bonding, etc.), protein unfolding and subsequent unbinding from the surface, desorption from CP surfaces, and interactions with no adhesion. They found that the fibronectin adhesion with PPy films could be mediated by interactions with chondroitin sulfate and hyaluronic acid presented on the PPy surface, indicating that the specific interaction plausibly arose from the electrostatic attraction to sulfate/anionic groups of the dopants.

The application of bioelectronic implants is limited by implant failure during chronic implantation. Addressing poor interaction between electrodes and targeted tissue, and alleviating adverse host responses triggered by protein adsorption, are two main issues that remained unsolved for long-term bioelectronic implantation. Therefore, A clear understanding of the interaction between biomolecules and CP materials is helpful for the rational design of conducting materials for bioelectronic implants.

2.4. Biofunctionalization of conducting polymers

The performance of electrodes is frequently reported to degrade with time when operating in biological systems, which has been widely accepted to be related to the implant-induced inflammatory response [21]. Foreign body responses may lead to the glial scar formation, which results in a dense cellular sheath around the neural probe and insulates the electrode from nearby neurons. In this case, the charge transfer from the electrode to the neural cells/tissues will be impeded [137], resulting in a weakened strength and a low quality of the recorded electrical signal. Building a selective interaction between target neurons and electrodes would depress the tissue response, and thus improve the recording quality and chronic electrode performance [138]. That is, for a long-term neural signal recording and stimulation, it is desired to reduce inflammatory responses, facilitating an intimate contact between recording sites of the neural robe and neural cells/tissues. Incorporating biomolecules with CPs has recently attracted wide attention due to its potential to ensure close electrocoupling between electrodes and neurons, promoting the proliferation and differentiation of neurons and increasing nerve recording quality. Some related research results of biofunctionalized CPs are summarized in Table 2.

Neurotrophic factors are widely used to dope CPs of neural electrodes. For example, using nerve growth factor (NGF) improves the differentiation of neural cells on CPs [83]. Neurotrophin-3 (NT-3) and brain-derived neurotrophic factor (BDNF), ligands for Trk receptors expressed on cochlear neuron surfaces, have been used in cochlear implants to control cellular responses [149,150]. Richardson et al. [150] used NT-3 functionalized PPy electrodes to electrically stimulate guinea pig cochlear nerve to promote the preservation of spiral ganglion neurons (SGNs) function. Compared with the control guinea pigs (no implant or nonfunctionalized polypyrrole implants), the guinea pigs treated with the NT-3-functionalized PPy electrodes presented lower electrically evoked auditory brainstem response thresholds and higher SGNs densities. However, the effects of neurotrophic factors functionalized CPs are subjected to neurotrophin loading and might disappear once neurotrophin is exhausted [151].

Moreover, cell adhesion biomolecules can effectively enhance adhesion and outgrowth for neurons on CP surfaces. Polylysine, a cell adhesion biomolecule, has been widely used to enhance the electrostatic interaction between CPs and cell membranes [23,142]. Kim et al. [23]

Table 2
Biomolecule-functionalized conducting polymers: diverse bioligands, modification methods, biological models, and advantages.

Conducting polymers	Bioligand	Modification method	Cell type/animal type	Key results	References
PEDOT	NGF and dexamethasone phosphate	Doping	Sprague–Dawley (SD) rats	Increasing charge storage capacitance and decreasing electrochemical impedance (reduced by ~96%) at 1 kHz. Reducing inflammation and promoting neuron survival.	[83]
PEDOT-poly(vinyl alcohol)	Heparin, sericin, gelatin, and NGF	Doping (heparin) Grafting (serin and gelatin)	PC12 cells	Enhancing neural cell adhesion and proliferation and differentiation of neurons.	[139]
PEDOT:PSS-*co*-MA	N-Cadherin and L1 protein	Grafting	Cortical neurons	Promoting axonal elongation and collateralization on the polymer.	[140]
PEDOT:PSS-*co*-MA	N-Cadherin	Grafting	Rat hippocampal slices	Increasing the amplitude and SNR of neural recordings.	[141]
PEDOT- PPy	Polylysine and glutamine	Doping	Cortical neurons	Improving neural cell adhesion, outgrowth, and viability.	[142]
PPyCl	A 12-amino acid peptide (T59), IKVAV and T59-IKVAV	Adsorption	PC 12 cells and cortical astrocytes, SD rats	Enhancing cell attachment and promoting neurites outgrowth on PPyCl-T59-IKVAV surface.	[143]
PEDOT	RNIAEIIKDI (p20)	Grafting	Cortical neurons	Accelerating neurite outgrowth.	[144]
PEDOT	PEG-CDPGYIGSR,	Adsorption and grafting	PC12 cells	Improving neurite expression without compromising the electrochemical properties.	[145]
PEDOT-PC-*co*-PEDOT-MI	CSSSSIKVAV	Grafting	PC12 cells, NIH3T3, and primary rat Schwann cells	High resistance toward nonspecific enzyme/cell binding and specific recognition of PC12 cells for electrical communication.	[131]
PEDOT	Polylysine, heparin, basic fibroblast growth factor, fibronectin	Grafting	Adult male Wistar rats	Promoting tissue healing, enhancing blood vessel formation and axonal regeneration without increasing inflammation.	[146]
PEDOT	YIGSR and RGD	Grafting	PC12 cells and SD rats	Enhancing cell attachment and neurite extension.	[147]
PEDOT-PEDOTacid	Peptide GGGGRGDS	Grafting	Rat primary motor neurons	Increasing the adhesion of neurons between 3 and 9 times higher than controls.	[46]
PEDOT-exomethylene side group (PEDOT-EM)	Aptamer Laminin	Grafting	NIH3T3 cells and primary neuron cells	Obtaining stable and low impedance state PEDOT-EM. Achieving facile post-functionalization of PEDOT -EM with molecules of varying size and functionality (from small molecules to DNAs and proteins).	[148]
PPy	Hyaluronic acid (HA)	Doping	NIH 3T3 and human SH-SY5Y neuroblastoma	Improving adhesion and proliferation of neuronal cells and resisting cell attachment by doping small and high molecular weight HA, respectively, into PPy.	[26]
PEDOT	Polydopamine	Doping	Rat hippocampi	Lowering impedance and improving CSC, CIL and SNR	[14]

reported that layer-by-layer assembly of poly(L-lysine) (pLys) onto a poly(glutamic acid) (pGlu)-doped PPy electrode [PPy(pGlu)-pLys$_n$] enhanced neuron adhesion, as shown in Fig. 2A. As the number of pLys layers increased, the PPy(pGlu)-pLys$_n$ impedance slightly increased but significantly enhanced cell adhesion and neurite outgrowth (Fig. 2B). Alves-Sampaio et al. [146] showed that PEDOT-coated carbon microfibers (PEDOT-MFs), when functionalized by a multilayer complex of polylysine/heparin/basic fibroblast growth factor/fibronectin, achieved close contact with the spinal nerve with weak inflammation and fibrosis. The biofunctionalized PEDOT-MFs were also used to bridge the damaged spinal cord of adult rats through topographic and chemical cues, guiding axonal extension and cell migration in longitudinal alignment (Fig. 2C–I). Their results indicated that biofunctionalized PEDOT-MFs are attractive for neuroprostheses and lesion-bridging scaffolds used to treat neurological diseases. Collazos-Castro et al. [140] grafted the N-cadherin (Ncad) and L1 recombinant proteins simultaneously onto poly[(4-styrene sulfonic acid)-*co*-(maleic acid)] (PEDOT:PSS-*co*-MA) electrodes and revealed that the covalent modification slightly influenced the electrode electrochemical properties but significantly promoted dendrite and axonal growth on these electrodes. Their group also coated Ncad-functionalized PEDOT:PSS-*co*-MA onto carbon microfibers for nerve recording, resulting in improved electrode−neuron contact and enhanced signal recording stability and fidelity [141]. As shown in Fig. 3, the PEDOT:PSS-*co*-MA-coated carbon microfibers reduced the recording noise but did not affect the recorded biopotential amplitude. In contrast, the Ncad-functionalized PEDOT:PSS-*co*-MA-coated electrodes were found to reduce the recording noise and increase the amplitude of the recorded multiunit activity (MUA), leading to a doubled signal-to-noise ratio relative to the control carbon microfibers.

The YIGSR and IKVAV (active sequences of laminin) peptide-modified CP electrodes demonstrated improved adhesion and differentiation of neural cells, including PC12 cells, granule cells, Purkinje cells, neural progenitor cells, and hippocampal neurons [131,143,145]. Various approaches, including physical adsorption, entrapment, and covalent bonding, were used to modify the CP electrodes, endowing them with specific interactions with neural cells. Bhagwat et al. [145] discovered that the chemical conjugation of PEDOT electrodes with YIGSR peptides increased cell attachment and enhanced neurite development on CP surfaces compared to the physical adsorption (PA)-modified electrodes (Fig. 4A and B). Meanwhile, the chemical modification did not greatly undermine the electrochemical properties of the PEDOT electrodes. One of the most effective methods for incorporating biofunctional molecules or moieties is to utilize CPs with bioconjugate groups, which have a highly selective conjugation reaction [131,140]. Zhu and Yu et la [131]. synthesized a biomimetic conducting copolymer with phosphorylcholine-functionalized EDOT (EDOT-PC) and a maleimide-functionalized EDOT (EDOT-MI), and they further grafted IKVAV peptides onto the copolymer surfaces through maleimide-thiol chemistry (Fig. 4C). As the PEDOT-PC films exhibited high resistance toward nonspecific protein binding (Fig. 4D), the CSSSSIKVAV-conjugated poly(EDOT-MI-*co*-EDOT-PC) could construct a neuron-targeted specific interaction on the nonspecific interaction resistant background, supporting the proliferation (Fig. 4E) and differentiation (Fig. 4F) of PC12 cells well.

In addition to proteins and peptides, some other hydrophilic biomolecules, such as hyaluronic acid, chondroitin sulfate, and dextran sulfate, are also applicable for CPs to improve their biocompatibility with tissues by depressing surface biofouling [22,26]. For example, Kim et al. [26] incorporated hyaluronic acid (HA) into PPy (PPy/HA) and found that PPy/HA films were compatible with tissue after four weeks of subcutaneous implantation. The PPy/HA electrodes were more sensitive

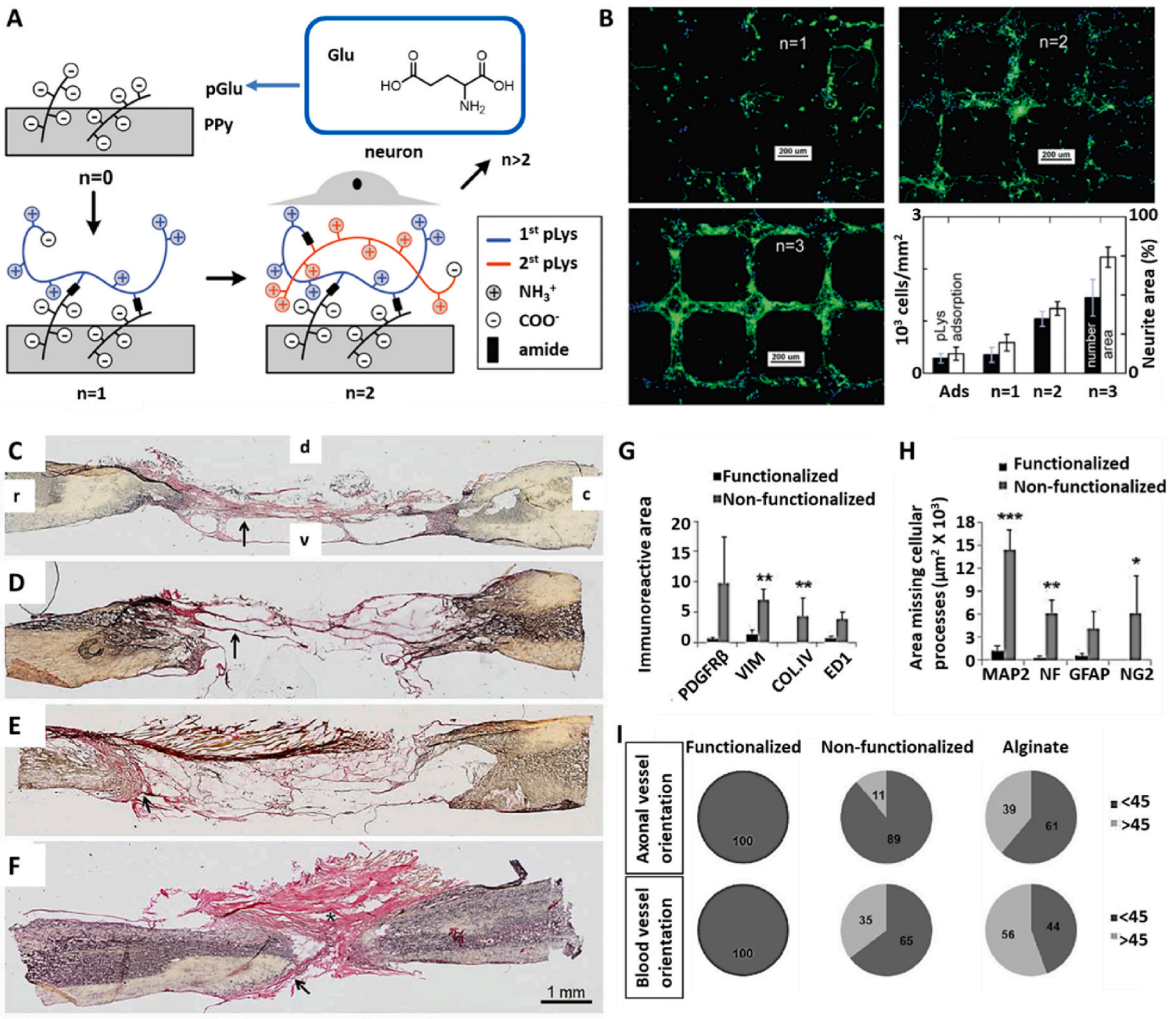

Fig. 2. (A) Schematic representation of a neuron adhered to a substrate consisting of PPy doped with poly(glutamic acid) (pGlu) and subsequently modified with multiple layers of polylysine (PPy[pGlu]-pLys$_n$) via reaction with protruding carboxylic acid groups of the pGlu dopant. (B) Immunofluorescence images of hippocampal neurons on PPy(pGlu)-pLys$_n$ 4 days after plating the with number of pLys layers n = 1, n = 2, and n = 3. The number of cells adhered to the patterns of PPy (pGlu)-pLys$_n$ (black bars) and the area of PPy(pGlu)-pLys$_n$ covered by neurites (white bars). Reproduced with permission [23]. Copyright 2010, American Chemical Society. (C–I) Spinal cord sections processed for Weigert's hematoxylin and van Gieson's stain, taken from animals treated with (C) polylysine/heparin/bFGF/fibronectin functionalized PEDOT-coated carbon microfibers (PEDOT-MFs); (D) nonfunctionalized MFs; (E) alginate alone; and (F) no treatment (control). Arrows in (C) and (D) signal the tissue growing along the MFs. Arrows in (E) and (F) point to the transverse fibrotic scar that sealed the spinal cord stumps. d, dorsal; v, ventral; r, rostral; c, caudal. (G) Quantification of the area of immunoreactivity for perivascular fibroblasts (PDGFR β), vimentin (VIM), collagen type IV (COL. IV), or inflammatory cells (ED1) around the MFs. (H) Quantification of the area missing neural processes for neurons (MAP2, NF), astrocytes (GFAP), and polydendrocytes (NG2) around the MFs. (I) Axon and blood vessel orientation at the transition zone, expressed as a percentage of elements forming an angle $<45°$ or $>45°$ with the longitudinal axis of the spinal cord. Reproduced with permission [146]. Copyright 2016, Elsevier Ltd.

to tiny signals than unmodified electrodes. Moreover, the PPy/HA electrode recording sensitivity increased with HA molecular weight, resulting in improved electromyography (EMG) signal detection and enhanced SNR (Fig. 5). This was primarily attributed to their higher CSC and decreased impedance due to their enhanced hydrophilicity.

Recently, polydopamine (PDA) was also used to functionalize CPs. Chalmers et al. [152] developed PDA-modified PPy hydrogels, which exhibited improved conductivity (2720%) and cell adhesion (2140%) compared to unmodified PPy hydrogels. Kim et al. [14] fabricated a PDA-incorporated PEDOT microelectrode (Fig. 6) with reduced impedance and higher CSC and CIL. These PEDOT/PDA microelectrodes were more biocompatible and exhibited much lower noise than gold electrodes. Moreover, they also successfully measured extracellular neuronal spikes from hippocampal neurons and evoked electrical activity of neuronal networks in response to current stimulations.

Although the biofunctionalization approach can effectively enhance CP-neuron interactions, implant-induced inflammation is still frequently observed in response to biofunctionalized CP implants [25,83,153]. Thus, extensive studies have been conducted to identify alternative materials and methods to further improve the long-term stability of neural electrodes. A practical approach to attenuating early implant inflammation is to load anti-inflammatory drugs into CPs. Wadhwa et al. [154] electrochemically doped dexamethasone (DEX) into a neuro-recording PPy electrode and verified its effect on preventing scar formation in the brain (Fig. 7A). Heo [25] and Boehler [155] also reported that drug-incorporated CP electrodes reduced the inflammatory response and significantly increased the density of axons around the electrodes (Fig. 7B and C). To achieve long-term electrical recording and stimulation in vivo, Zhong et al. [83] electrochemically codeposited PEDOT:PSS/NGF/DEX/poly(vinyl alcohol)/poly(acrylic acid) onto electrodes. The CSC value of the modified electrode was significantly enhanced, and the electrode impedance at 1 kHz was reduced by approximately 96% compared to the control. The immunochemical analysis revealed that the NGF- and DEX-functionalized CP electrodes

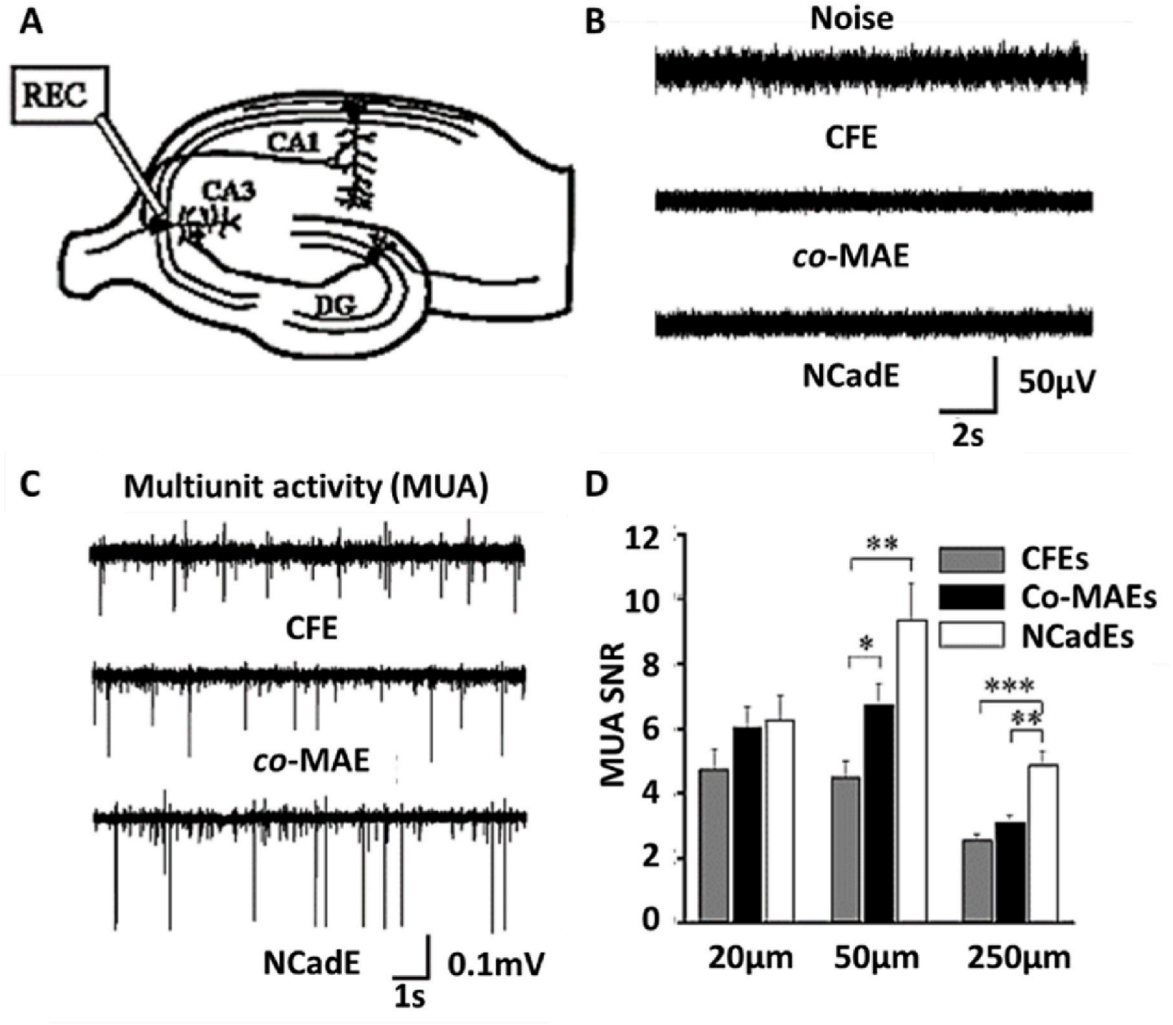

Fig. 3. (A) Schematic of a rat hippocampal slice showing the disposition of the recording electrode (REC); DG, dentate gyrus. (B) Representative traces of basal background noise remaining after tetrodotoxin perfusion in spontaneous activity recordings using 50 μm electrodes. (C) Representative traces of multiunit activity (MUA) activity segments extracted from recordings of spontaneous activity acquired using 50 μm electrodes. (D) Signal-to-noise ratio calculated for MUA. Reproduced with permission [141]. Copyright 2015, American Chemical Society.

alleviate the inflammatory response and improved neuronal survival at the interface after six weeks of cortical implantation in rats (Fig. 7D). Their results indicated that the combination of nerve growth factors and anti-inflammatory drugs improve the long-term stability of CP electrodes for chronic electrophysiological applications.

2.5. Challenges of biofunctionalized conducting polymers

Biofunctionalized CPs improve biocompatibility, promote neuron growth, notably increase SNR and reduce inflammation when utilized as implantable materials. However, several critical challenges remain unaddressed for CPs before their chronic applications.

There are three main methods to functionalize CPs by biomolecules: physical adsorption, entrapment, and chemical conjugation. The physical adsorption and entrapment of molecules are straightforward methods for modifying CPs. However, it is not easy to control the amount of biomolecules adsorbed or entrapped in CPs [156]. Protein adsorption or entrapment usually disrupts the CP surface morphology and electrical properties [157]. Furthermore, the physical adsorption of biomolecules with CP is pH-sensitive. The biomolecules might also leak from the polymer films, damaging the electrodes' stability [158,159]. Chemical conjugation allows the biological molecules to be covalently grafted onto CP surfaces, thereby enhancing the biofunctional stability of the CP electrodes [156]. However, the polymer conductivity might be compromised [158], and the activity of the biomolecules might be damaged in the chemical reactions [160].

Although the biomolecule modification approach can improve the biocompatibility of CP electrodes, it might increase the electrical impedance, resulting in poor electrical signal exchange at the interfaces. Liu et al. [22] Bhagwat et al. [145] found that after modifying CP electrodes with proteins or peptides, these modified electrodes had higher impedances than the pristine CP electrodes, which might be related to the reduced CP-solution interface area due to the biomolecule coating. Green et al. [157] demonstrated that doping laminin peptide significantly decreased the charge storage capacity of PEDOT. These peptide modifications also affected the mechanical, electrochemical, stability, and biological properties of CPs [157].

Last but not least, biomolecule-functionalized CPs cannot prevent gliosis formation in long-term implantation. Cui et al. [153] implanted DCDPGYIGSR peptide-coated PPy electrodes into guinea pig brains and monitored their foreign body reaction for three weeks. During the second week, a layer of non-neuronal tissue, consisting primarily of meningeal fibroblasts and ECM proteins, formed around the neural probe. By the end of the third week, astrocytes began to form loose tissue layers. Some other biofunctionalized CP-coated electrodes also remained scar tissue after being implanted in vivo for several weeks [25,

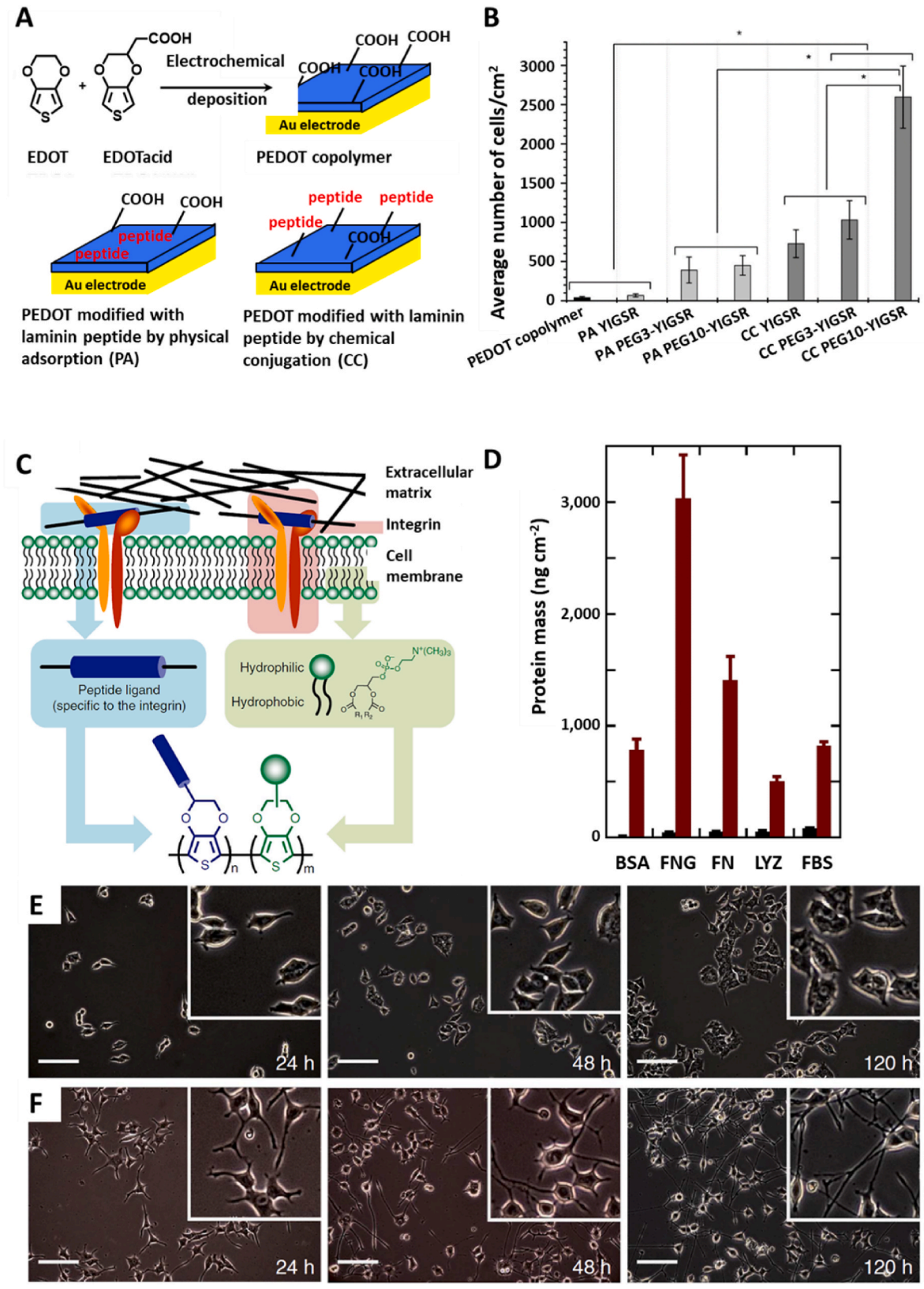

Fig. 4. (A) Schematic of surface modification of COOH-functionalized PEDOT films with YIGSR-based peptides through physical adsorption and chemical conjugation. (B) Average number of PC12 cells/cm^2 attached to the surface of COOH-functionalized PEDOT films modified with YIGSR-based peptides. Reproduced with permission [145]. Copyright 2016, Elsevier Ltd. (C) Schematic representation of a biomimetic conducting polymer. (D) Adsorption of various proteins on poly (EDOT-PC) (black) and poly(EDOT-OH) (red). (E) Proliferation and (F) differentiation (in the presence of NGF) of PC12 cells attached to CSSSSIKVAV-conjugated poly(EDOT-MI-*co*-EDOT-PC) films after 24, 48 and 120 h. Scale bar: 200 μm. Reproduced with permission [131]. Copyright 2014, Macmillan Publishers Limited.

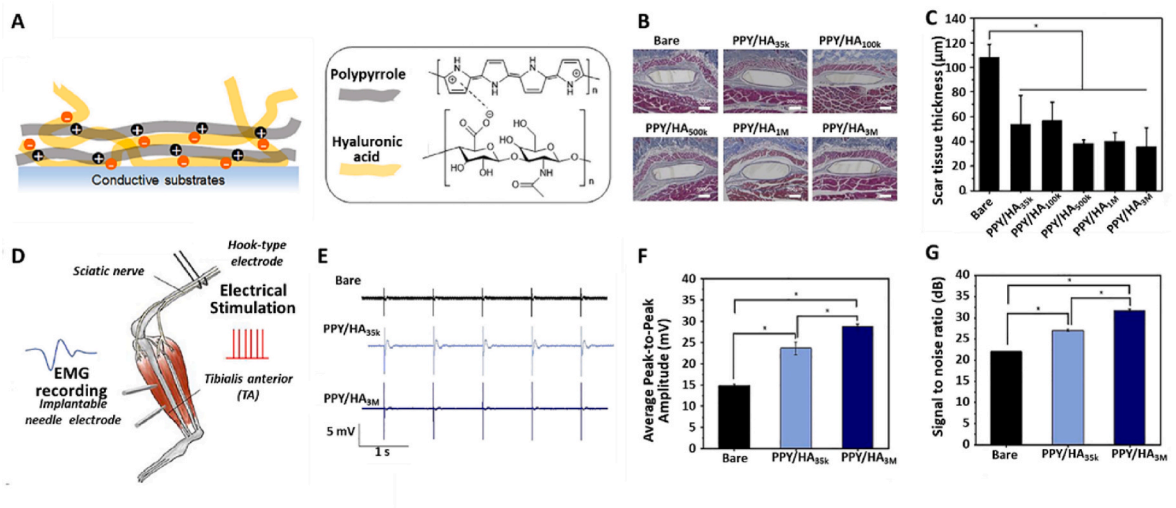

Fig. 5. (A) Schematic structures of hyaluronic acid-doped PPy (PPy/HA). (B) Masson's trichrome staining images of the tissues implanted with bare electrodes and PPy/HA-modified electrodes with different molecular weights. Scale bars: 200 μm. (C) Scar tissue thickness in tissues implanted with various PPy/HA substrates. (D) A schematic illustration of the electromyography (EMG) signal measurement at the tibialis anterior using an implantable concentric needle electrode by stimulating the sciatic nerve using a hook-type electrode. (E) In vivo EMG signals obtained from bare, PPy/HA_{35k}, and PPy/HA_{3M} electrodes. (F) Average peak-to-peak amplitudes and (G) signal-to-noise ratios of the obtained EMG signals. Reproduced with permission [26]. Copyright 2018, Elsevier Ltd.

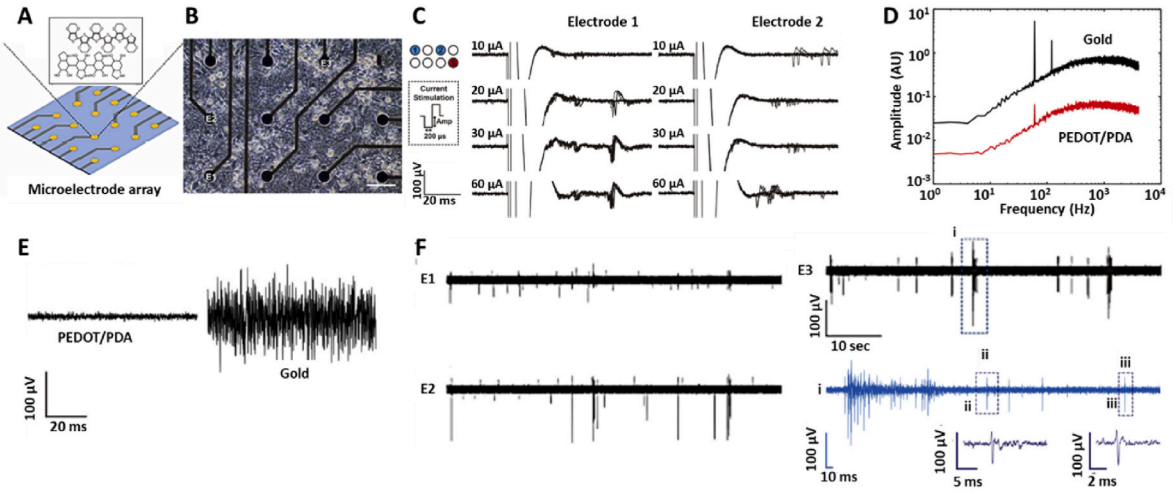

Fig. 6. (A) Schematic illustration of polydopamine and PEDOT hybrid (PEDOT/PDA) microelectrode microelectrodes. (B) Phase image of cultured neural networks on a microelectrode array. Scale bar: 100 μm. E1–E3 represent the electrodes that collected neural signals in (E). (C–F) Recording and stimulation with PEDOT/PDA microelectrodes. (C) Evoked neural signals after current stimulations (10 response signals overlapped). S: Stimulated electrode. (D and E) Noise of PEDOT/PDA and gold electrodes. Noise spectra in the frequency domain (D) and signals in the time domain (E). (F) Spontaneous neural signals recorded from PEDOT/PDA microelectrodes. Burst activities (i) and single spikes (ii, iii) were repetitively recorded. Reproduced with permission [14]. Copyright 2019, Elsevier Ltd.

26]. Given these findings, further revision of these biofunctionalized CPs is necessary to achieve long-term stability of CP electrodes. Modifying CP with anti-inflammatory drugs was also reported to reduce the immune response [25,83,154,155]. However, its effect is influenced by the amount of drug loaded and unsuitable for chronic application.

The interface between the implant surface and surrounding tissues is where the incorporated biomolecules meet with the body's immune system. Implanting a foreign implant into the brain will break the blood–brain barrier, leading to the influx of proteins, monocytes, and other blood-borne cells and their nonspecific adsorption onto the implant's surface [7–9,161]. The entire process was reported to occur within seconds [161]. During the early stages of inflammation, monocytes differentiate into macrophages. They recognize implants as foreign objects through nonspecifically adsorbed proteins and attempt to phagocytose and digest implants [8,9,11]. The local glia and neurons injured during implantation release acute cytokines and factors, e.g., ATP and macrophage colony-stimulating factor (*M*-CSF), which activate microglia. Activated microglia further release cytokines, including monokines, chemokines, and interleukins [162]. These cytokines facilitate cell-to-cell interactions during the immune response, promote proliferation, and attract microglia and astrocytes to the implant site [163,164]. During the chronic phase, the implant is ultimately encapsulated by a dense glial sheath, which may take more than six weeks to stabilize. Based on this immune response pathway, the nonspecific interaction of proteins/cells plays a crucial role in triggering the immune response.

Nonspecific cell/protein adsorption has been verified as the primary factor triggering inflammation [7,10,11]. Previous studies have demonstrated that nonspecifically adsorbed proteins enhance macrophage adhesion to foreign materials, triggering the early stage of the

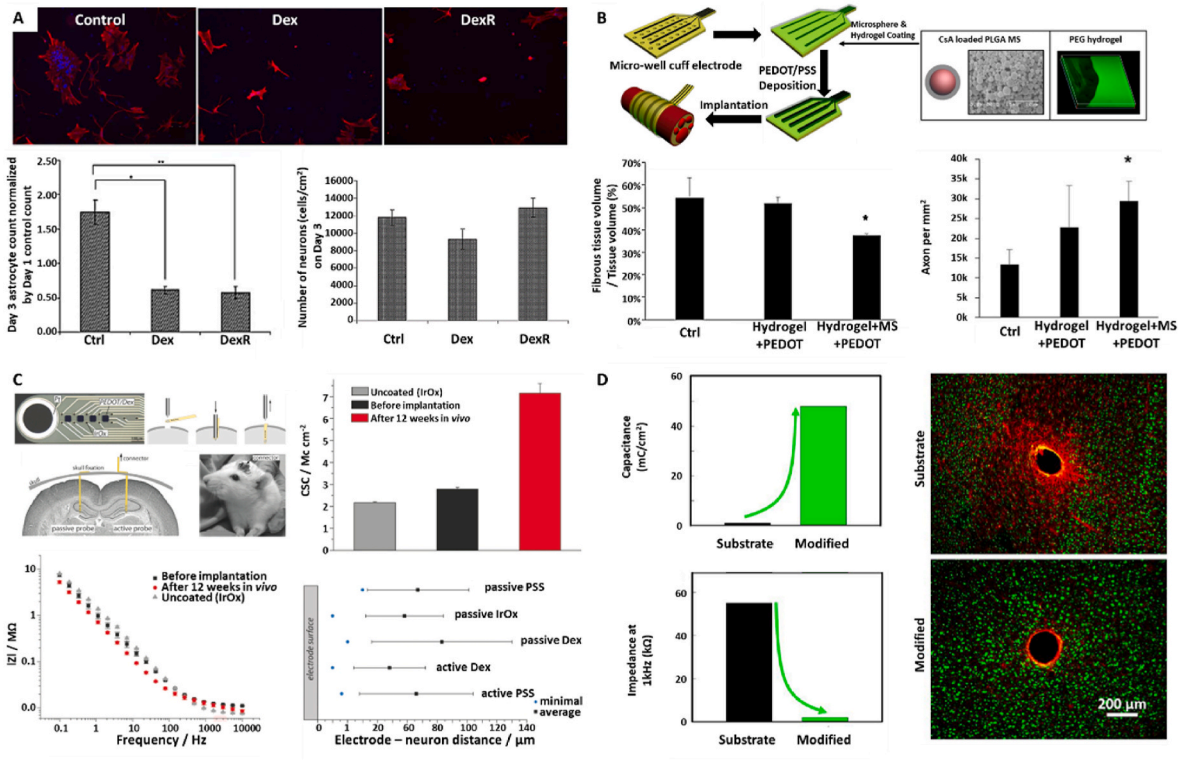

Fig. 7. In vitro or in vivo studies of the effects of anti-inflammatory drugs on CPs. (A) In vitro studies for the effect of dexamethasone (Dex) on reactive astrocytes number, as shown by GFAP staining. Control group: no drug, Dex group: Dex was added to the media at a concentration of 10^6 M, and DexR: drug was electrically released in PBS from the PPy–Dex electrode, and the resulting solution was added to media with a final Dex concentration of 10^6 M. Histograms showing the normalized number of astrocytes on day 3 and the effect of Dex on neuron viability on day 3 for Ctrl-, Dex- and DexR-treated cells. Reproduced with permission [154]. Copyright 2005, Elsevier Ltd.
(B) Schematic illustration of the fabrication process for the cyclosporin A (CsA)- and PEDOT:PSS-functionalized nerve cuff electrode. Histograms showing quantification of the fibrotic tissue area of the nerve tissue and axonal density of sciatic nerves after implantation with control (Ctrl), Hydrogel + PEDOT, and Hydrogel + MS + PEDOT coated electrodes. Reproduced with permission [25]. Copyright 2016, Elsevier Ltd.
(C) Microscope image of a polyimide neural probe with 4 PEDOT/Dex-coated electrode sites. Comparison of CSC and impedance magnitude for a PEDOT/Dex-coated probe before implantation and 12 weeks later in vivo. Neuron distance around different material-coated probes. Passive probe: no stimulation, the active probe: CV-stimulation. Reproduced with permission [155]. Copyright 2017, Elsevier Ltd.
(D) Comparison of CSC and impedance magnitude of Pt/Ir implant (substrate) and CP/NGF/DEX/hydrogel electrode (modified). GFAP (red) and NeuN (green) immunostaining around implants at 6 weeks after implantation in the rat brain. Reproduced with permission [83]. Copyright 2017, Elsevier Ltd.

inflammatory response [24]. Furthermore, the compositions and three-dimensional structures of adsorbed proteins are crucial for immune cells to recognize the foreign surface and trigger a complex immune response [24,165]. Several works have already shown that reducing protein adsorption benefits device neural recording in long-term implantation [166,167]. Thus, given these results, antifouling CPs, which resist nonspecific protein/cell binding, should be much more promising, as they can prevent the electrode from nonspecifically binding proteins/cells, thus abrogating the first step toward triggering the immune response.

3. Zwitterionic conducting polymers for bioelectronic devices

3.1. Zwitterionic conducting polymers

Antifouling CPs have recently received extensive attention due to their strong resistance to nonspecific protein/cell interactions and their exciting potential for depressing immune responses. A common structural feature of these antifouling CPs is their grafting of hydrophilic groups or polymers. Depending on the chemical structures, three main kinds of antifouling CPs were developed for bioelectronic applications. Oligo(ethylene glycol) (OEG)- or poly(ethylene glycol) (PEG)-functionalized CPs were the earliest reported antifouling CPs [168,169]. During the past ten years, the most commonly studied antifouling CPs have been zwitterion-functionalized CPs [29,131,132,170–179], which are grafted by zwitterionic groups or polymer chains with an equal number of oppositely charged groups. The zwitterionic groups and zwitterionic polymers usually present strong hydrophilicity and neutral charge, which helps the CPs prevent proteins/cells from approaching via nonspecific interactions (originating from hydrophobic-hydrophobic, electrostatic, dipole–dipole, or van der Waals interactions). Hydrophilic biomolecules, e.g., hydrophilic peptides and phytic acid [170,180,181], have also been used to functionalize CPs with antifouling properties. Table 3 summarizes some recent studies of antifouling CPs.

PEG- or OEG-functionalized CPs are susceptible to oxidative degradation, as ethylene glycol groups were reported to decompose when in contact with transition metals and oxygen in biological solutions [187,188]. PEG-functionalized CPs were also unstable after being applied in an oxidation potential for a few hours [30]. In addition, OEG and PEG were reported to be immunogenic and thus might not be applicable for long-term implants [189]. Their immunogenic feature was attributed to the hydrophobic C–C backbone and –O(CH_3) terminal group. The hydrophobic feature of OEG and PEG moieties exposes it to the immune system, leading to the generation of PEG-specific antibodies [190]. In addition, several studies revealed that zwitterion polymers are chemically more stable and superior in antifouling performance [191–195]. Thus, we focus on the synthesis, properties, and bioelectronic applications of zwitterionic CPs.

Table 3
Hydrophilic and zwitterionic group functionalized conducting polymers, applications, and key results (Abbreviation: PC = phosphorylcholine, SB = sulfobetaine, CB = carboxybetaine, BSA = bovine serum albumin, FN = fibronectin, FNG = fibrinogen, MA = methacrylate, MI = maleimide, HQ = hydroquinone, Th = thiophene, MAA = methacrylamide, PTh-CB-*co*-ThAA = carboxybetaine thiophene-*co*-thiophene-3-acetic acid, and PThAA = poly(thiophene-3-acetic acid)).

Antifouling moieties	Antifouling CPs	Impedance	Application	Protein/cell/ bacteria/animal	In vitro and in vivo stability	Key results	References
PC	PEDOT-PC	/	Dopamine biosensor	BSA, rat	The PEDOT-PC electrode could retain 92% sensitivity, while the PEDOT electrode only 43%.	The biosensor maintained its high sensitivity to dopamine in rat brains.	[182]
PC	PPy-PC	/	Anti-inflammtion electrode	BSA, Escherichia coli, Staphylococcus aureus, and mice	PPy-PC suppressed scar tissue formation by 80% after 4 weeks of subcutaneous implantation.	PPy-PC electrodes displayed high resistance to proteins, bacterials and cell, and suppressed scar tissue formation.	[129]
SB	PEDOT:PSS-SB	Au: ~252 Ω; PEDOT:PSS-SB: ~160 Ω at 1 kHz	Neural interface	PC 12 cells, rat	PEDOT:PSS-SB device induced a stable compound action potential for at least 4 weeks of implantation.	PEDOT:PSS-SB electrode showed improved impedance, charge storage capacity, and charge injection capability and demonstrated efficient stimulating and recording during chronic neuromodulation.	[183]
Zwitterionic peptide (sequence EKEKEKE)	PEDOT–COOH–EKEKEKE	/	DNA sensor	Human plasma	/	The DNA biosensor displayed high selectivity and low detection limit.	[170]
PEG	PPy/GCE-PEG	Glassy carbon electrode (GCE): 121.4 Ω; PPy coated GCE (PPy/GCE): 12.4 Ω; PPy/GCE-PEG:498.0 Ω.	DNA sensor	Serum	The Rct value of PPy/GCE increased dramatically after the protein solution incubation, while those of PEG/PPy/GCE did not.	The detection range of targeted miRNA is from 0.10 pM to 1.0 nM.	[184]
SB and PEG	Poly(OEGMA) grafted PEDOT (PEDOT-POEGMA), poly(SBMA) grafted PEDOT(PEDOT-PSBMA)	PEDOT-PSBMA showed a lower impedance than PEDOT-POEGMA at low frequency.	Antifouling electrode	BSA, FNG, NIH3T3	/	PEG and SB grated PEDOT electrode prevented cell adhesion. Protein binding properties of the surface can be modulated by the density of polymer brushes.	[29]
SB	PEDOT-C_4-SB, PEDOT-C_5-SB	PEDOT-C4-SB: 82 Ω; PEDOT-C5-SB: 55Ω; PEDOT-SB: 1630 Ω at 1 Hz.	Antifouling electrode	FNG	After being applied 1000 cycles of CV scans, the total charge of PEDOT-SB decreased to 60%, while those of PEDOT- C5-SB and PEDOT- C4-SB retained 70% and 80%, respectively.	The antifouling CP electrode showed excellent antifouling properties. The 1 Hz impedance of PEDOT-C_4-SB (-C_5-SB) was 20 times lower than PEDOT-SB.	[174]
SB	PEDOT-SB	/	Antifouling electrode	BSA, NIH3T3	/	Only a minimal amount (<1% of surface coverage) of cell adhesion was observed on the surface.	[173]
PC, SB, and CB	Poly(EDOT-*co*-EDOT-PC), poly (EDOT-*co*-EDOT-CB), poly(EDOT-*co*-EDOT-SB)	Poly(EDOT-*co*-EDOT-PC) had the lowest impedance at the low frequency.	Antifouling electrode	NIH3T3	/	Poly(EDOT-*co*-EDOTPC) gave the lowest impedance and the best resistance to protein adsorption and cell adhesion.	[132]
PC, SB, and EG	PEDOT-EG3, PEDOT-EG4, PEDOT-PC, PEDOT-SB	PEDOT-SB and PEDOT-EG4 had a higher impedance than PEDOT-PC, PEDOT-EG3, and PEDOT.	Antifouling stability under stimulation	HAPI, NIH3T3	PEDOT-PC demonstrated the best stability in the antifouling and electrochemical properties during the electrical stimulation.	After the electrical stimulation, the PEDOT-PC electrode still exhibited good electrochemical stability, low impedance, small voltage excursion, and excellent resistance toward proteins and HAPI microglial cells.	[28]
PEG and PC	PEDOT-PC, PEDOT-EG	/	Antifouling conducting biointerface	BSA and lysozyme	/	PEDOT-PC has a higher desorption rate and film regeneration compared with PEDOT-EG.	[30]
PC	Peptide grafted Poly (EDOT-MI-*co*-EDOT-PC)	Poly(EDOT-MI-*co*-EDOT-PC) showed lower impedance than PEDOT and Au.	Selective cell interaction on PEDOT	BSA, FN, FNG, LYZ, FBS, NIH/ 3T3, PC 12	The PEDOT-PC film still could retain its electroactivity and excellent antifouling property after being	Peptide grafted poly(EDOT-MI-*co*-EDOT-PC) could selectively interact with cells, ensuring efficient electrical communication	[131]

(*continued on next page*)

Table 3 (*continued*)

Antifouling moieties	Antifouling CPs	Impedance	Application	Protein/cell/ bacteria/animal	In vitro and in vivo stability	Key results	References
					applied 1000 cycles of CV scans.	with neural model cells over five days.	
PC	EDOT-PC copolymers	Copolymers had a much lower impedance than gold.	Cell-repulsive cues for electrodes	PC 12 cells	/	The strong repulsive force of PEDOT-PC could control the neurite outgrowth well and enhance it by 179%.	[185]
PC	Poly(EDOT-HQ-*co*-EDOT-PC)	Poly(EDOT-HQ-*co*-EDOT-PC) and PEDOT had a similar impedance.	Dynamic Cell Capture and Release	NIH3T3, PC12 cells	The poly(EDOT-HQ) film displayed a reversible electrochemical switch.	This PEDOT copolymer presented a dynamic interaction with cells through redox bioconjugation; it further demonstrated the electrically stimulated cell differentiation and subsequent safe cell release on this copolymer.	[186]
CB	PThCB-*co*-ThAA, PThCB-*co*-ThMAA, PCBTh-*co*-ThRGD	/	Specific cell interaction	Bovine aortic endothelial cells	/	RGD grafted PThCB-*co*-Th specifically interacted with cells through RGD.	[177]

3.2. Synthesis of zwitterionic conducting polymers

Zwitterionic CPs are composed of a conjugated backbone and hydrophilic side groups and chains with equal amounts of cationic and anionic units. Phosphorylcholine (PC), sulfobetaine (SB), and carboxybetaine (CB) moieties are the most popular zwitterions used to functionalize CPs. The following sections highlight their synthesis and their molecular design.

3.2.1. Phosphorylcholine (PC)-functionalized conducting polymers

Zhu and Yu et al. [131] reported the first zwitterionic PEDOT, i.e., phosphorylcholine-functionalized PEDOT (PEDOT-PC); its synthesis pathway is shown in Fig. 8A–i. EDOT-OH was first reacted with 2-chloro-2-oxo-1,3,2-dioxaphospholane. Then, in the presence of trimethylamine, the dioxaphospholane ring was opened to yield phosphorylcholine-functionalized EDOT (EDOT-PC). A surfactant-assisted electropolymerization was used to deposit the EDOT-PC homopolymer and its copolymers, which displayed strong resistance to nonspecific protein/cell binding. Goda et al. [171] later also synthesized phosphorylcholine-functionalized EDOT and its polymer, which is slightly different from the above chemical structure (Fig. 8A–ii). First, in the presence of p-toluene sulfonic acid, 3,4-dimethoxythiophene was reacted with 3-chloro-1,2-propanediol to prepare EDOT-Cl. Then, its chloromethyl was reacted with potassium thioacetate to form methanethioester-functionalized EDOT through nucleophilic substitution. The methanethiol-functionalized EDOT (EDOT-SH) was then available by deprotection in a basic medium. Finally, it was reacted with 2-methacryloyloxyethyl phosphorylcholine (MPC) through thiol−ene chemistry to yield EDOT-PC. Electrocopolymerization of EDOT and EDOT-PC monomers was performed to prepare random copolymers. In a later study from the same group, they used EDOT-SH to react with zwitterionic methacrylates to prepare three zwitterionic EDOTs bearing phosphorylcholine (EDOT-PC), carboxybetaine (ECOT-CB), and sulfobetaine (EDOT-SB) (Fig. 8A–iii) [132]. Subsequently, copolymers of zwitterion EDOT with EDOT were synthesized by electrochemical copolymerization. Their results further revealed that the structure and composition of zwitterions exerted pronounced effects on the protein adsorption and cell adhesion of these polymer films.

3.2.2. Sulfobetaine (SB)-functionalized zwitterionic conducting polymers

As mentioned above, the EDOT-SB monomer was synthesized from EDOT-SH through thiol-ene chemistry. This synthesis method is straightforward and efficient with a high yield. In addition, Cao et al. [172] recently synthesized EDOT-SB using a simple three-step method (Fig. 8B–i). First, 3,4-dimethoxythiophene was reacted with 3-chloro-1,2-propanediol to synthesize EDOT-Cl through acid-catalyzed transesterification. Then, the amination of EDOT-Cl was performed to yield aminated EDOT. Subsequently, the substance was reacted with 1,3-propanesultone by quaternization to generate EDOT-SB. Finally, the EDOT-SB polymer (PEDOT-SB) was prepared by electrochemical polymerization. The PEDOT-SB surface exhibited excellent conductivity, stability, and switchable antifouling/antimicrobial properties. Shen et al. [173] developed another approach to preparing sulfobetaine-functionalized EDOT from hydroxymethyl-EDOT (EDOT-OH) (Fig. 8B–ii). EDOT-OH and dimethylglycine were condensed via Steglich esterification to yield tertiary amino-functionalized EDOT. Then, it was reacted with 1,3-propanesultone to produce EDOT-SB through quaternization. The PEDOT-SB films were prepared by electrochemical deposition, which inhibited 95% of the nonspecific binding of proteins and fibroblast cells. Lee et al. [174] synthesized two derivatives of PEDOT-SB, PEDOT-C_4-SB, and PEDOT-C_5-SB by introducing alkoxyl spacers of different lengths between the PEDOT backbone and sulfobetaine (Fig. 8B–iii). First, 4-bromobutoxy methyl-EDOT or 5-bromobutoxy methyl-EDOT was synthesized from EDOT-OH through nucleophilic substitution, and then a procedure similar to that shown in Fig. 7B–i was conducted to prepare PEDOT-C_4-SB and PEDOT-C_5-SB. PEDOT-C_4-SB and PEDOT-C_5-SB were found to be significantly different from PEDOT-SB with respect to oxidation potential and surface morphology.

In addition to bottom-up synthesis, post-modification approaches, i.e., surface-initiated polymerization or the direct grafting-to method, have also been used to introduce zwitterionic groups or polymers onto CP surfaces. Pei et al. [175] successfully grafted zwitterionic betaine polymers onto PPy using atom transfer radical polymerization (ATRP). Pyrrole was electrocopolymerized with 4-(3-pyrrolyl) butyric acid to yield poly(Py-*co*-PBA), followed by conversion of carboxylate to hydroxyl and subsequent coupling of ATRP initiators through the nucleophilic substitution reaction. Then, poly(3-(methacryloylamido) propyl)-N,N′-dimethyl(3-sulfopropyl)-ammonium hydroxide) (PMPDSAH) and poly(methyl methacrylate)-*b*-PMPDSAH (PMMA-*b*-PMPDSAH) were grafted from the initiator via ATRP. In this way, zwitterionic polymer-grafted PPy materials and electrodes were successfully synthesized. In another earlier study, Zhao et al. [29] first synthesized the ATRP initiator (-Br)-grafted 3,4-ethylene dioxythiophene (EDOT-Br) from EDOT-OH and 2-bromoisobutyryl bromide by nucleophilic substitution. Then, poly(EDOT-Br-*co*-EDOT) films were deposited as thin films using electropolymerization. Finally, surface-initiated ATRP was used to graft poly((oligo(ethylene glycol) methacrylate), poly(OEGMA), and zwitterionic poly([2-(methacryloyloxy)ethyl]dimethyl-(3-sulfopropyl) ammonium hydroxide), poly(SBMA) onto PEDOT surfaces.

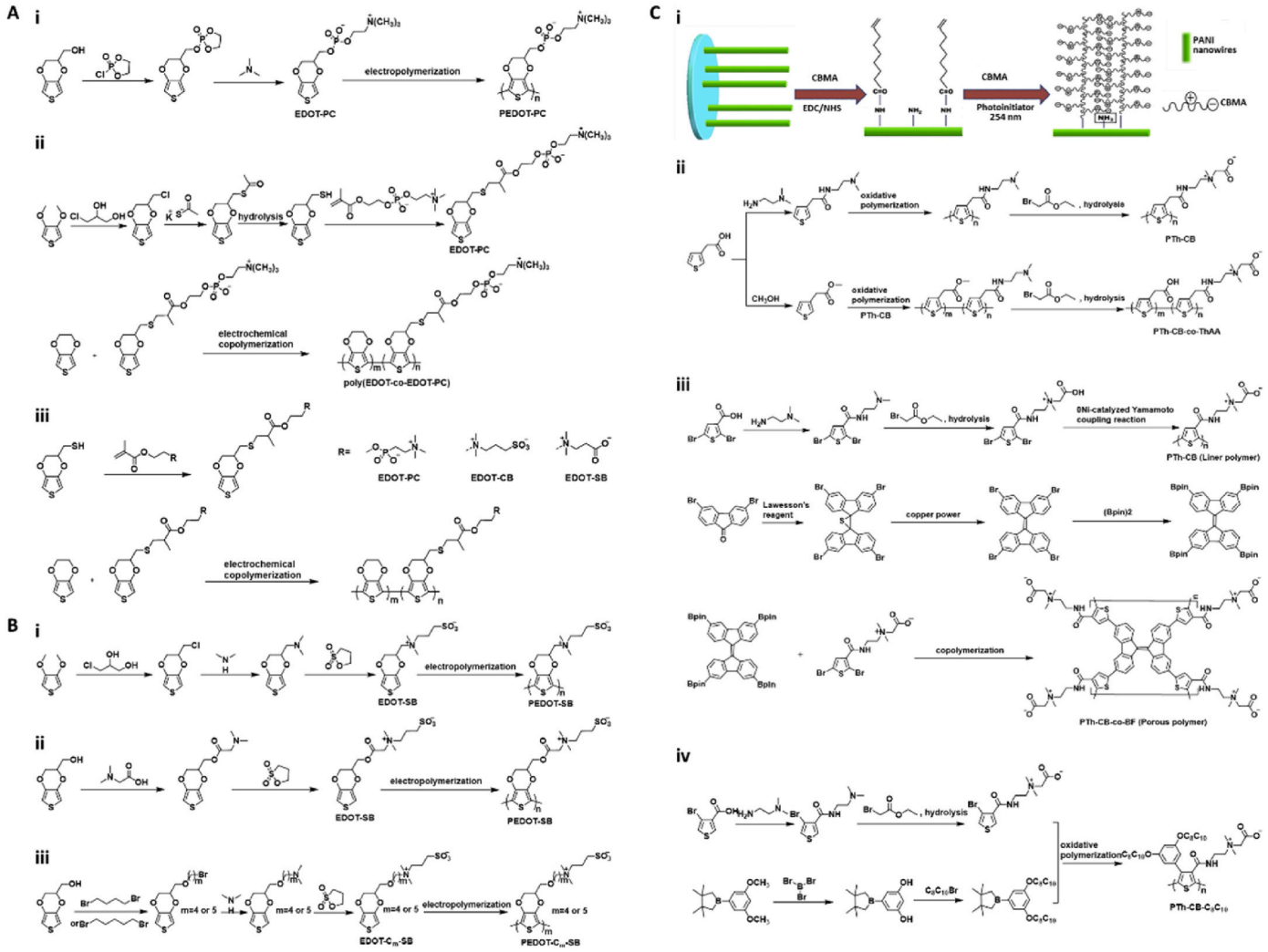

Fig. 8. (A) Syntheses of phosphorylcholine functionalized conducting polymers. i) Syntheses of PEDOT-PC from EDOT-OH [131]. ii) Synthesis route for EDOT-PC from 3, 4-dimethoxythiophene. Electrochemical copolymerization of EDOT and EDOT-PC [171]. iii) Synthesis of zwitterionic EDOTs from EDOT-SH, and electropolymerization of zwitterionic EDOTs and EDOT [132]
(B) Syntheses of sulfobetaine functionalized conducting polymers. i) Synthetic route of PEDOT-SB from 3, 4-dimethoxythiophene [172]. ii) Synthesis of PEDOT-SB from EDOT-OH [173]. iii) Synthetic route of PEDOT-C_4-SB and PEDOT-C_5-SB from EDOT-OH [174]
(C) Syntheses of carboxybetaine functionalized conducting polymers. i) Schematic illustration of the construction process of antifouling PANI. Reproduced with permission [176]. Copyright 2018, Elsevier Ltd. ii) Synthetic routes to PCBTh homopolymer and its random copolymers: PCBTh-*co*-ThAA, PCBTh-*co*-ThMAA and PCBTh-*co*-ThSH [177]. iii) Synthetic routes to obtain PCBTh and PCBTh-*co*BF [178]. iv) Synthetic routes for polymer PCBTh–C_8C_{10} [179].

Their results revealed that nonspecific protein adsorption on CPs could be modulated by zwitterionic polymer brush density, which is tuned by the feed composition of EDOT-Br in the solution for electropolymerization.

3.2.3. Carboxybetaine (CB)-functionalized zwitterionic conducting polymers

Wang et al. [176] synthesized poly(carboxybetaine methacrylate) (polyCBMA)-modified polyaniline (PANI) nanowires by postgrafting. As shown in Fig. 8C–i, CBMA monomers were first anchored onto PANI surfaces using EDC-NHS chemistry; thus, these methacrylates anchored onto surfaces could function as monomers to join the photocatalyzed radical polymerization and grafted polymer chains onto PANI surfaces. Thus, the prepared polyCBMA-grafted PANI nanowires displayed excellent antifouling and electrical conductivity. In another study, Cao et al. [177] synthesized carboxybetaine-functionalized thiophene monomer (Th-CB), its homopolymer (PTh-CB), and its random copolymer (PTh-CB-*co*-ThAA) with thiophene-3-acetic acid (ThAA). ThAA was reacted with N,N′-dimethylethylenediamine through the condensation reaction to give (N-(2-(dimethylamino)ethyl)-2-(-thiophene-3-yl)acetamide). Then, it was further reacted with ethyl bromoacetate through the dimethylamino group, and the product was subsequently hydrolyzed to regenerate the final product via the ion exchange resin column. PTh-CB and PTh-CB-*co*-20%ThAA were then synthesized using oxidative polymerization with iron(III) chloride as an oxidant. PTh-CB-*co*-ThAA could further react with methacrylamide and thiol to install the desired functional groups (Fig. 8C–ii). These polymers effectively prevented nonspecific BSA and fibrinogen adsorption. Recently, the Lee group synthesized two multifunctional zwitterionic conducting polymers, i.e., linear poly(carboxybetaine thiophene) (PTh-CB) and porous poly(carboxybetaine thiophene-*co*-9,9′-bifluoreneylidene) (PTh-CB-*co*-BF). Its synthesis pathway is similar to those mentioned before, as shown in Fig. 8C–iii [178]. The same group further synthesized a multifunctional zwitterionic liquid crystalline polymer PCBTh–C_8C_{10} (Fig. 8C–iv) as an intriguing approach for implanting organic bioelectronics [179]. These conducting biomaterials exhibited significant antimicrobial properties and were highly resistant to protein adsorption and cell attachment.

3.3. Antifouling of zwitterionic conducting polymers

Zwitterionic biointerfaces have been well demonstrated to resist the nonspecific adhesion of proteins and cells [29,131,132,172,173,177,185,186]. Schlenoff has provided a systematic review of all antifouling mechanisms of zwitterionic biointerfaces based on the surface energy, the water structure around zwitterions, the excluded volume effect (including the contribution of enthalpy and entropy), the ion coupling effect, the mobility of surface functional groups, and salt resistance [196]. Thus, this review will not discuss those subjects in detail but will instead focus on zwitterion superiority in hydration and the effect of zwitterionic CP structures.

3.3.1. Hydration of zwitterions

The hydration of antifouling interfaces is critical for cell/protein resistance. The hydration layer formed at the zwitterion-modified interface originates from ionic interactions [194]. This makes the hydration layer more compact and stable than those formed at PEG/OEG-modified interfaces. As PEG/OEG chains are neutral hydrophilic components, their hydration occurs via hydrogen bonding instead. Through molecular dynamics simulations or sum frequency generation techniques, it was confirmed that water molecules close to zwitterionic surfaces exhibit decreased mobility, wider dipole orientation distribution, and longer residence time than those of the OEG surfaces or nonmodified surfaces [191,192]. The free energy of hydration for zwitterionic CB and SB (−404 and −519 kJ mol^{-1}, respectively) was much lower than that for nonionic EG_4 moieties (−182 kJ mol^{-1}) [193], revealing that zwitterionic materials have more substantial hydration capability [194]. Furthermore, more water molecules were demonstrated to interact with zwitterionic units than with EG units; the hydrated water molecules on SB units were more tightly bound than those on EG units before saturation [195]. Given these results, water molecules tend to steadily stay on zwitterionic surfaces and are less favored to move away, indicating that zwitterionic polymers strongly repulse nonspecific protein adsorption.

Intriguingly, zwitterions have a more reliable antifouling property than some other hydrophilic moieties. Zhang et al. [197] found that proteins binding on zwitterion surfaces could be removed entirely by water washing and did not substantially stick to the interface. In comparison, the polysaccharide-modified surface could not be regenerated by washing. It indicates that irreversible binding is predominant. This can be explained well by the fact that the water bonding strength for zwitterionic surfaces is much more robust than that for polysaccharide surfaces.

A simulation by Shao et al. revealed that the self-assembled PC monolayers are highly ordered [198]. Moreover, poly (2-methacryloyloxyethyl phosphorylcholine) (PMPC) persisted in a relatively stiff structure in an aqueous NaCl solution within a wide range of concentrations (0–5.0 M) [199]. In another study by Kobayashi et al. [200], it was demonstrated that the most characteristic property of PC-based polymer compared to SB-based polymer is its independence of the chain dimensions on salt concentration. This is primarily because the trimethylammonium cation and phosphate anion bind covalently in the PC unit to form the inner salt situation. The two ions are situated close to one another, with three methyl groups bound to the nitrogen atom of the PC unit located outside of the polymer chains. This provides a site that can form favorable interactions with water through hydrophobic hydration, including a more ordered water structure similar to that of free water in the bulk phase. This hydrophobic hydration layer did not disturb the hydrogen bonding between the water molecules [201]. These results could explain why zwitterionic PC groups have extreme resistance to nonspecific protein/cell interactions.

3.3.2. pH, spacer length, composition, and chemical structure effects

All three zwitterionic CPs have the same positively charged unit, the ammonium group, but have different negatively charged units. Their difference in the negatively charged units should lead to different surface charges and thus different antifouling performance under the same acid environments. The sulfonic and phosphate groups can remain unprotonated over a wide pH range of approximately 2–14 [202–204]. Thus, both sulfobetaine- and phosphorylcholine-functionalized CPs are expected to retain their zwitterionic nature over a wide pH range from 2 to 14. However, the carboxylic groups of carboxybetaine-functionalized CPs would be protonated at pH $\leq$ 4, as carboxylic acid is a weaker acid [203,205]. This result indicates that carboxybetaine groups could be neutral or positively charged, depending on the pH. Thus, it is not unexpected that the antifouling performance of carboxybetaine is highly dependent on the pH value of the environment.

In another research by Zhang et al. [28], it was found that the antifouling performance of the PEDOT-SB electrode was slightly worse than that of the PEDOT-PC electrode. One plausible explanation is that the charge densities of the cationic (3.0 e/nm^3) and anionic groups (−4.5 e/nm^3) of SB groups are unbalanced, which may change the configuration of self-associated SB moieties [206]. Zwitterionic PC moieties have a charge density balance between the cationic group (3.0 e/nm^3) and the anionic group (−3.0 e/nm^3), enhancing the self-association of PC moieties and stabilizing their configuration [206].

The distance between the two oppositely charged groups in a zwitterion also influences the antifouling property of zwitterionic polymers. Usually, the hydrophobic alkyl group is used to connect and gap the two oppositely charged groups. Although the hydrophilicity increases with spacer extension [203], the longer hydrophobic alkyl compromises more hydrophilicity [207]. As simulated by Shao et al. [207], the hydration free energy of carboxybetaine groups decreases with the extension of the alkyl spacer, when the number of methyl groups is smaller or equal to 3. It was also indicated that the charges groups of CB moieties with longer alkyl spacer are more highly charged, and those of CB moieties with spacer length $\geq$3 methyl groups present identical charges. Another concern is that the hydrophobic alkyl chain would compromise the hydrophilicity. However, based on the study by Shao et al. [207] there is only a slight variation in the hydration free energy for CB molecules with longer hydrophobic spacer.

Their simulation results further indicated that the interactions between CB moieties and guest ions strongly depend on the spacer length. The longer the carbon spacer length is, the stronger the Na^+ association preference for CB moieties due to the higher partial charge of carboxylic groups. Mi et al. [208]experimentally verified that CB moieties with methylene spacers did not associate with Mg^{2+} or resist polysaccharide attachment, whereas CB moieties with longer spacers bound polysaccharides due to their association with Mg^{2+}. The previous study by Weers et al. [203] has found that the methylene spacer length has a very small effect on the sulfobetaine hydration while having a distinctive effect on the carboxybetaine hydration. It could be explained by that increasing methylene spacer length would increase the pKa value of carboxybetaine, and enhance the carboxybetaine hydrophilicity as the protonated moiety is more hydrophilic than the zwitterionic one.

Zhu and Yu [131]. studied the effect of polymer composition on resistance to proteins/cells for PC-functionalized CPs. Its resistance to nonspecific protein/cell interactions was sigmoidally dependent on the EDOT-PC monomer feed composition. When the feed composition of EDOT-PC in the electrolyte solution was greater than 50%, the copolymer films were consistently highly resistant to cells and proteins. This finding is critical for applying zwitterionic CPs in bioelectronic devices, as it provides a composition window to combine conjugatable comonomers for building biomolecule-defined specific interactions without damaging the nonspecific interaction resistance. Goda [132] developed three zwitterionic conducting copolymers by copolymerizing EDOT with EDOT-PC, EDOT-CB, or EDOT-SB. They also verified that the antifouling property of the copolymer films remains constant when the composition of the zwitterionic monomer is more than 50 mol%. They further demonstrated that PEDOT-PC exhibited more resistance to protein adsorption and cell adhesion than PEDOT-SB and PEDOT-CB.

3.4. Low impedance of zwitterionic conducting polymers

3.4.1. Enhanced ion conductivity

For bioelectronic implants, the low impedance of electrodes is critical to ensure their efficient electrocoupling with cells/tissues. High impedance usually results in increased noise and signal loss in the neural recording. Furthermore, the higher CSC and CIC of implants are crucial for preventing tissues/cells from being damaged by the side electrochemical reaction under higher potential. Zhu and Yu demonstrated that the impedance of phosphorylcholine-functionalized PEDOT was even lower than that of unfunctionalized PEDOT [131]. Zhao et al. [29] found that the impedance of OEG functionalized PEDOT was significantly increased, whereas that of the sulfobetaine functionalized PEDOT remained almost unchanged, possibly due to the zwitterion-enhanced ionic conductivity. In a recent study, Zhang et al. [28] demonstrated that the CSC and CIC values of zwitterionic PEDOT electrodes are higher than those of OEG-functionalized PEDOT electrodes. This should be due to zwitterions promoting ion dissociation and transportation compared to nonionic oligo(ethylene glycol) [209]. Cao et al. [177] also found that the carboxybetaine-functionalized thiophene polymer displayed higher electrical conductivity than the thiophene polymer.

The improved electrical properties of zwitterionic CPs should arise from the ionic conductivity enhancement with zwitterion incorporation. Many studies have demonstrated that adding zwitterionic moieties into conducting polymer electrolytes significantly enhances ion conductivities [210,211]. The enhanced ionic conductivity is primarily due to the large dipole moment of zwitterions, which is 7–8 times larger than those of polar solvents [212]. The large dipole moment endows the materials with a large dielectric constant that shields the electrostatic attraction between anions and cations (Fig. 9A–D) [213]. As shown in Fig. 9D, the Li 1s binding energy of PBP-*g*-Li(PSI)$_2$ slightly shifts to a higher value of 54.95 eV, compared to that of PBP-*g*-LiPSI (54.60 eV). In PBP-*g*-LiPSI, the lithium is close to the bis(sulfonyl)imide anion due to the strong electrostatic force. It increases the probability of transferring electrons from the anion to the cation. However, in the case of PBP-*g*-Li(PSI)$_2$, the zwitterion dipole would weaken this electrostatic attraction, and reduce the probability of electron transfer. It is the reason why the core electrons of the lithium cation of PBP-*g*-Li(PSI)$_2$ are harder to excite than that of PBP-*g*-LiPSI. The molecular dynamics simulations indicated that zwitterions weaken the association between anions and cations (Fig. 9E–H) [214]. The anionic and cationic groups of zwitterions act as sites that interact with cations and anions, respectively, benefiting the dissociation of oppositely charged ions [215]. Zwitterionic molecules also provide migration channels for ions under the applied electric field, in which one ion can hope to the following combining site to achieve migration (Fig. 9I–K) [209,215].

Furthermore, Stavrinidou et al. [216] suggested that the extent of hydration is critical for ion transport in polymer materials. Ion mobility usually decreases when hydration is decreased. Because zwitterionic polymers have compact and stable hydration layers and robust water retention ability, enriching zwitterions inside also benefits ionic transport in zwitterionic CPs [209].

The dipole moment of zwitterions can be adjusted by zwitterion structures and linker length; zwitterions with more prominent dipole moments are likely to improve the ion dissociation and ionic conductivity of polymer materials [217]. Thus, further studies are needed to determine how the structure of zwitterionic CPs affects the whole ionic conductivity.

3.4.2. Interface of metal with zwitterionic CPs

Several review papers by Emrick and Russell et al. [218–220] have discussed the interaction between zwitterionic CPs and metals in

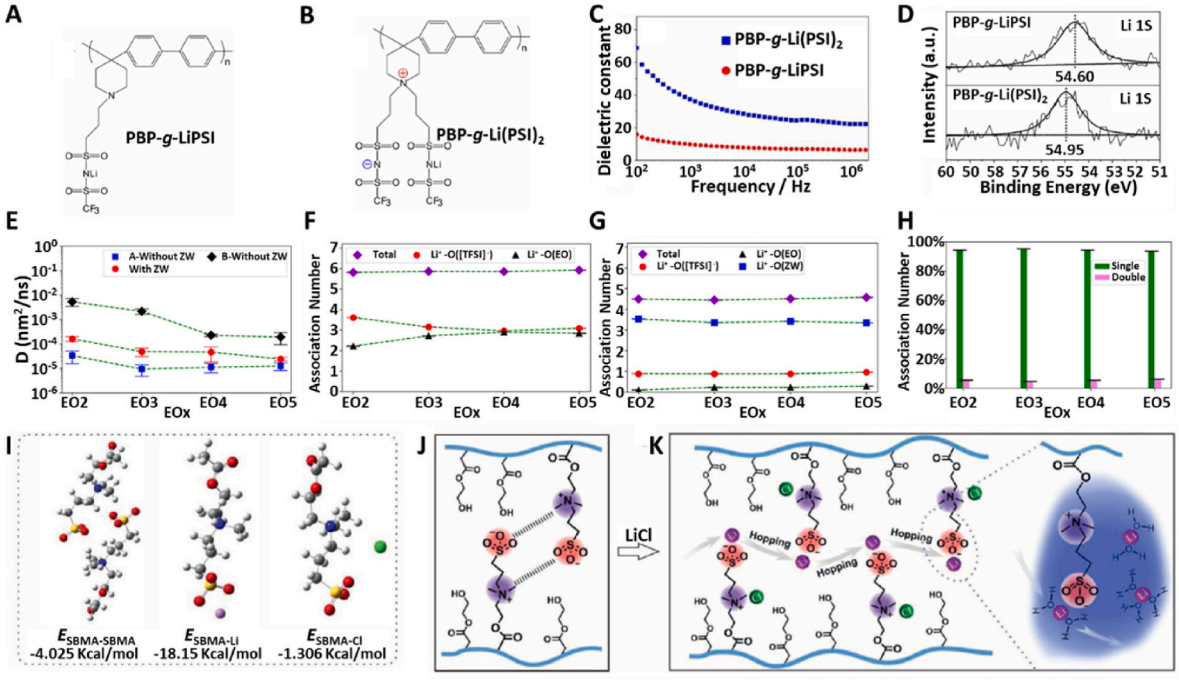

Fig. 9. (A and B) Poly(biphenylpiperidinium) (PBP)-grafted poly(biphenylpiperidinium)s, including (A) PBP-*g*-LiPSI and (B) PBP-*g*-Li(PSI)$_2$. (C) Dielectric spectra of PBP-*g*-LiPSI and PBP-*g*-Li(PSI)$_2$. (D) Li 1s XPS spectra of PBP-*g*-LiPSI and PBP-*g*-Li(PSI)$_2$. Reproduced with permission [213]. Copyright 2022, Elsevier Ltd.
(E) Diffusion coefficients of Li^+ in LiTFSI/EOx/ZW and LiTFSI/EOx in cases A (same Li^+ feeding concentration as the LiTFSI/EOx/ZW group) and case B (higher Li^+ feeding concentration than case A). (F and G) Association number of Li^+-O(EOx), Li^+-O([TFSI]-) and Li^+-O(ZW) and their sum. (F) Case A without ZW, (G) electrolytes with ZW. (H) Percentage of "single" and "double" status of Li^+-ZW associations. (LiTFSI = lithium bis (trifluoromethanesulfonyl); EO = oligo(ethylene oxide); ZW = zwitterionic molecules). Reproduced with permission [214]. Copyright 2020, Elsevier Ltd.
(I) Density functional theory (DFT) calculation of the interaction between different components in zwitterionic polymer hydrogel (polySH) electrolyte. (J) Schematic diagram of electrostatic interaction between anionic and cationic groups in polySH hydrogel without salt and K) Proposed Li^+ migration mechanism in polySH electrolyte, where hydrated Li^+ hopping through SO_3^- sites. Reproduced with permission [215]. Copyright 2021, John Wiley & Sons, Inc.

electronic devices. These reviews shed light on the function of zwitterionic CPs in field-effect transistors, light-emitting diodes, and photovoltaics. However, to the best of our knowledge, there are no reviews evaluating the impact of zwitterionic CPs on the performance of bioelectronic devices. Similar to the above electronic devices, the zwitterionic CP-coated electrodes also consist of multilayer structures, where zwitterionic polymers directly contact the metal and work as an interfacial layer between the metal and the aqueous buffer. Zwitterions are non-migrating and exhibit strong dipoles near the metals [212,214,215]. When coating a thin layer of zwitterionic conjugated polymers on a metal surface, the zwitterionic pendant groups should significantly alter the work function of metal electrodes due to the presence of an interfacial dipole [221–223]. Liu et al. [222] proposed a model in which dipoles electrostatically self-align at the metal surface to account for the interfacial dipoles observed for these electrodes (Fig. 10A–C). The self-induced torque of the dipole directs the negative charge to the metal surface by rotating the fixed interfacial dipole around its positive charge. This redistribution of charges by dipole orientation alters the electrode's work function [220–223]. The net direction of the dipoles is determined by the geometrical size and migration performance of the charged constituents of the dipole [224–226]. When the dipoles direct the negative charges toward the metal surface, it decreases the work function of the metals; otherwise, an increase in the work function of the metals occurs (Fig. 10D and E) [221,226].

The length of zwitterionic side chains was also crucial for the performance of the devices. Zwitterionic conjugated polymers with longer side chains resulted in larger interfacial dipoles [221,222]. This is likely due to improved flexibility of the side chains, benefiting the molecular reorientation along the surface normal of the metal electrode.

As discussed in 2.2.3, the highly doped p-type CPs significantly decrease the interfacial barrier to a considerable degree and facilitate efficient charge transfer across the interface. Thus, the synergy of the CPs and zwitterionic side chains further promotes tuning the metal and CP work function, reducing the interfacial barrier height and facilitating efficient charge injection and collection in organic electronic devices.

3.4.3. Zwitterion structure and spacer length

For zwitterionic CPs, the zwitterionic structures and the spacer between the backbone and zwitterions play critical roles in the electrochemical performance of zwitterionic CPs. Zhang et al. [28] demonstrated that the CSC of PEDOT-PC (0.28 mC/cm^2) electrodes was higher than that of PEDOT-SB (0.26 mC/cm^2). A similar tendency was observed in CIC, with a value of 15.92 μC/cm^2 for PEDOT-PC, which was also higher than for PEDOT-SB (13.38 μC/cm^2). PEDOT-PC electrodes had a lower voltage excursion, meaning that they were safer for chronic stimulation. Moreover, PEDOT-PC electrodes displayed good resistance to proteins and HAPI microglia cells (inflammatory cell model) after electrical stimulation. Goda et al. [132] also found that PC-functionalized PEDOT exhibited the lowest impedance and highest capacitance among three different zwitterionic CPs.

Lee et al. [174] synthesized PEDOT-SB, PEDOT-C_4-SB, and PEDOT-C_5-SB (Fig. 7B–iii), which had different lengths of alkyl spacers, and explored how the zwitterionic sulfobetaine side chain affected the electrochemical properties of the polymer and polymerization of the monomer. PEDOT-SB, PEDOT-C_4-SB, and PEDOT-C_5-SB exhibited comparable resistance to fibrinogen adhesion, indicating that the spacer would not affect the antifouling performance. However, the interfacial impedance of the CPs significantly decreased with the introduction of the alkoxyl spacer. In addition, these derivatives of PEDOT-SB were more stable in electropolymerization, leading to an increase in the mean conjugate length and cyclic stability and better packing.

It should be mentioned here that it is not appropriate to directly compare the impedance values of zwitterionic conducting polymer electrodes, as the impedance value is also coherently related to, besides the inherent property of conducting polymer, the surface area and morphology of conducting polymer electrodes and the mass of the conducting polymer deposited.

3.5. Bioelectronic application of zwitterionic CPs

The immune response is one of the most critical issues for bioelectronic implants. Immune activation usually results in scar tissue formation, which either dramatically increases the signal noise in recording or significantly depresses the neuron excitation in stimulation. Over the past 10 years, extensive efforts have been made to optimize electronic materials and devices to minimize inflammation, improve device-host tissue interactions, and extend implant life.

Endowing implants with antifouling properties is an effective method to reduce implant-induced inflammation. Many studies have confirmed that zwitterionic polymer coatings significantly improve implant anti-inflammatory, anti-infection, and anti-hyperplasia properties [11,167,227–231]. Jiang et al. [11] observed that the poly(carboxybetaine methacrylate) hydrogel has not induced foreign body reaction after implantation. After 3 months of implantation in a mouse, no collagenous capsule could be observed on the surface of the zwitterionic materials, and the microvessel formation in the tissue surrounding the implanted materials was much enhanced. In contrast, the poly(2-hydroxyethyl methacrylate) control samples were encapsulated by dense and avascular collagen. Recently, Anderson et al. [228] also demonstrated that poly(2-methacryloyloxyethyl phosphorylcholine) modified alginate microspheres improved the biocompatibility of these implanted materials by reducing the surface mediated in vivo fibrotic reaction. The most recent studies further revealed that the zwitterionic polymer coating protected in vivo electrodes from foreign body reactions. Xie et al. [229] demonstrated that the zwitterionic polymer coating could significantly suppress the foreign body reaction of implanted electrodes, eliminate signal noise in detection, and freed the sensor from recalibration within at least two weeks of implantation. In contrast, the control sensors presented a significant noise even on the first day after implantation. Cui et al. [167,230] demonstrated that the poly(sulfobetaine methacrylate) coating could greatly reduce the acute microglial encapsulation of neural electrodes. They further proved that this zwitterionic coating could effectively prevent the protein adsorption and the attachment of fibroblasts and microglia cells for at least 4 weeks. Zhang et al. [231] recently utilized sulfobetaine-functionalized polydopamine to modify neural electrodes. These coatings were found to largely reduce the acute neuroinflammatory responses, and thus retained the 92% sensitivity of the device, much higher than that of the control electrode (only 39%). In recent research by Chen et al. [232], the zwitterion polymer coating was also found to significantly inhibit macrophage activation and inflammatory factor release in cochlear implantation. It is the reason why the rats implanted by the zwitterion polymer coated cochlear electrodes could preserve much better the hearing capability than those with uncoated electrodes after 4-week implantation. Interestingly, the poly(sulfobetaine methacrylate) coating was found to significantly reduce the frictional coefficients of surfaces and thus reduce the insertional forces and invasiveness for implanting a cochlear electrode array [233]. These results encourage the potential of zwitterionic electrodes to extend the life of neural implants.

Despite these promising findings, the zwitterionic polymer coating might also increase the electrode impedance due to poor electrical conductivity. In contrast, the zwitterionic CP-modified electrodes supply an alternative solution to meet the synergetic requirement for low impedance and antifouling. As mentioned in section 3.4, the zwitterionic CP coating did not increase but reduced electrode impedance. The low impedance of zwitterionic CP electrodes was attributed to the zwitterion-enhanced ion conductivity, and the interface dipole orientation dominated electron transfer.

It has been shown that zwitterionic CPs exhibit excellent resistance to bacterial (e.g., Escherichia coli and Streptococcus mutans) [52,129,172], proteins (e.g., BSA, FBS, fibrinogen, etc.) [29,132,172,173] and cells (e.g., NIH 3T3, BAECs, HAPI, etc.) [131,132,172,177,185,186].

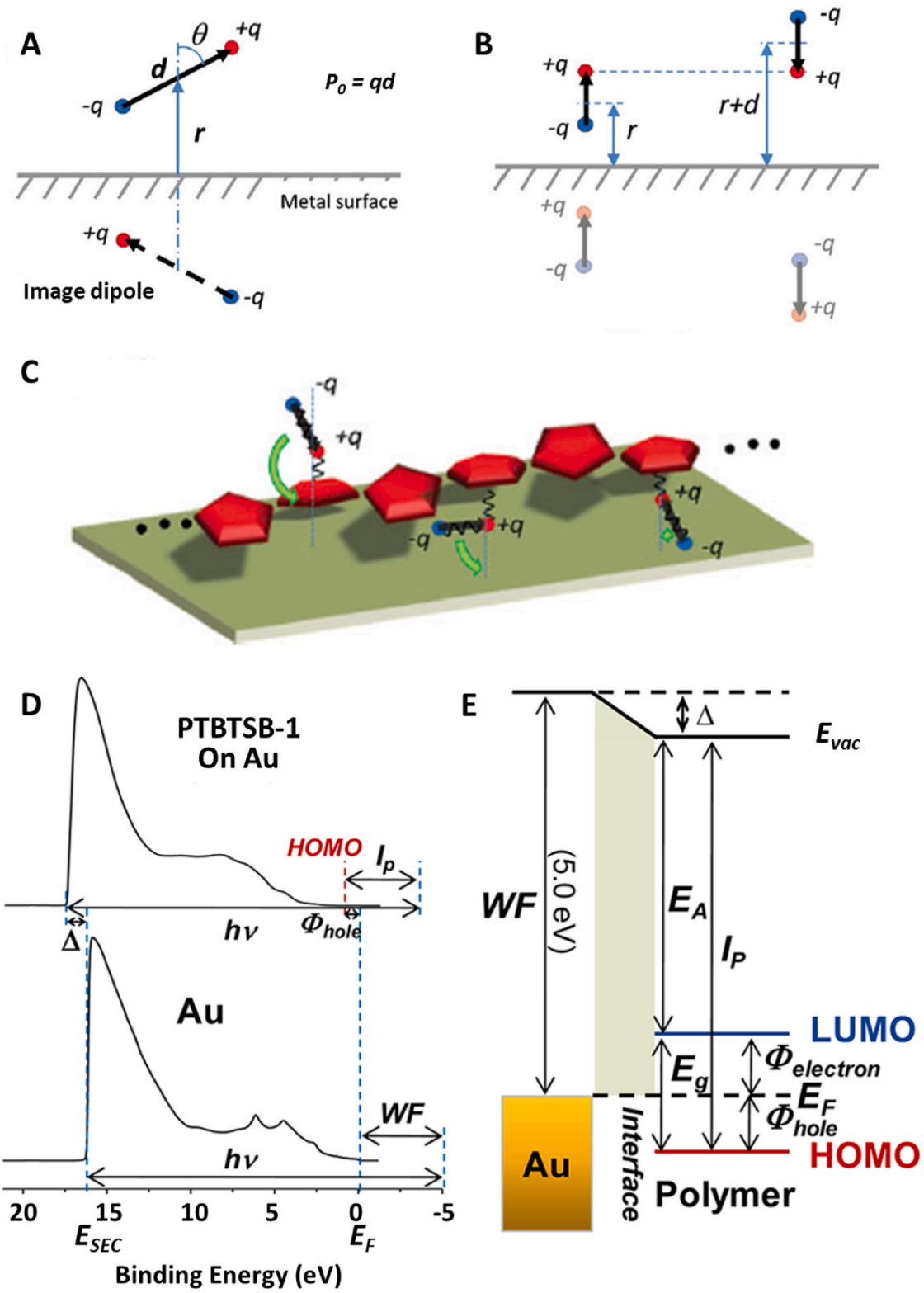

Fig. 10. (A) Schematic illustration of an "image" dipole where $p_o = qd$ (q is the elementary charge, d is a vector pointing from a negative charge, $-q$, to a positive charge, $+q$, which is equal to the separation distance between the charges) located a distance r from a metal surface. (B) Two possible orientations of an electrostatic dipole fixed rigidly at the point of positive charge, where an upward orientation (left side) is a state with lower energy. (C) Alignment of dipolar side chains of a zwitterionic polymer on a metal surface. Reproduced with permission [222]. Copyright 2013, John Wiley & Sons, Inc.
(D and E) Schematic representation of electronic energy levels at the polymer–metal interface characterized by UPS. (D) Overlay of UPS spectra of thiophene–benzothiadiazoles (PTBTSB-1) on gold (top) and bare gold (bottom). (E) Diagram showing the effect of the interfacial dipole, Δ, on vacuum and other energy level alignments. The values of Eg (EA and LUMO) were determined using UV–vis spectroscopy. Reproduced with permission [221]. Copyright 2012, American Chemical Society.

They can be used in scaffolds/implants, especially to control cell alignment and cell differentiation. Zhang et al. [185] modulated the interaction of PEDOT copolymers with proteins/cells by adjusting the comonomer compositions. Electrochemical polymerization was used to assemble phosphorylcholine-functionalized EDOT and other functionalized EDOTs as tunable copolymers (Fig. 11A). The cell-repulsive force generated from PC groups can spatially guide neurite outgrowth, forming a neuron network at single-cell resolution and enhancing neurite outgrowth by 179% (Fig. 11B–G) [185]. Zwitterionic CPs have also been applied to in bioelectronic devices due to their combination of antifouling properties and low impedance, which benefits interface charge transfer and improves device sensitivity and response rates [176,182,234]. Mao et al. [182] recently coated phosphorylcholine -functionalized PEDOT (PEDOT-PC) onto a carbon fiber microelectrode for in vivo monitoring of brain dopamine (Fig. 12). This PEDOT-PC electrode could retain its sensitivity and response rate well after being implanted in the rat brain. The ratio of post-calibration sensitivity to pre-calibration sensitivity of the PEDOT-PC electrode was 0.92 ± 0.07, whereas that of PEDOT and PEDOT-OH electrodes fell in the range of 0.43 ± 0.04 to 0.52 ± 0.05, indicating a large loss of sensitivity in the absence of PEDOT-PC modification (Fig. 12E). Recently, Jeong et al. [129] grafted poly(2-methacryloyloxyethyl phosphorylcholine) (PMPC) onto the PPy electrodes (PPy-PC) (Fig. 13) to improve their long-term implantation stability. The PPy-PC electrode demonstrated excellent resistance to nonspecific protein adsorption, bacterial attachment, and cell adhesion. Importantly, it could suppress scar tissue formation by 80% after 4 weeks of subcutaneous implantation. Yang et al. [183] developed a sulfobetaine polymer-modified PEDOT:PSS material and used it to fabricate a novel neural electrode. This device features a low impedance and a large charge storage capacity and a high charge injection capability, enabling effective electrical stimulation at a high current density (1 mA cm^{-2}) but an ultralow voltage (±25 mV). The presence of zwitterion largely improved the biocompatibility of the neural electrodes, making the device induce a stable compound action potential for at least 4 weeks of implantation. In contrast, the Au electrode could not maintain stable neural signal recording because of the severe inflammation that occurred around it. Furthermore, the zwitterion functionalized CP electrode evoked a much stronger neural response than that of the Au electrode when the same stimulating voltage was applied. These results provide a bright future for the application of zwitterionic CPs in bioelectronic implants. The unique combination of anti-inflammation and low impedance makes the zwitterionic conducting polymer promising for long-term bioelectronic implants.

However, zwitterionic CPs alone cannot supply the neural implants with an intimate electrocoupling with nerve cells/tissues, as they also resist the approaching neurons. One of the most critical challenges for this purpose is constructing an electrode surface with conjugation sites for grafting biomolecules or other biological cues of a solid interaction with nerve cells/tissue while retaining antifouling properties for zwitterionic electrodes. Zhu and Yu et al. [131] copolymerized zwitterionic EDOT with maleimide-functionalized EDOT (EDOT-MI) and deposited zwitterionic EDOT copolymers onto electrodes to conjugate neuron-specific peptides (Fig. 14A-L). The conjugation of IKVAV with CPs was achieved through the highly selective reaction of maleimide groups with cysteine terminal moieties of CSSSSIKVAV peptides, supplying active cues for neuron adhesion. The IKVAV-conjugated copolymer demonstrated a strong selective interaction with neurons, combined with solid resistance to NIH3T3 cells (Fig. 14D). Its unique performance stems from two molecular design principles: enriching phosphorylcholine moieties on the surface to prevent nonspecific interactions and decorating ligands to define specific cell interactions of surfaces on the antifouling background. Cao et al. [177] also used a similar approach to prepare the CRGDS-grafted zwitterionic thiophene copolymer. After being grafted with CRGDS peptides, the bioinert carboxybetain-functionalized thiophene copolymer strongly interacted with bovine aorta endothelial cells (Fig. 14M-Q). In a recent study by Zou et al., a neural probe modified by antifouling zwitterionic peptides was used for the long-term neural activity recording test (Fig. 15) [166]. The antifouling zwitterionic peptide consists of an EKEKEK head (negatively charged glutamic acids alternates with positively charged lysines) and a tail IKVAV. The IKVAV tail was utilized to endow the microelectrodes with adhesion to neuronal cells. It was demonstrated that EKEKEK-IKVAV-modified microelectrodes could present a stable neuronal activity recording for at least 16 weeks and significantly reduced neuronal cell loss. Particularly, the recording SNR was found to increase after 7 weeks of implantation instead, indicating IKVAV might attract neural cells closer to electrodes. This study highlights a promising future for zwitterionic CPs combined with neural-specific peptides to realize stable and intimate interactions with neurons.

To create an ideal neural interface for implanted bioelectronics, one issue that cannot be overcome for clinical trials is device reimplantation or removal after the implants stop functioning or the therapy is completed. For example, of 487 cochlear implantations, 3.8% of adults

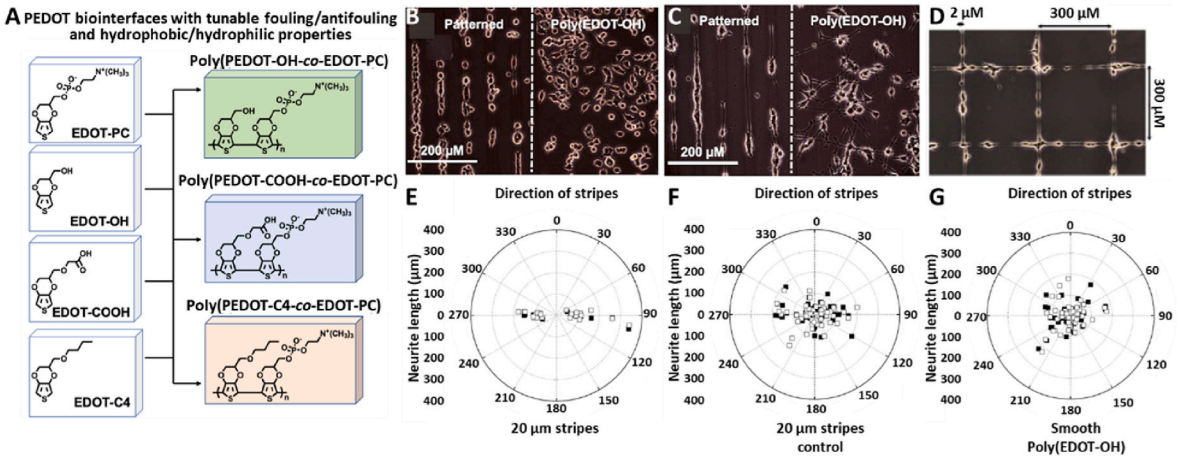

Fig. 11. (A) Zwitterionic biointerfaces form different chemical structures of functionalized EDOT monomers to PEDOT copolymers. (B) Difference in cell arrangement between patterned and adjacent nonpatterned substrates. (C) Cell arrangement and differentiation between patterned and adjacent nonpatterned substrates. (D) Formation of a neuron network of PC12 cells on the PEDOT platform with cell-binding stripes of width 2 μm after differentiation for 120 h. (E) Polar plots of the lengths and orientation angles of the neurites of PC12 cells differentiated for 24 h on PEDOT copolymer films with cell-binding stripes of width 20 μm and cell-resistance stripes of width 50 μm. Control platform (F) with cell adhesive stripes of width 20/50 μm and (G) with smooth poly(EDOT-OH). Reproduced with permission [185]. Copyright 2020, American Chemical Society.

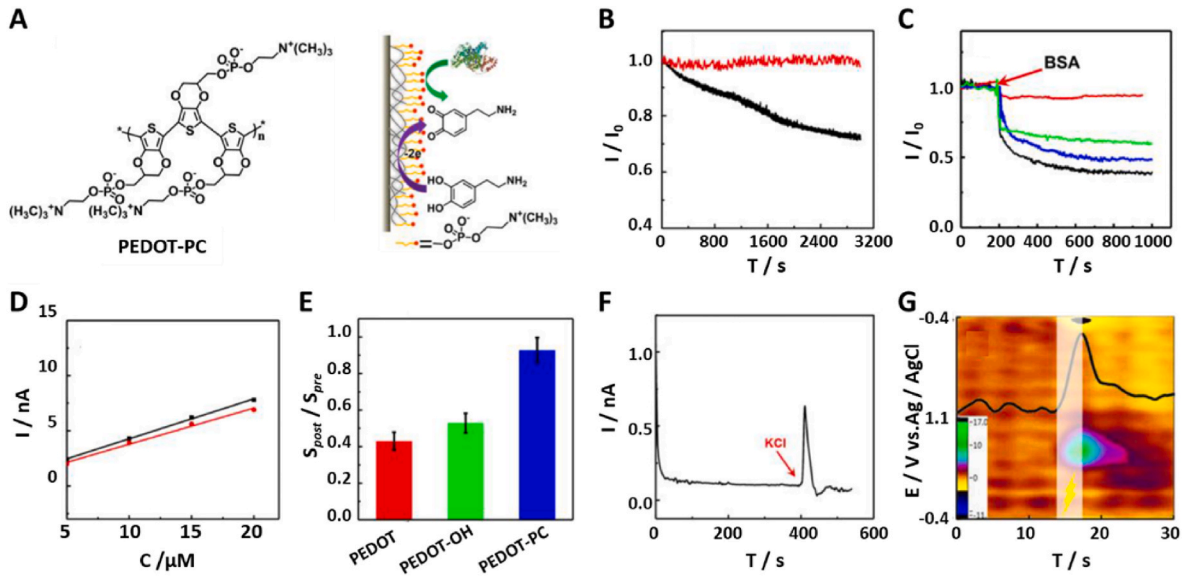

Fig. 12. (A) The structure of PEDOT-PC and the schematic of the interface between PEDOT-PC/carbon fiber microelectrode (CFE) and solution. (B) Amperometric current response toward 20 μM dopamine (DA) recorded with using CFE (black) and PEDOT-PC/CFE (red) at +0.20 V I_0 and I are the current values at the starting time and given time, respectively. (C) Amperometric current response toward 20 μM DA recorded with CFE (black), PEDOT/CFE (blue), PEDOT-OH/CFE (green), and PEDOT-PC/CFE (red) at +0.20 V upon the addition of 10 mg mL^{-1} BSA, as indicated in the figure. I_0 and I are the current values at the starting and measurement times, respectively. (D) Pre- and post-calibration curves obtained using PEDOT-PC/CFE upon successive additions of DA (each addition, 5 μM) in aCSF before (black curve) and after (red curve) in vivo implantation of the electrode in the striatum of the rat brain for 2 h. (E) The ratios of sensitivities by postcalibration of PEDOT/CFE (red column), PEDOT-OH/CFE (green column) and PEDOT-PC/CFE (blue column) to that by pre-calibration after in vivo electrode implantation for 2 h. (F) Amperometric response recorded with PEDOT-PC/CFE in the striatum by locally injecting KCl to evoke DA release. (G) In vivo fast-scan cyclic voltammetry (FSCV) recorded using PEDOT-PC/CFE by stimulating a medial forebrain bundle (MFB) (white shadow, 3 s at 60 Hz, ±250 μA, 2 ms per phase). The current versus time trace (black line) was extracted from the color plot at the peak oxidation potential (ca. +0.50 V) for DA. Reproduced with permission [182]. Copyright 2017, Wiley Periodicals, Inc.

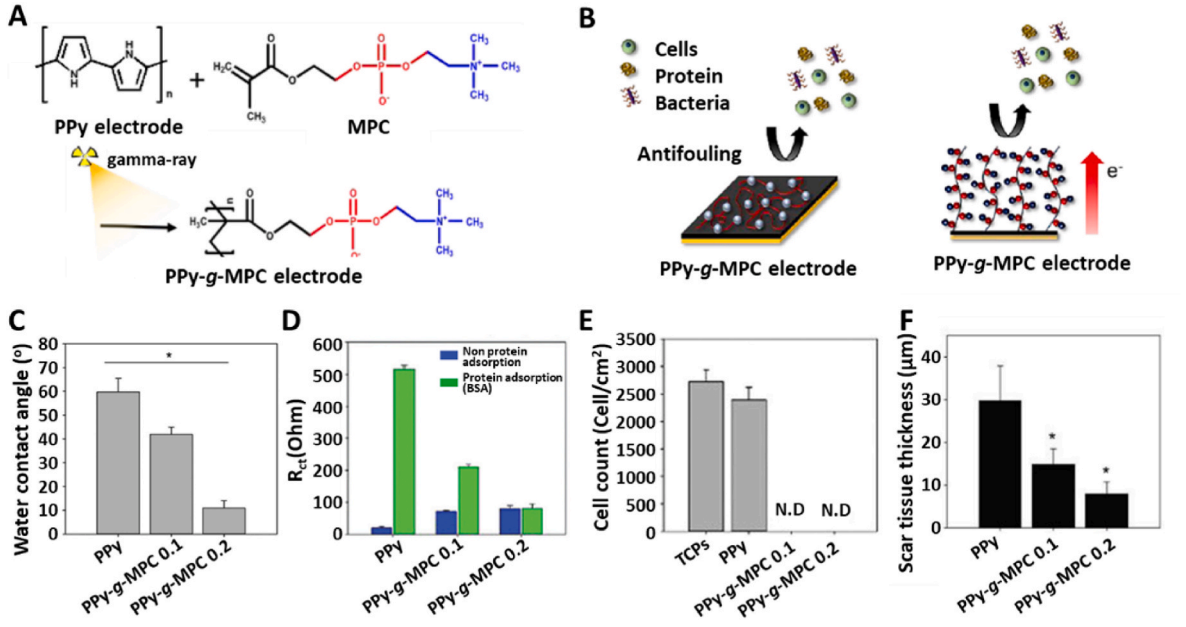

Fig. 13. (A) A schematic illustration of in situ polymerization and grafting of 2-methacryloyloxyethyl phosphorylcholine (MPC) polymer on the PPy electrode by gamma irradiation to form the PPy-*g*-MPC electrode. (B) Anti-biofouling properties of the PPy-*g*-MPC electrode. (C) A plot of water contact angles of PPy, PPy modified with 0.1 M MPC (PPy-*g*-MPC 0.1), and PPy modified with 0.2 M MPC (PPy-*g*-MPC 0.2) films. (D) The charge transfer resistance (R_{ct}) values of the PPy and PPy-*g*-MPC electrodes before and after incubation in BSA solution. (E) Number of NIH 3T3 cells on the PPy and PPy-*g*-MPC electrodes after 3 days in culture (N.D. = Not Detected). (F) Scar tissue thickness around the implants. Reproduced with permission [129]. Copyright 2020, The Royal Society of Chemistry.

and 4.5% of children underwent revisionary surgery [235]. However, the reimplantation of an active device is more complicated than its initial implantation because the second procedure might cause tissue damage and weaken physical function after reimplantation [236]. Therefore, it is desirable to develop a neural interface that specifically couples and decouples with neural cells/tissues with negligible

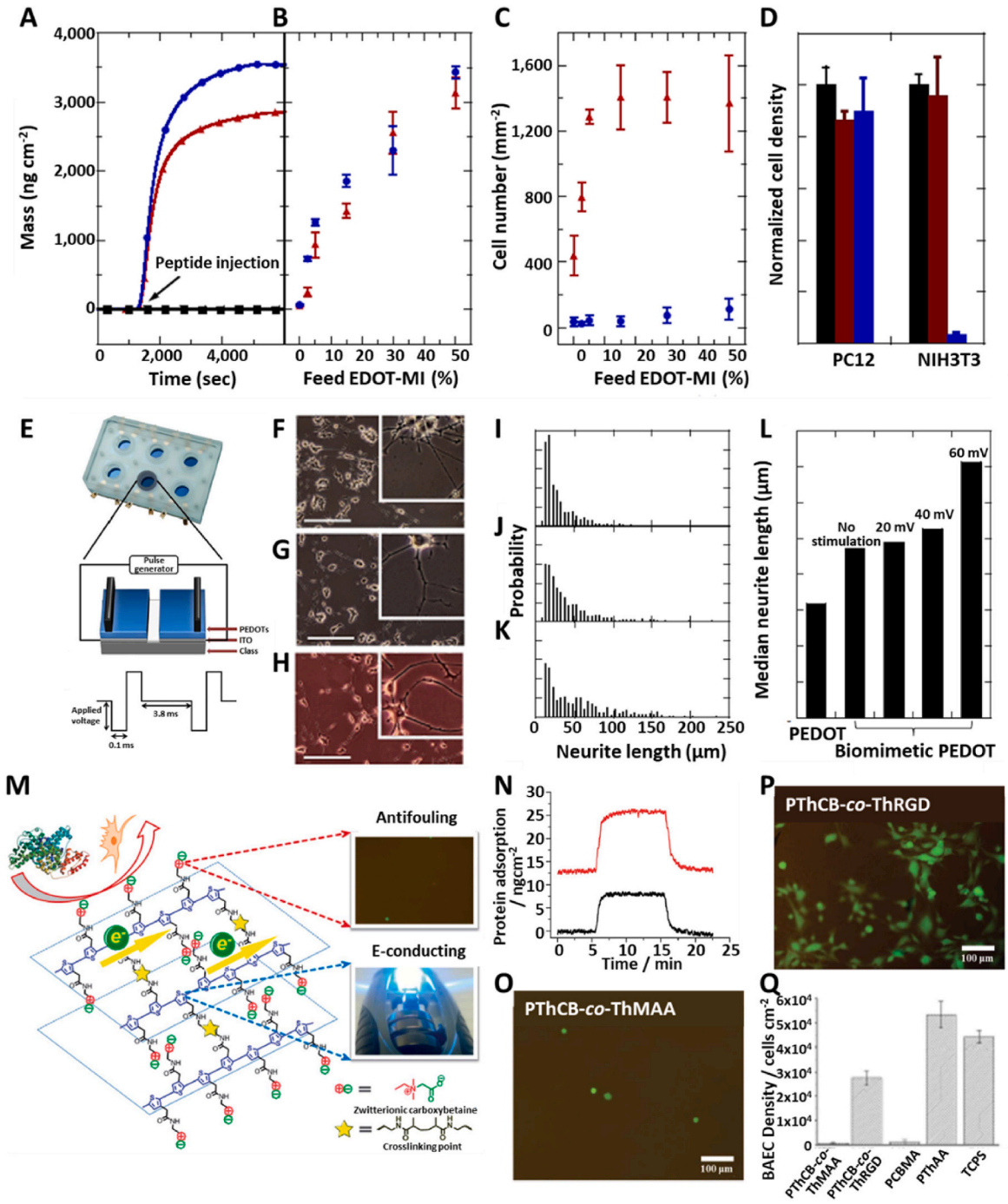

Fig. 14. (A) In situ monitoring of CSSSSIKVAV (red), CSSSSGKVAV (blue) and SSSSIKVAV (black) conjugation on poly(EDOT-MI-*co*-EDOT-PC) films polymerized from a monomer solution containing 5 mM EDOT-MI and 5 mM EDOT-PC. (B) Conjugation of CSSSSIKVAV (red) and CSSSSGKVAV (blue) on poly(EDOT-MI-*co*-EDOT-PC) films. (C) Density of PC12 cells attached to poly(EDOT-MI-*co*-EDOT-PC) films after conjugation with the ligands CSSSSIKVAV (red) and CSSSSGKVAV (blue). (D) Selective adhesion of PC12 and NIH3T3 cells on a polystyrene culture dish (black), poly(EDOT-OH) (red) and a biomimetic PEDOT (blue). (E) Schematic representation of the device used for cell growth with applied electrical stimulation and illustration of the electrical pulse used. (F–H) Microscopy images of differentiated PC12 cells cultured in NGF-supplemented medium on (F) a PEDOT film, (G) a biomimetic PEDOT film, and (H) the biomimetic PEDOT film with applied pulsed electrical stimulation at an amplitude of 60 mV. Scale bars: 200 mm. (I–K) Corresponding neurite length distributions of (F–H). (L) Median neurite length of PC12 cells on PEDOT and biomimetic PEDOT. The biomimetic PEDOT used in (D–L) was prepared from 3 mM EDOT-MI and 7 mM EDOT-PC conjugated with IKVAV. Reproduced with permission [131]. Copyright 2014, Macmillan Publishers Limited. (M) Schematic illustration of the PTh-CB-*co*-ThMAA hydrogel that consists of a conducting backbone and multifunctional zwitterionic side chains. (N) Adsorption of BSA (bottom curve) and FNG (top curve) in PBS buffer on PThCB-*co*-ThSH-modified SPR substrates. (O and P) Representative fluorescence microscopy images of attached bovine aortic endothelial cells (BAECs) on the (O) PThCB-*co*-ThMAA hydrogel and (P) PThCB-*co*-ThRGD hydrogel. (H) Quantitative cell density on different surfaces. (PThCB-*co*-ThAA = carboxybetaine thiophene-*co*-thiophene-3-acetic acid, PTh-CB-*co*-ThMAA = PThCB-*co*-ThAA was further modified with 2-aminoethyl methacrylamide, PCBMA = carboxybetaine methacrylate, and PThAA = poly(thiophene-3-acetic acid, PThCB-*co*-ThSH = cysteamine conjugated PCBTh-*co*-ThAA, TCPS = tissue culture polystyrene). Reproduced with permission [177]. Copyright 2015, The Royal Society of Chemistry.

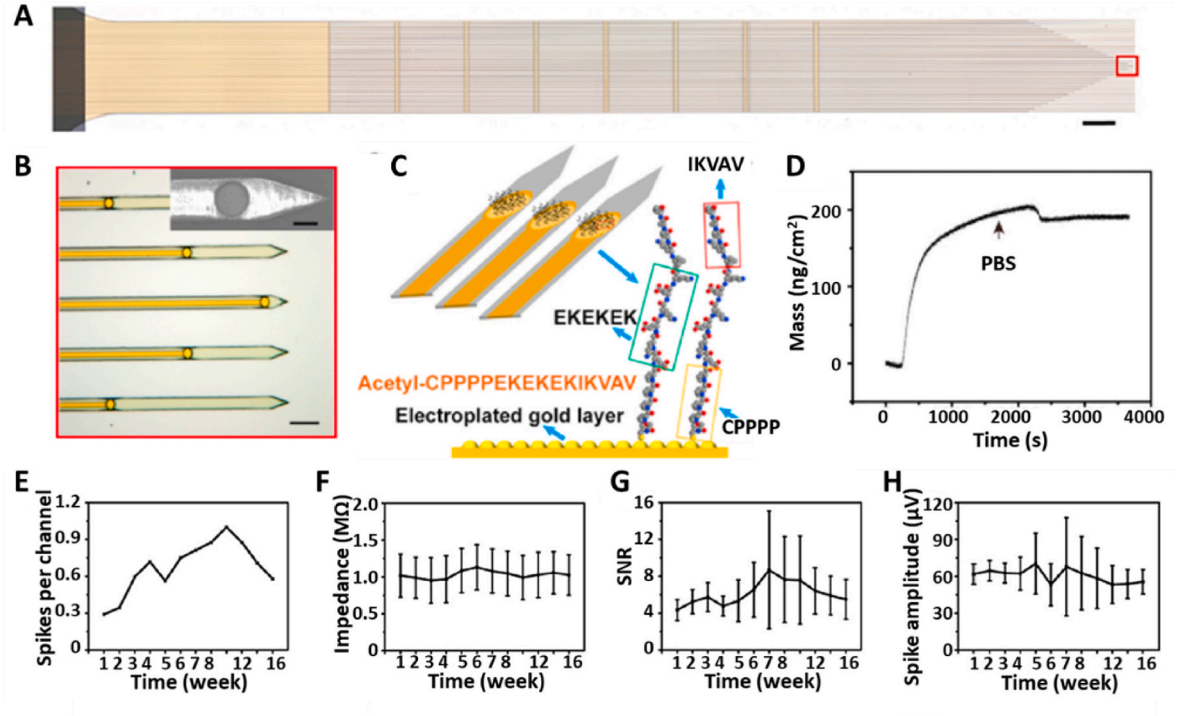

Fig. 15. Fabrication of the EK-IKVAV functionalized neural probe and chronic stable neural activity recording by EK-IKVAV functionalized probe. (A) Free-standing segment of the microelectrode on the aluminum sacrificial layer. Scale bar: 500 μm. (B) Zoomed-in view of the microelectrode filaments. Scale bar: 35 μm. Inset: SEM image of a 12-μm-wide microelectrode filament with a 10-μm-diameter recording site. Scale bar: 7 μm. (C) Schematic of the EK-IKVAV-modified recording sites. The EK-IKVAV was anchored on the surface by cystine with a functional segment IKVAV, antifouling segment EKEKEK and linker segment PPPP. (D) The EK-IKVAV modification process characterized by QCM-D. (E) Recorded unit yield of each week. (F–H) Average impedance, SNR, and spike amplitude of all sortable neurons recorded by EK-IKVAV functionalized microelectrode from 1 to 16 weeks after implantation. Reproduced with permission [166]. Copyright 2021, Elsevier Ltd.

disruption of the viability and functions of cells in a controlled manner. Lin et al. [186] developed a dynamic zwitterionic EDOT copolymer for the controlled adhesion and release of cells (Fig. 16). Simulating the dynamic integrin-extracellular matrix interactions of nature, they electropolymerized hydroquinone-functionalized EDOT (EDOT-HQ) with phosphorylcholine-functionalized EDOT (EDOT-PC) to fabricate a poly (EDOT-HQ-*co*-EDOT-PC) electrode with dynamic interaction with neurons. After converting the hydroquinone moieties into benzoquinone moieties (BQ) by applying oxidation potential, the amino-oxy terminated RGD peptides were grafted onto the zwitterionic EDOT copolymer, providing a solid specific interaction toward targeted cells. They subsequently demonstrated that neuron model cells could be released on demand by applying reduction potential to cut off the redox linkage to RGD peptides. The demonstration of electrically differentiating neurons and the subsequent release of differentiated cells with high viability was also successfully achieved [186].

4. Conclusions and future scope

Future electronic implants should induce little inflammation, a high signal-to-noise ratio, and close electrocoupling with neurons. CPs are attractive alternatives to traditional materials for bioelectrodes and are being extensively explored for high-performance bioelectronic implants. Their tissue-mimicking softness, mixed ionic-electronic conductivity, low electrochemical impedance, and facile chemistry and processing render CP electrodes and implants significantly improve neural recording and stimulation performance. However, similar to other implants, their long-term implantation is being fiercely challenged by the implant-induced inflammatory response and formation of insulated scar tissues. This review primarily outlined the most recent progress on biofunctionalized and zwitterionic CPs for long-term bioelectronic implants, with concerns about their biocompatibility and electrochemical performance.

Biofunctionalized CPs have been extensively used to revise the neuron-electrode interaction or modulate the surface immune response. Functionalizing CPs using neurotrophic factors, cell-adhesive biomolecules, and anti-inflammatory drugs promotes neuron adhesion, proliferation, and differentiation in vitro and increases the signal-to-noise ratio or reduces acute inflammation in vivo. Unfortunately, most previous results have indicated that functionalizing CPs with biomolecules, especially giant molecules such as proteins and biopolymers, exposes CPs to the risk of damage in electrochemical performance [157–159]. Moreover, although this side effect might be partially suppressed by the incorporated biomolecules, the nonspecific interaction of CP surfaces remains one of the most critical concerns for the long-term implantation of CP electrodes since it is one significant factor triggering the implant inflammatory response.

Zwitterionic CPs have recently emerged as intriguing electrode materials to resist immune responses combined with excellent electrochemical performance. Zwitterionic CPs demonstrate excellent resistance to nonspecific protein/cell interactions due to their substantial ionic hydration and neutral charge. Moreover, they retain low impedance and large CSC/CIC, which, in some cases, are even superior to those of the unfunctionalized CPs [28,131,177]. Their surface and electrochemical properties are coherently related to the molecular structures of zwitterionic moieties and spacer length of oppositely charged groups. Studies attribute their superior electrochemical properties to the high ionic conductivity and close CP-metal electrocoupling that is enhanced by zwitterions. The zwitterionic polymer-grafted electrodes have been demonstrated to maintain stable neural activity recording for over 16 weeks, with significantly suppressed scar tissue formation [166]. The pioneering work on zwitterionic CPs by Mao et al. demonstrated that the phosphorylcholine-functionalized PEDOT neural probe, due to its strong resistance to the in vivo nonspecific protein

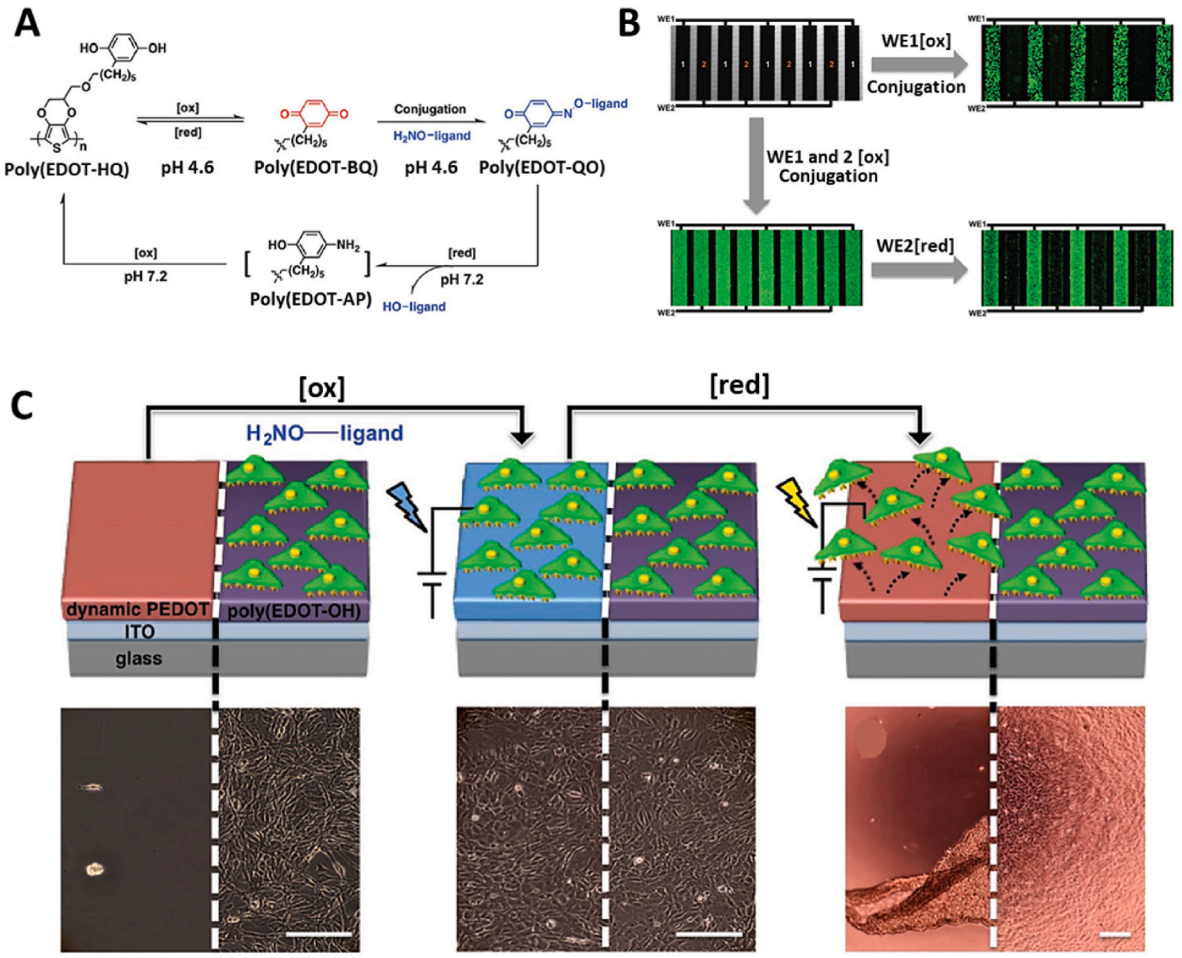

Fig. 16. (A) Schematic illustration of poly(EDOT-HQ)/poly(EDOT-BQ) switching and the formation/cleavage of oxime linkages on poly(EDOT-HQ) films. (B) Bright-field image of a poly(EDOT-HQ) film coated on two sets of interdigitated Au working microelectrodes (WE1, WE2) (top left); fluorescence images by two-photon excitation microscopy showing the selective immobilization and release of aminooxy-functionalized Alexa-488 dyes on poly(EDOT-HQ)-coated interdigitated Au microelectrodes. When the oxidative potential was only applied to WE1 to convert poly(EDOT-HQ) to poly(EDOT-BQ), the Alexa dyes were selectively immobilized on WE1 through oxime conjugation (top-right); when the oxidative potential was applied to both WE1 and WE2, Alexa dyes were immobilized on both electrodes (bottom-left). Alexa dyes were selectively released from WE2 by applying a reductive potential to cleave the oxime conjugate (bottom right). (C) The controlled attachment and release of NIH3T3 cells on RGD peptide-conjugated poly(EDOT-HQ-*co*-EDOT-PC) film compared to those nonspecifically attached to poly(EDOT-OH) controls paired on patterned ITO glass; bright-field images of PC12 cells on RGD-conjugated poly(EDOT-HQ-*co*-EDOT-PC) films. Reproduced with permission [186]. Copyright 2018, John Wiley & Sons, Inc.

interaction, did not compromise its sensitivity or response rate but dramatically improved its electrochemical performance [182]. One recent study by Jeong et al. further revealed that the PMPC-grafted PPy electrode reduced scar tissue formation by 80% after four weeks of implantation [129].

However, to develop a long-term bioelectronic implant for real-world application, several critical issues remain to be addressed. First, the long-term implantation of zwitterionic CP electrodes in the brain needs further exploration. Their molecular structures, especially those of zwitterionic moieties, are critical for resistance to in vivo nonspecific protein/cell interactions and immune responses. A molecular-level investigation of this concern is necessary to select and design zwitterionic CPs that are reliable for actual applications. In addition, a thorough evaluation of their long-term implantation concerning the acute and chronic brain immune response is crucial for their applications in the real world. Second, understanding how zwitterions tune mixed ionic-electronic transport and charge transport at CP-metal and CP-water interfaces is crucial for electrocoupling implants with tissues, requiring detailed experimental and theoretical investigations. Previous studies have extensively investigated these two issues in organic electronic devices, but few have addressed with their function in water. Third, most zwitterionic CP electrodes were prepared using the electrodeposition approach, which is straightforward but conducting-substrate-dependent and unsuitable for large-scale production. Developing chemical approaches to prepare soluble zwitterionic CPs would make it cost-efficient to fabricate electrode implants and open the door to integrating zwitterionic CPs into other electronic devices, such as organic thin-film transistors, organic ion pumps, and organic electrochemical transistors [237–240], leading to novel implantable bioelectronic implants. In addition, combining biofunctionalized CPs with zwitterionic CPs is promising for shaping a close selective electrocoupling with targeted nerve cells/tissues for implants, as evidenced by the in vitro data [131,177,186]. Further verifying and optimizing this approach in vivo will allow the bioelectronic implant to stably function in the brain for a long time. We envision the progress of zwitterionic CPs combined with biomolecules will endow bioelectronic implants with properties to suppress inflammation and to facilitate close electrocoupling to nerve cells/tissues at low impedance, significantly advancing the long-term monitoring, stimulation, and recording of nerve cells/tissues.

Credit authorship contribution statement

B.Z., H.-A.L., and S.Q. conceived the work; S.Q, H.-A.L. and Q.P. wrote the initial draft; S.Q., B.Z., and H.-A.L. proposed, curated, and prepared all the figures; and S.Q. and H.-A.L. collected data on various biomolecules and zwitterion-functionalized conducting polymers. B.Z., S.Q., S.Z., Y.Z., Z.G., and Q.W. revised the manuscript. B.Z. and Y.H. supervised the work. All authors contributed to the discussion and writing of the manuscript.

Ethics approval and consent to participate

Ethics approval and consent to participate does not apply to this review manuscript.

Declaration of competing interest

There is no conflict of interest to publish this review article.

Acknowledgment

This study was supported by NSFC (22175111, 21474014, 21704013, and 51903149), the Program for Professor of Special Appointment (Eastern Scholar) at the Shanghai Institutions of Higher Learning (TP2019043), and the Program of Shanghai Academic/Technology Research Leader (20XD1400100).

References

[1] T. Someya, Z. Bao, G.G. Malliaras, The rise of plastic bioelectronics, Nature 540 (7633) (2016) 379–385.
[2] E. Song, J. Li, S.M. Won, W. Bai, J.A. Rogers, Materials for flexible bioelectronic systems as chronic neural interfaces, Nat. Mater. 19 (6) (2020) 590–603.
[3] F.G. Zeng, S. Rebscher, W. Harrison, X. Sun, H. Feng, Cochlear implants: system design, integration, and evaluation, IEEE Rev. Biomed. Eng. 1 (2008) 115–142.
[4] D.C. Rodger, A.J. Fong, W. Li, H. Ameri, A.K. Ahuja, C. Gutierrez, I. Lavrov, H. Zhong, P.R. Menon, E. Meng, Flexible parylene-based multielectrode array technology for high-density neural stimulation and recording, Sens. Actuators, B 132 (2) (2008) 449–460.
[5] B. Wester, R. Lee, M. LaPlaca, Development and characterization of in vivo flexible electrodes compatible with large tissue displacements, J. Neural. Eng. 6 (2) (2009), 024002.
[6] S.A. Hara, B.J. Kim, J.T. Kuo, C.D. Lee, E. Meng, V. Pikov, Long-term stability of intracortical recordings using perforated and arrayed Parylene sheath electrodes, J. Neural. Eng. 13 (6) (2016), 066020.
[7] D. Zhang, Q. Chen, C. Shi, M. Chen, K. Ma, J. Wan, R. Liu, Dealing with the foreign-body response to implanted biomaterials: strategies and applications of new materials, Adv. Funct. Mater. 31 (6) (2021), 2007226.
[8] J. Groothuis, N.F. Ramsey, G.M. Ramakers, G. van der Plasse, Physiological challenges for intracortical electrodes, Brain Stimul. 7 (1) (2014) 1–6.
[9] C. Bennett, M. Samikkannu, F. Mohammed, W.D. Dietrich, S.M. Rajguru, A. Prasad, Blood brain barrier (BBB)-disruption in intracortical silicon microelectrode implants, Biomaterials 164 (2018) 1–10.
[10] I. Banerjee, R.C. Pangule, R.S. Kane, Antifouling coatings: recent developments in the design of surfaces that prevent fouling by proteins, bacteria, and marine organisms, Adv. Mater. 23 (6) (2011) 690–718.
[11] L. Zhang, Z. Cao, T. Bai, L. Carr, J.-R. Ella-Menye, C. Irvin, B.D. Ratner, S. Jiang, Zwitterionic hydrogels implanted in mice resist the foreign-body reaction, Nat. Biotechnol. 31 (6) (2013) 553–556.
[12] M.E. Spira, A. Hai, Multi-electrode array technologies for neuroscience and cardiology, Nat. Nanotechnol. 8 (2) (2013) 83–94.
[13] D.-H. Kim, J. Viventi, J.J. Amsden, J. Xiao, L. Vigeland, Y.-S. Kim, J.A. Blanco, B. Panilaitis, E.S. Frechette, D. Contreras, Dissolvable films of silk fibroin for ultrathin conformal bio-integrated electronics, Nat. Mater. 9 (6) (2010) 511–517.
[14] R. Kim, Y. Nam, Polydopamine-doped conductive polymer microelectrodes for neural recording and stimulation, J. Neurosci. Methods 326 (2019), 108369.
[15] T. Nyberg, A. Shimada, K. Torimitsu, Ion conducting polymer microelectrodes for interfacing with neural networks, J. Neurosci. Methods 160 (1) (2007) 16–25.
[16] D.-H. Kim, J.A. Wiler, D.J. Anderson, D.R. Kipke, D.C. Martin, Conducting polymers on hydrogel-coated neural electrode provide sensitive neural recordings in auditory cortex, Acta Biomater. 6 (1) (2010) 57–62.
[17] B.D. Paulsen, K. Tybrandt, E. Stavrinidou, J. Rivnay, Organic mixed ionic–electronic conductors, Nat. Mater. 19 (1) (2020) 13–26.
[18] J. Rivnay, S. Inal, B.A. Collins, M. Sessolo, E. Stavrinidou, X. Strakosas, C. Tassone, D.M. Delongchamp, G.G. Malliaras, Structural control of mixed ionic and electronic transport in conducting polymers, Nat. Commun. 7 (1) (2016) 1–9.
[19] A.V. Volkov, K. Wijeratne, E. Mitraka, U. Ail, D. Zhao, K. Tybrandt, J. W. Andreasen, M. Berggren, X. Crispin, I.V. Zozoulenko, Understanding the capacitance of PEDOT: PSS, Adv. Funct. Mater. 27 (28) (2017), 1700329.
[20] S.F. Cogan, Neural stimulation and recording electrodes, Annu. Rev. Biomed. Eng. 10 (2008) 275–309.
[21] C. Vallejo-Giraldo, A. Kelly, M.J. Biggs, Biofunctionalisation of electrically conducting polymers, Drug Discov. Today 19 (1) (2014) 88–94.
[22] X. Liu, Z. Yue, M.J. Higgins, G.G. Wallace, Conducting polymers with immobilised fibrillar collagen for enhanced neural interfacing, Biomaterials 32 (30) (2011) 7309–7317.
[23] S.Y. Kim, K.-M. Kim, D. Hoffman-Kim, H.-K. Song, G.T.R. Palmore, Quantitative control of neuron adhesion at a neural interface using a conducting polymer composite with low electrical impedance, ACS Appl. Mater. Interfaces 3 (1) (2011) 16–21.
[24] M.D. Swartzlander, C.A. Barnes, A.K. Blakney, J.L. Kaar, T.R. Kyriakides, S. J. Bryant, Linking the foreign body response and protein adsorption to PEG-based hydrogels using proteomics, Biomaterials 41 (2015) 26–36.
[25] D.N. Heo, S.-J. Song, H.-J. Kim, Y.J. Lee, W.-K. Ko, S.J. Lee, D. Lee, S.J. Park, L. G. Zhang, J.Y. Kang, Multifunctional hydrogel coatings on the surface of neural cuff electrode for improving electrode-nerve tissue interfaces, Acta Biomater. 39 (2016) 25–33.
[26] S. Kim, Y. Jang, M. Jang, A. Lim, J.G. Hardy, H.S. Park, J.Y. Lee, Versatile biomimetic conductive polypyrrole films doped with hyaluronic acid of different molecular weights, Acta Biomater. 80 (2018) 258–268.
[27] J.-G. Wu, J.-H. Chen, K.-T. Liu, S.-C. Luo, Engineering antifouling conducting polymers for modern biomedical applications, ACS Appl. Mater. Interfaces 11 (24) (2019) 21294–21307.
[28] Y.-Q. Zhang, H.-A. Lin, Q.-C. Pan, S.-H. Qian, S.-Y. Zhang, A. Zhuang, S.-H. Zhang, G. Qiu, M. Cieplak, P.S. Sharma, A trade-off between antifouling and the electrochemical stabilities of PEDOTs, J. Mater. Chem. B 9 (11) (2021) 2717–2726.
[29] H. Zhao, B. Zhu, S.-C. Luo, H.-A. Lin, A. Nakao, Y. Yamashita, H.-h. Yu, Controlled protein absorption and cell adhesion on polymer-brush-grafted poly(3,4-ethylenedioxythiophene) films, ACS Appl. Mater. Interfaces 5 (11) (2013) 4536–4543.
[30] Y. Chen, S.-C. Luo, Synergistic effects of ions and surface potentials on antifouling poly (3, 4-ethylenedioxythiophene): comparison of oligo (ethylene glycol) and phosphorylcholine, Langmuir 35 (5) (2018) 1199–1210.
[31] P. Du, X. Lin, X. Zhang, A multilayer bending model for conducting polymer actuators, Sens. Actuators, A 163 (1) (2010) 240–246.
[32] M. Salvadori, I. Brown, A. Vaz, L. Melo, M. Cattani, Measurement of the elastic modulus of nanostructured gold and platinum thin films, Phys. Rev. B 67 (15) (2003), 153404.
[33] S.N. Sarangi, B.C. Behera, N.K. Sahoo, S.K. Tripathy, Schottky junction devices by using bio-molecule DNA template-based one dimensional CdS-nanostructures, Biosens. Bioelectron. 190 (2021), 113402.
[34] A. Hussain, S. Sarangi, J. Kesarwani, S. Sahu, Au-nanocluster emission based glucose sensing, Biosens. Bioelectron. 29 (1) (2011) 60–65.
[35] S. Sarangi, K. Goswami, S. Sahu, Biomolecular recognition in DNA tagged CdSe nanowires, Biosens. Bioelectron. 22 (12) (2007) 3086–3091.
[36] M. Rivas, R.Q. Rudy, B. Sanchez, M.B. Graziano, G.R. Fox, P. Sunal, L. Nataraj, E. Sandoz-Rosado, A.C. Leff, B.D. Huey, Iridium oxide top electrodes for piezo- and pyroelectric performance enhancements in lead zirconate titanate thin-film devices, J. Mater. Sci. 55 (2020) 10351–10363.
[37] M.A. Moffitt, C.C. McIntyre, Model-based analysis of cortical recording with silicon microelectrodes, Clin. Neurophysiol. 116 (9) (2005) 2240–2250.
[38] R. Green, M.R. Abidian, Conducting polymers for neural prosthetic and neural interface applications, Adv. Mater. 27 (46) (2015) 7620–7637.
[39] D.O. Adewole, M.D. Serruya, J.A. Wolf, D.K. Cullen, Bioactive neuroelectronic interfaces, Front. Neurosci. 13 (2019) 269.
[40] A. Vázquez-Guardado, Y. Yang, A.J. Bandodkar, J.A. Rogers, Recent advances in neurotechnologies with broad potential for neuroscience research, Nat. Neurosci. 23 (12) (2020) 1522–1536.
[41] M.D. Serruya, J.P. Harris, D.O. Adewole, L.A. Struzyna, J.C. Burrell, A. Nemes, D. Petrov, R.H. Kraft, H.I. Chen, J.A. Wolf, Engineered axonal tracts as “living electrodes” for synaptic-based modulation of neural circuitry, Adv. Funct. Mater. 28 (12) (2018), 1701183.
[42] S. Park, S.W. Heo, W. Lee, D. Inoue, Z. Jiang, K. Yu, H. Jinno, D. Hashizume, M. Sekino, T. Yokota, Self-powered ultra-flexible electronics via nano-grating-patterned organic photovoltaics, Nature 561 (7724) (2018) 516–521.
[43] Q. Yang, T. Wei, R.T. Yin, M. Wu, Y. Xu, J. Koo, Y.S. Choi, Z. Xie, S.W. Chen, I. Kandela, Photocurable bioresorbable adhesives as functional interfaces between flexible bioelectronic devices and soft biological tissues, Nat. Mater. 20 (11) (2021) 1559–1570.
[44] M. Jorfi, J.L. Skousen, C. Weder, J.R. Capadona, Progress towards biocompatible intracortical microelectrodes for neural interfacing applications, J. Neural. Eng. 12 (1) (2014), 011001.
[45] B. Wei, J. Liu, L. Ouyang, C.-C. Kuo, D.C. Martin, Significant enhancement of PEDOT thin film adhesion to inorganic solid substrates with EDOT-acid, ACS Appl. Mater. Interfaces 7 (28) (2015) 15388–15394.
[46] L.K. Povlich, J.C. Cho, M.K. Leach, J.M. Corey, J. Kim, D.C. Martin, Synthesis, copolymerization and peptide-modification of carboxylic acid-functionalized 3, 4-ethylenedioxythiophene (EDOTacid) for neural electrode interfaces, Biochim. Biophys. Acta, Gen. Subj. 1830 (9) (2013) 4288–4293.

[47] L. Ouyang, B. Wei, C.-c. Kuo, S. Pathak, B. Farrell, D.C. Martin, Enhanced PEDOT adhesion on solid substrates with electrografted P (EDOT-NH2), Sci. Adv. 3 (3) (2017), e1600448.

[48] C.m. Bodart, N. Rossetti, J.E. Hagler, P. Chevreau, D. Chhin, F. Soavi, S. B. Schougaard, F. Amzica, F. Cicoira, Electropolymerized poly (3, 4-ethylene-dioxythiophene)(PEDOT) coatings for implantable deep-brain-stimulating microelectrodes, ACS Appl. Mater. Interfaces 11 (19) (2019) 17226–17233.

[49] D. Chhin, D. Polcari, C. Bodart-Le Guen, G. Tomasello, F. Cicoira, S. B. Schougaard, Diazonium-based anchoring of PEDOT on Pt/Ir electrodes via diazonium chemistry, J. Electrochem. Soc. 165 (12) (2018) G3066.

[50] W. Zhang, F.K. Yang, Z. Pan, J. Zhang, B. Zhao, Bio-Inspired dopamine functionalization of polypyrrole for improved adhesion and conductivity, Macromol. Rapid Commun. 35 (3) (2014) 350–354.

[51] S. Kim, L.K. Jang, H.S. Park, J.Y. Lee, Electrochemical deposition of conductive and adhesive polypyrrole-dopamine films, Sci. Rep. 6 (1) (2016) 1–8.

[52] B.-S. Lee, Y.-C. Lin, W.-C. Hsu, C.-H. Hou, J.-J. Shyue, S.-Y. Hsiao, P.-J. Wu, Y.-T. Lee, S.-C. Luo, Engineering antifouling and antibacterial stainless steel for orthodontic appliances through layer-by-layer deposition of nanocomposite coatings, ACS Appl. Bio Mater. 3 (1) (2019) 486–494.

[53] M.P. Ward, P. Rajdev, C. Ellison, P.P. Irazoqui, Toward a comparison of microelectrodes for acute and chronic recordings, Brain Res. 1282 (2009) 183–200.

[54] A. Prasad, Q.-S. Xue, V. Sankar, T. Nishida, G. Shaw, W.J. Streit, J.C. Sanchez, Comprehensive characterization and failure modes of tungsten microwire arrays in chronic neural implants, J. Neural. Eng. 9 (5) (2012), 056015.

[55] K. Scholten, E. Meng, Materials for microfabricated implantable devices: a review, Lab Chip 15 (22) (2015) 4256–4272.

[56] J. Rivnay, H. Wang, L. Fenno, K. Deisseroth, G.G. Malliaras, Next-generation probes, particles, and proteins for neural interfacing, Sci. Adv. 3 (6) (2017), e1601649.

[57] E. Mariani, G. Lisignoli, R.M. Borzì, L. Pulsatelli, Biomaterials: foreign bodies or tuners for the immune response? Int. J. Mol. Sci. 20 (3) (2019) 636.

[58] O. Veiseh, A.J. Vegas, Domesticating the foreign body response: recent advances and applications, Adv. Drug Deliv. Rev. 144 (2019) 148–161.

[59] T.D.Y. Kozai, N.B. Langhals, P.R. Patel, X. Deng, H. Zhang, K.L. Smith, J. Lahann, N.A. Kotov, D.R. Kipke, Ultrasmall implantable composite microelectrodes with bioactive surfaces for chronic neural interfaces, Nat. Mater. 11 (12) (2012) 1065–1073.

[60] A. Susloparova, S. Halliez, S. Begard, M. Colin, L. Buée, S. Pecqueur, F. Alibart, V. Thomy, S. Arscott, E. Pallecchi, Low impedance and highly transparent microelectrode arrays (MEA) for in vitro neuron electrical activity probing, Sens. Actuators, B 327 (2021), 128895.

[61] S.H. Bauquier, K.J. McLean, J.L. Jiang, R.C. Boston, A. Lai, Z. Yue, S.E. Moulton, A.J. Halliday, G. Wallace, M.J. Cook, Evaluation of the biocompatibility of polypyrrole implanted subdurally in GAERS, Macromol. Biosci. 17 (5) (2017), 1600334.

[62] M. Nourbakhsh, P. Zarrintaj, S.H. Jafari, S.M. Hosseini, S. Aliakbari, H. G. Pourbadie, N. Naderi, M.I. Zibaii, S.S. Gholizadeh, J.D. Ramsey, Fabricating an electroactive injectable hydrogel based on pluronic-chitosan/aniline-pentamer containing angiogenic factor for functional repair of the hippocampus ischemia rat model, Mater. Sci. Eng. C 117 (2020), 111328.

[63] M. Han, E. Yildiz, H.N. Kaleli, S. Karaz, G.O. Eren, I.B. Dogru-Yuksel, E. Senses, A. Şahin, S. Nizamoglu, Tissue-like optoelectronic neural interface enabled by PEDOT: PSS hydrogel for cardiac and neural stimulation, Adv. Healthc. Mater. (2021), 2102160.

[64] C.-C. Hsu, Y.-R. Wang, A. Tripathi, Y.-L. Wang, J.-C. Chen, Polyaniline as a Hippocampus-Inspired Biomimetic Device for Electrochemical Monitoring of Phosphorylated Tau Induced Neurodegenerative Processes, 2021.

[65] A. Zhuang, Y. Bian, J. Zhou, S. Fan, H. Shao, X. Hu, B. Zhu, Y. Zhang, All-organic conductive biomaterial as an electroactive cell interface, ACS Appl. Mater. Interfaces 10 (41) (2018) 35547–35556.

[66] X. Ren, M. Yang, T. Yang, C. Xu, Y. Ye, X. Wu, X. Zheng, B. Wang, Y. Wan, Z. Luo, Highly conductive PPy–PEDOT: PSS hybrid hydrogel with superior biocompatibility for bioelectronics application, ACS Appl. Mater. Interfaces 13 (21) (2021) 25374–25382.

[67] A. Zhuang, Q. Pan, Y. Qian, S. Fan, X. Yao, L. Song, B. Zhu, Y. Zhang, Transparent conductive silk film with a PEDOT–OH nano layer as an electroactive cell interface, ACS Biomater. Sci. Eng. 7 (3) (2021) 1202–1215.

[68] L. Wang, R. Vivek, W. Wu, G. Wang, J.-Y. Wang, Fabrication of stable and well-dispersed polyaniline–polypyrrolidone nanocomposite for effective photothermal therapy, ACS Biomater. Sci. Eng. 4 (5) (2018) 1880–1890.

[69] S. Abasi, J.R. Aggas, A. Guiseppi-Elie, Physiochemical and morphological dependent growth of NIH/3T3 and PC-12 on polyaniline-chloride/chitosan bionanocomposites, Mater. Sci. Eng., C 99 (2019) 1304–1312.

[70] A.R. Harris, G.G. Wallace, Organic electrodes and communications with excitable cells, Adv. Funct. Mater. 28 (12) (2018), 1700587.

[71] K.J. Wynne, G.B. Street, Poly (pyrrol-2-ylium tosylate), electrochemical synthesis and physical and mechanical properties, Macromolecules 18 (12) (1985) 2361–2368.

[72] S. Wang, G. Guo, X. Lu, S. Ji, G. Tan, L. Gao, Facile soaking strategy toward simultaneously enhanced conductivity and toughness of self-healing composite hydrogels through constructing multiple noncovalent interactions, ACS Appl. Mater. Interfaces 10 (22) (2018) 19133–19142.

[73] C. Huang, Q. Zhang, J. Su, High-dielectric-constant all-polymer percolative composites, Appl. Phys. Lett. 82 (20) (2003) 3502–3504.

[74] J. Hur, K. Im, S.W. Kim, J. Kim, D.-Y. Chung, T.-H. Kim, K.H. Jo, J.H. Hahn, Z. Bao, S. Hwang, Polypyrrole/agarose-based electronically conductive and reversibly restorable hydrogel, ACS Nano 8 (10) (2014) 10066–10076.

[75] C. Rinoldi, M. Lanzi, R. Fiorelli, P. Nakielski, K. Zembrzycki, T. Kowalewski, O. Urbanek, V. Grippo, K. Jezierska-Woźniak, W. Maksymowicz, Three-dimensional printable conductive semi-interpenetrating polymer network hydrogel for neural tissue applications, Biomacromolecules 22 (7) (2021) 3084–3098.

[76] C. Yu, C. Wang, X. Liu, X. Jia, S. Naficy, K. Shu, M. Forsyth, G.G. Wallace, A cytocompatible robust hybrid conducting polymer hydrogel for use in a magnesium battery, Adv. Mater. 28 (42) (2016) 9349–9355.

[77] X. Wang, X. Sun, D. Gan, M. Soubrier, H.-Y. Chiang, L. Yan, Y. Li, J. Li, S. Yu, Y. Xia, Bioadhesive and conductive hydrogel-integrated brain-machine interfaces for conformal and immune-evasive contact with brain tissue, Matter 5 (4) (2022) 1204–1223.

[78] E. Spedden, J.D. White, E.N. Naumova, D.L. Kaplan, C. Staii, Elasticity maps of living neurons measured by combined fluorescence and atomic force microscopy, Biophys. J. 103 (5) (2012) 868–877.

[79] S. Budday, R. Nay, R. de Rooij, P. Steinmann, T. Wyrobek, T.C. Ovaert, E. Kuhl, Mechanical properties of gray and white matter brain tissue by indentation, J. Mech. Behav. Biomed 46 (2015) 318–330.

[80] Y.-B. Lu, K. Franze, G. Seifert, C. Steinhäuser, F. Kirchhoff, H. Wolburg, J. Guck, P. Janmey, E.-Q. Wei, J. Käs, Viscoelastic properties of individual glial cells and neurons in the CNS, Proc. Natl. Acad. Sci. U.S.A. 103 (47) (2006) 17759–17764.

[81] A. Sridharan, S.D. Rajan, J. Muthuswamy, Long-term changes in the material properties of brain tissue at the implant–tissue interface, J. Neural. Eng. 10 (6) (2013), 066001.

[82] Z.J. Du, C.L. Kolarcik, T.D.Y. Kozai, S.D. Luebben, S.A. Sapp, X.S. Zheng, J. A. Nabity, X.T. Cui, Ultrasoft microwire neural electrodes improve chronic tissue integration, Acta Biomater. 53 (2017) 46–58.

[83] C. Zhong, D. Ke, L. Wang, Y. Lu, L. Wang, Bioactive interpenetrating polymer networks for improving the electrode/neural-tissue interface, Electrochem. Commum. 79 (2017) 59–62.

[84] A. Kalra, A. Lowe, A. Al-Jumaily, Mechanical behaviour of skin: a review, J. Mater. Sci. Eng. 5 (4) (2016), 1000254.

[85] C. Boehler, T. Stieglitz, M. Asplund, Nanostructured platinum grass enables superior impedance reduction for neural microelectrodes, Biomaterials 67 (2015) 346–353.

[86] C.G. Eleftheriou, J.B. Zimmermann, H.D. Kjeldsen, M. David-Pur, Y. Hanein, E. Sernagor, Carbon nanotube electrodes for retinal implants: a study of structural and functional integration over time, Biomaterials 112 (2017) 108–121.

[87] F. Koch, A.-M. Möller, M. Frenz, U. Pieles, K. Kuehni-Boghenbor, M. Mevissen, An in vitro toxicity evaluation of gold-, PLLA-and PCL-coated silica nanoparticles in neuronal cells for nanoparticle-assisted laser-tissue soldering, Toxicol, In Vitro 28 (5) (2014) 990–998.

[88] C.A. Chapman, H. Chen, M. Stamou, J. Biener, M.M. Biener, P.J. Lein, E. Seker, Nanoporous gold as a neural interface coating: effects of topography, surface chemistry, and feature size, ACS Appl. Mater. Interfaces 7 (13) (2015) 7093–7100.

[89] M. Lapierre-Landry, A.Y. Gordon, J.S. Penn, M.C. Skala, In vivo photothermal optical coherence tomography of endogenous and exogenous contrast agents in the eye, Sci. Rep. 7 (1) (2017) 1–9.

[90] A. Cruz, L. Abad, N. Carretero, J. Moral-Vico, J. Fraxedas, P. Lozano, G. Subías, V. Padial, M. Carballo, J. Collazos-Castro, Iridium oxohydroxide, a significant member in the family of iridium oxides. Stoichiometry, characterization, and implications in bioelectrodes, J. Phys. Chem. C 116 (8) (2012) 5155–5168.

[91] A. Cruz, N. Casañ-Pastor, Graded conducting titanium–iridium oxide coatings for bioelectrodes in neural systems, Thin Solid Films 534 (2013) 316–324.

[92] C. Xu, S. Guan, S. Wang, W. Gong, T. Liu, X. Ma, C. Sun, Biodegradable and electroconductive poly (3, 4-ethylenedioxythiophene)/carboxymethyl chitosan hydrogels for neural tissue engineering, Mater. Sci. Eng. C 84 (2018) 32–43.

[93] D. Mawad, A. Artzy-Schnirman, J. Tonkin, J. Ramos, S. Inal, M.M. Mahat, N. Darwish, L. Zwi-Dantsis, G.G. Malliaras, J.J. Gooding, Electroconductive hydrogel based on functional poly (ethylenedioxy thiophene), Chem. Mater. 28 (17) (2016) 6080–6088.

[94] V. Saunier, E. Flahaut, M.-C. Blatché, C. Bergaud, A. Maziz, Carbon nanofiber-PEDOT composite films as novel microelectrode for neural interfaces and biosensing, Biosens. Bioelectron. 165 (2020), 112413.

[95] N. Chen, B. Luo, A.C. Patil, J. Wang, G.G.L. Gammad, Z. Yi, X. Liu, S.-C. Yen, S. Ramakrishna, N.V. Thakor, Nanotunnels within poly (3, 4-ethylenedioxythiophene)-carbon nanotube composite for highly sensitive neural interfacing, ACS Naano 14 (7) (2020) 8059–8073.

[96] Z.J. Du, X. Luo, C.L. Weaver, X.T. Cui, Poly (3, 4-ethylenedioxythiophene)-ionic liquid coating improves neural recording and stimulation functionality of MEAs, J. Mater. Chem. C 3 (25) (2015) 6515–6524.

[97] F. Gisbert Roca, F.M. André, J. Mas Estelles, M. Monleon Pradas, L.M. Mir, C. Martínez-Ramos, BDNF-Gene transfected schwann cell-assisted axonal extension and sprouting on new PLA–PPy microfiber substrates, Macromol. Biosci. 21 (5) (2021), 2000391.

[98] V. Lundin, A. Herland, M. Berggren, E.W. Jager, A.I. Teixeira, Control of neural stem cell survival by electroactive polymer substrates, PLoS One 6 (4) (2011), e18624.

[99] M. Gajendiran, J. Choi, S.-J. Kim, K. Kim, H. Shin, H.-J. Koo, K. Kim, Conductive biomaterials for tissue engineering applications, J. Ind. Eng. Chem. 51 (2017) 12–26.

[100] B. Sun, T. Wu, J. Wang, D. Li, J. Wang, Q. Gao, M.A. Bhutto, H. El-Hamshary, S. S. Al-Deyab, X. Mo, Polypyrrole-coated poly (l-lactic acid-co-ε-caprolactone)/silk fibroin nanofibrous membranes promoting neural cell proliferation and differentiation with electrical stimulation, J. Mater. Chem. B 4 (41) (2016) 6670–6679.
[101] X.Y. Lee, H.W. Fan, H.J. Koh, Characterization of electrically conductive hydrogels-polyaniline/polyacrylamide and graphene/polyacrylamide, Mater. Sci. Forum, Trans. Tech. Publ. (2020) 59–64.
[102] S. Caponi, S. Mattana, M. Ricci, K. Sagini, L. Juarez-Hernandez, A. Jimenez-Garduño, N. Cornella, L. Pasquardini, L. Urbanelli, P. Sassi, A multidisciplinary approach to study the functional properties of neuron-like cell models constituting a living bio-hybrid system: SH-SY5Y cells adhering to PANI substrate, AIP Adv. 6 (11) (2016), 111303.
[103] J.W. Onorato, C.K. Luscombe, Morphological effects on polymeric mixed ionic/electronic conductors, Mol. Syst. Des. Eng. 4 (2) (2019) 310–324.
[104] B.D. Paulsen, S. Fabiano, J. Rivnay, Mixed ionic-electronic transport in polymers, Annu. Rev. Mater. Res. 51 (2021) 73–99.
[105] S. Wang, M. Ha, M. Manno, C. Daniel Frisbie, C. Leighton, Hopping transport and the Hall effect near the insulator–metal transition in electrochemically gated poly (3-hexylthiophene) transistors, Nat. Commun. 3 (1) (2012) 1–7.
[106] S. Nam, H. Han, J. Seo, M. Song, H. Kim, T.D. Anthopoulos, I. McCulloch, D. D. Bradley, Y. Kim, Ambipolar organic phototransistors with p-type/n-type conjugated polymer bulk heterojunction light-sensing layers, Adv. Electron. Mater. 2 (12) (2016), 1600264.
[107] N.A. Kukhta, A. Marks, C.K. Luscombe, Molecular design strategies toward improvement of charge injection and ionic conduction in organic mixed ionic–electronic conductors for organic electrochemical transistors, Chem. Rev. 122 (4) (2021) 4325–4355.
[108] S.G. Bucella, A. Luzio, E. Gann, L. Thomsen, C.R. McNeill, G. Pace, A. Perinot, Z. Chen, A. Facchetti, M. Caironi, Macroscopic and high-throughput printing of aligned nanostructured polymer semiconductors for MHz large-area electronics, Nat. Commun. 6 (1) (2015) 1–10.
[109] D.A. Koutsouras, M.H. Amiri, P.W. Blom, F. Torricelli, K. Asadi, P. Gkoupidenis, An iontronic multiplexer based on spatiotemporal dynamics of multiterminal organic electrochemical transistors, Adv. Funct. Mater. 31 (22) (2021), 2011013.
[110] M. Braendlein, T. Lonjaret, P. Leleux, J.M. Badier, G.G. Malliaras, Voltage amplifier based on organic electrochemical transistor, Adv. Sci. 4 (1) (2017), 1600247.
[111] J. Rivnay, P. Leleux, M. Ferro, M. Sessolo, A. Williamson, D.A. Koutsouras, D. Khodagholy, M. Ramuz, X. Strakosas, R.M. Owens, High-performance transistors for bioelectronics through tuning of channel thickness, Sci. Adv. 1 (4) (2015), e1400251.
[112] S.J. Wilks, S.M. Richardson-Burn, J.L. Hendricks, D. Martin, K.J. Otto, Poly (3, 4-ethylene dioxythiophene)(PEDOT) as a micro-neural interface material for electrostimulation, Front. Neuroeng. 2 (2009) 7.
[113] G. Yang, K.L. Kampstra, M.R. Abidian, High performance conducting polymer nanofiber biosensors for detection of biomolecules, Adv. Mater. 26 (29) (2014) 4954–4960.
[114] X. Cui, J.F. Hetke, J.A. Wiler, D.J. Anderson, D.C. Martin, Electrochemical deposition and characterization of conducting polymer polypyrrole/PSS on multichannel neural probes, Sens. Actuators, A 93 (1) (2001) 8–18.
[115] T. Komura, S. Goisihara, T. Yamaguti, K. Takahasi, Electron and ion transport in polypyrrole/polystyrenesulfonate composite films, J. Electroanal. Chem. 456 (1–2) (1998) 121–129.
[116] J.F. Rubinson, Y.P. Kayinamura, Charge transport in conducting polymers: insights from impedance spectroscopy, Chem. Soc. Rev. 38 (12) (2009) 3339–3347.
[117] C.G. Tang, M.C. Ang, K.-K. Choo, V. Keerthi, J.-K. Tan, M.N. Syafiqah, T. Kugler, J.H. Burroughes, R.-Q. Png, L.-L. Chua, Doped polymer semiconductors with ultrahigh and ultralow work functions for ohmic contacts, Nature 539 (7630) (2016) 536–540.
[118] J. Janata, M. Josowicz, Conducting polymers in electronic chemical sensors, Nat. Mater. 2 (1) (2003) 19–24.
[119] S. Fletcher, Contribution to the theory of conducting-polymer electrodes in electrolyte solutions, J. Chem. Soc., Faraday Trans. 89 (2) (1993) 311–320.
[120] A. Kahn, Fermi level, work function and vacuum level, Mater. Horiz. 3 (1) (2016) 7–10.
[121] Q. Chen, C. Wang, Y. Li, L. Chen, Interfacial dipole in organic and perovskite solar cells, J. Am. Chem. Soc. 142 (43) (2020) 18281–18292.
[122] M. Petrosino, A. Rubino, The effect of the PEDOT: PSS surface energy on the interface potential barrier, Synthetic Met 161 (23–24) (2012) 2714–2717.
[123] A.E. Mansour, H. Kim, S. Park, T. Schultz, D.X. Cao, T.Q. Nguyen, W. Brütting, A. Opitz, N. Koch, Conductive polymer work function changes due to residual water: impact of temperature-dependent dielectric constant, Adv. Electron. Mater. 6 (10) (2020), 2000408.
[124] N. Kirova, S. Brazovskii, Contact kinetics in conducting polymers, Synthetic Met 76 (1–3) (1996) 229–232.
[125] M. Willatzen, Z.L. Wang, Contact electrification by quantum-mechanical tunneling, Research (2019).
[126] F. Musumeci, G.H. Pollack, Influence of water on the work function of certain metals, Chem. Phys. Lett. 536 (2012) 65–67.
[127] N. Koch, A. Vollmer, A. Elschner, Influence of water on the work function of conducting poly (3, 4-ethylenedioxythiophene)/poly (styrenesulfonate), Appl. Phys. Lett. 90 (4) (2007), 043512.
[128] P.J. Molino, M.J. Higgins, P.C. Innis, R.M. Kapsa, G.G. Wallace, Fibronectin and bovine serum albumin adsorption and conformational dynamics on inherently conducting polymers: a QCM-D study, Langmuir 28 (22) (2012) 8433–8445.
[129] J.-O. Jeong, S. Kim, J. Park, S. Lee, J.-S. Park, Y.-M. Lim, J.Y. Lee, Biomimetic nonbiofouling polypyrrole electrodes grafted with zwitterionic polymer using gamma rays, J. Mater. Chem. B 8 (32) (2020) 7225–7232.
[130] Y. Zhu, H.-A. Lin, S. Zhang, Q. Pan, S. Qian, S. Zhang, Y. Zhang, S.-C. Luo, H.-H. Yu, B. Zhu, A straightforward strategy to spatially organize repulsive and attractive cues on Zwitterionic PEDOTs, Colloid Interface Sci. 50 (2022), 100656.
[131] B. Zhu, S.-C. Luo, H. Zhao, H.-A. Lin, J. Sekine, A. Nakao, C. Chen, Y. Yamashita, H.-h. Yu, Large enhancement in neurite outgrowth on a cell membrane-mimicking conducting polymer, Nat. Commun. 5 (2014) 4523.
[132] T. Goda, Y. Miyahara, Electrodeposition of zwitterionic PEDOT films for conducting and antifouling surfaces, Langmuir 35 (5) (2018) 1126–1133.
[133] A. Gumus, J.P. Califano, A.M. Wan, J. Huynh, C.A. Reinhart-King, G.G. Malliaras, Control of cell migration using a conducting polymer device, Soft Matter 6 (20) (2010) 5138–5142.
[134] A. Gelmi, M. Higgins, G.G. Wallace, Resolving sub-molecular binding and electrical switching mechanisms of single proteins at electroactive conducting polymers, Small 9 (3) (2013) 393–401.
[135] H. Zhang, P.J. Molino, G.G. Wallace, M.J. Higgins, Quantifying molecular-level cell adhesion on electroactive conducting polymers using electrochemical-single cell force spectroscopy, Sci. Rep. 5 (1) (2015) 1–13.
[136] A. Gelmi, M.J. Higgins, G.G. Wallace, Quantifying fibronectin adhesion with nanoscale spatial resolution on glycosaminoglycan doped polypyrrole using Atomic Force Microscopy, Biochim. Biophys. Acta, Gen. Subj. 1830 (9) (2013) 4305–4313.
[137] C. Marin, E. Fernández, Biocompatibility of intracortical microelectrodes: current status and future prospects, Front. Neuroeng. (2010) 8.
[138] S.J. O'Leary, R.R. Richardson, H.J. McDermott, Principles of design and biological approaches for improving the selectivity of cochlear implant electrodes, J. Neural. Eng. 6 (5) (2009), 055002.
[139] G.L. Mario Cheong, K.S. Lim, A. Jakubowicz, P.J. Martens, L.A. Poole-Warren, R. A. Green, Conductive hydrogels with tailored bioactivity for implantable electrode coatings, Acta Biomater. 10 (3) (2014) 1216–1226.
[140] J.E. Collazos-Castro, G.R. Hernandez-Labrado, J.L. Polo, C. Garcia-Rama, N-Cadherin- and L1-functionalised conducting polymers for synergistic stimulation and guidance of neural cell growth, Biomaterials 34 (14) (2013) 3603–3617.
[141] H. Vara, J.E. Collazos-Castro, Biofunctionalized conducting polymer/carbon microfiber electrodes for ultrasensitive neural recordings, ACS Appl. Mater. Interfaces 7 (48) (2015) 27016–27026.
[142] J. Moral-Vico, N.M. Carretero, E. Pérez, C. Suñol, M. Lichtenstein, N. Casañ-Pastor, Dynamic electrodeposition of aminoacid-polypyrrole on aminoacid-PEDOT substrates: conducting polymer bilayers as electrodes in neural systems, Electrochim. Acta 111 (2013) 250–260.
[143] J.D. Nickels, C.E. Schmidt, Surface modification of the conducting polymer, polypyrrole, via affinity peptide, J. Biomed. Mater. Res., Part A 101A (5) (2013) 1464–1471.
[144] X. Luo, C.L. Weaver, S. Tan, X.T. Cui, Pure graphene oxide doped conducting polymer nanocomposite for bio-interfacing, J. Mater. Chem. B 1 (9) (2013) 1340–1348.
[145] N. Bhagwat, R.E. Murray, S.I. Shah, K.L. Kiick, D.C. Martin, Biofunctionalization of PEDOT films with laminin-derived peptides, Acta Biomater. 41 (2016) 235–246.
[146] A. Alves-Sampaio, C. García-Rama, J.E. Collazos-Castro, Biofunctionalized PEDOT-coated microfibers for the treatment of spinal cord injury, Biomaterials 89 (2016) 98–113.
[147] K. Wang, R.-Y. Tang, X.-B. Zhao, J.-J. Li, Y.-R. Lang, X.-X. Jiang, H.-J. Sun, Q.-X. Lin, C.-Y. Wang, Covalent bonding of YIGSR and RGD to PEDOT/PSS/MWCNT-COOH composite material to improve the neural interface, Nanoscale 7 (44) (2015) 18677–18685.
[148] B. Wu, B. Cao, I.M. Taylor, K. Woeppel, X.T. Cui, Facile synthesis of a 3, 4-Ethylene-Dioxythiophene (EDOT) derivative for ease of bio-functionalization of the conducting polymer PEDOT, Front. Chem. (2019) 178.
[149] B.C. Thompson, S.E. Moulton, R.T. Richardson, G.G. Wallace, Effect of the dopant anion in polypyrrole on nerve growth and release of a neurotrophic protein, Biomaterials 32 (15) (2011) 3822–3831.
[150] R.T. Richardson, A.K. Wise, B.C. Thompson, B.O. Flynn, P.J. Atkinson, N. J. Fretwell, J.B. Fallon, G.G. Wallace, R.K. Shepherd, G.M. Clark, S.J. O'Leary, Polypyrrole-coated electrodes for the delivery of charge and neurotrophins to cochlear neurons, Biomaterials 30 (13) (2009) 2614–2624.
[151] L.N. Gillespie, G.M. Clark, P.F. Bartlett, P.L. Marzella, BDNF-induced survival of auditory neurons in vivo: cessation of treatment leads to accelerated loss of survival effects, J. Neurosci. Res. 71 (6) (2003) 785–790.
[152] E. Chalmers, H. Lee, C. Zhu, X. Liu, Increasing the conductivity and adhesion of polypyrrole hydrogels with electropolymerized polydopamine, Chem. Mater. 32 (1) (2019) 234–244.
[153] X. Cui, J. Wiler, M. Dzaman, R.A. Altschuler, D.C. Martin, In vivo studies of polypyrrole/peptide coated neural probes, Biomaterials 24 (5) (2003) 777–787.
[154] R. Wadhwa, C.F. Lagenaur, X.T. Cui, Electrochemically controlled release of dexamethasone from conducting polymer polypyrrole coated electrode, J. Contr. Release 110 (3) (2006) 531–541.
[155] C. Boehler, C. Kleber, N. Martini, Y. Xie, I. Dryg, T. Stieglitz, U.G. Hofmann, M. Asplund, Actively controlled release of Dexamethasone from neural microelectrodes in a chronic in vivo study, Biomaterials 129 (2017) 176–187.

[156] R. Balint, N.J. Cassidy, S.H. Cartmell, Conductive polymers: towards a smart biomaterial for tissue engineering, Acta Biomater. 10 (6) (2014) 2341–2353.
[157] R.A. Green, N.H. Lovell, L.A. Poole-Warren, Impact of co-incorporating laminin peptide dopants and neurotrophic growth factors on conducting polymer properties, Acta Biomater. 6 (1) (2010) 63–71.
[158] N.K. Guimard, N. Gomez, C.E. Schmidt, Conducting polymers in biomedical engineering, Prog. Polym. Sci. 32 (8–9) (2007) 876–921.
[159] T. Ahuja, I.A. Mir, D. Kumar, Biomolecular immobilization on conducting polymers for biosensing applications, Biomaterials 28 (5) (2007) 791–805.
[160] S. Cosnier, Biomolecule immobilization on electrode surfaces by entrapment or attachment to electrochemically polymerized films, A review, Biosens. Bioelectron. 14 (5) (1999) 443–456.
[161] Q. Wei, T. Becherer, S. Angioletti-Uberti, J. Dzubiella, C. Wischke, A.T. Neffe, A. Lendlein, M. Ballauff, R. Haag, Protein interactions with polymer coatings and biomaterials, Angew. Chem., Int. Ed. 53 (31) (2014) 8004–8031.
[162] W.K. Ward, A review of the foreign-body response to subcutaneously-implanted devices: the role of macrophages and cytokines in biofouling and fibrosis, J. Diabetes Sci. Technol. 2 (5) (2008) 768–777.
[163] A. Takeuchi, O. Miyaishi, K. Kiuchi, K.i. Isobe, Macrophage colony-stimulating factor is expressed in neuron and microglia after focal brain injury, J. Neurosci. Res. 65 (1) (2001) 38–44.
[164] B. Basu, Biomaterials Science and Tissue Engineering: Principles and Methods, Cambridge University Press, 2017.
[165] V.P. Vu, G.B. Gifford, F. Chen, H. Benasutti, G. Wang, E.V. Groman, R. Scheinman, L. Saba, S.M. Moghimi, D. Simberg, Immunoglobulin deposition on biomolecule corona determines complement opsonization efficiency of preclinical and clinical nanoparticles, Nat. Nanotechnol. 14 (3) (2019) 260–268.
[166] Y. Zou, J. Wang, S. Guan, L. Zou, L. Gao, H. Li, Y. Fang, C. Wang, Anti-fouling peptide functionalization of ultraflexible neural probes for long-term neural activity recordings in the brain, Biosens. Bioelectron. 192 (2021), 113477.
[167] Q. Yang, B. Wu, J.R. Eles, A.L. Vazquez, T.D. Kozai, X.T. Cui, Zwitterionic polymer coating suppresses microglial encapsulation to neural implants in vitro and in vivo, Adv. Biosyst. 4 (6) (2020), 1900287.
[168] S.-C. Luo, J. Sekine, B. Zhu, H. Zhao, A. Nakao, H.-h. Yu, Polydioxythiophene nanodots, nonowires, nano-networks, and tubular structures: the effect of functional groups and temperature in template-free electropolymerization, ACS Nano 6 (4) (2012) 3018–3026.
[169] S.-C. Luo, E.A.B. Kantchev, B. Zhu, Y.W. Siang, H.-h. Yu, Tunable, dynamic and electrically stimulated lectin–carbohydrate recognition on a glycan-grafted conjugated polymer, Chem. Commun. 48 (55) (2012) 6942–6944.
[170] G. Wang, R. Han, X. Su, Y. Li, G. Xu, X. Luo, Zwitterionic peptide anchored to conducting polymer PEDOT for the development of antifouling and ultrasensitive electrochemical DNA sensor, Biosens. Bioelectron. 92 (2017) 396–401.
[171] T. Goda, M. Toya, A. Matsumoto, Y. Miyahara, Poly (3, 4-ethylenedioxythiophene) bearing phosphorylcholine groups for metal-free, antibody-free, and low-impedance biosensors specific for C-reactive protein, ACS Appl. Mater. Interfaces 7 (49) (2015) 27440–27448.
[172] B. Cao, C.-J. Lee, Z. Zeng, F. Cheng, F. Xu, H. Cong, G. Cheng, Electroactive poly (sulfobetaine-3, 4-ethylenedioxythiophene)(PSBEDOT) with controllable antifouling and antimicrobial properties, Chem. Sci. 7 (3) (2016) 1976–1981.
[173] M.-Y. Shen, T.-Y. Huang, C.-H. Luo, Y.-C. Huang, Y.-H. Tsai, T.-L. Wang, H.-h. Yu, Inexpensive synthesis of poly(ethylenedioxythiophene-sulfobetaine) films with high bio-antifouling ability, J. Chin. Chem. Soc. (Weinheim, Ger.) 65 (1) (2018) 149–155.
[174] C.-J. Lee, H. Wang, M. Young, S. Li, F. Cheng, H. Cong, G. Cheng, Structure-function study of poly(sulfobetaine 3,4-ethylenedioxythiophene) (PSBEDOT) and its derivatives, Acta Biomater. 75 (2018) 161–170.
[175] Y. Pei, J. Travas-Sejdic, D.E. Williams, Reversible electrochemical switching of polymer brushes grafted onto conducting polymer films, Langmuir 28 (21) (2012) 8072–8083.
[176] J. Wang, N. Hui, Zwitterionic poly (carboxybetaine) functionalized conducting polymer polyaniline nanowires for the electrochemical detection of carcinoembryonic antigen in undiluted blood serum, Bioelectrochemistry 125 (2019) 90–96.
[177] B. Cao, Q. Tang, L. Li, C.-J. Lee, H. Wang, Y. Zhang, H. Castaneda, G. Cheng, Integrated zwitterionic conjugated poly (carboxybetaine thiophene) as a new biomaterial platform, Chem. Sci. 6 (1) (2015) 782–788.
[178] J. Xu, J. Xu, H. Moon, H.O. Sintim, H. Lee, Zwitterionic porous conjugated polymers as a versatile platform for antibiofouling implantable bioelectronics, ACS Appl. Polym. Mater. 2 (2) (2020) 528–536.
[179] J. Xu, J. Xu, H. Moon, H.O. Sintim, H. Lee, Zwitterionic liquid crystalline polythiophene as an antibiofouling biomaterial, J. Mater. Chem. B 9 (2) (2021) 349–356.
[180] R. Han, G. Wang, Z. Xu, L. Zhang, Q. Li, Y. Han, X. Luo, Designed antifouling peptides planted in conducting polymers through controlled partial doping for electrochemical detection of biomarkers in human serum, Biosens. Bioelectron. 164 (2020), 112317.
[181] L. Yang, H. Wang, H. Lü, N. Hui, Phytic acid functionalized antifouling conducting polymer hydrogel for electrochemical detection of microRNA, Anal. Chim. Acta 1124 (2020) 104–112.
[182] X. Liu, T. Xiao, F. Wu, M.Y. Shen, M. Zhang, H.h. Yu, L. Mao, Ultrathin cell-membrane-mimic phosphorylcholine polymer film coating enables large improvements for in vivo electrochemical detection, Angew. Chem., Int. Ed. 129 (39) (2017) 11964–11968.
[183] M. Yang, P. Chen, X. Qu, F. Zhang, S. Ning, L. Ma, K. Yang, Y. Su, J. Zang, W. Jiang, Robust neural interfaces with photopatternable, bioadhesive, and highly conductive hydrogels for stable chronic neuromodulation, ACS Nano 17 (2) (2023) 885–895.
[184] J. Wang, N. Hui, Electrochemical functionalization of polypyrrole nanowires for the development of ultrasensitive biosensors for detecting microRNA, Sens. Actuators, B 281 (2019) 478–485.
[185] Y.-Q. Zhang, H.-A. Lin, Q.-C. Pan, S.-H. Qian, S.-H. Zhang, G. Qiu, S.-C. Luo, H.-h. Yu, B. Zhu, Tunable protein/cell binding and interaction with neurite outgrowth of low-impedance zwitterionic PEDOTs, ACS Appl. Mater. Interfaces 12 (10) (2020) 12362–12372.
[186] H.-A. Lin, B. Zhu, Y.-W. Wu, J. Sekine, A. Nakao, S.-C. Luo, Y. Yamashita, H.-H. Yu, Dynamic poly(3,4-ethylenedioxythiophene)s integrate low impedance with redox-switchable biofunction, Adv. Funct. Mater. 28 (12) (2018) (n/a).
[187] S. Han, C. Kim, D. Kwon, Thermal/oxidative degradation and stabilization of polyethylene glycol, Polymer 38 (2) (1997) 317–323.
[188] A. Venault, Y. Chang, Designs of zwitterionic interfaces and membranes, Langmuir 35 (5) (2018) 1714–1726.
[189] B. Li, P. Jain, J. Ma, J.K. Smith, Z. Yuan, H.-C. Hung, Y. He, X. Lin, K. Wu, J. Pfaendtner, Trimethylamine N-oxide–derived zwitterionic polymers: a new class of ultralow fouling bioinspired materials, Sci. Adv. 5 (6) (2019), eaaw9562.
[190] B. Li, Z. Yuan, H.C. Hung, J. Ma, P. Jain, C. Tsao, J. Xie, P. Zhang, X. Lin, K. Wu, Revealing the immunogenic risk of polymers, Angew. Chem., Int. Ed. 57 (42) (2018) 13873–13876.
[191] Y. He, J. Hower, S. Chen, M.T. Bernards, Y. Chang, S. Jiang, Molecular simulation studies of protein interactions with zwitterionic phosphorylcholine self-assembled monolayers in the presence of water, Langmuir 24 (18) (2008) 10358–10364.
[192] T. Kondo, K. Nomura, M. Gemmei-Ide, H. Kitano, H. Noguchi, K. Uosaki, Y. Saruwatari, Structure of water at zwitterionic copolymer film–liquid water interfaces as examined by the sum frequency generation method, Colloids Surf., B 113 (2014) 361–367.
[193] Q. Shao, Y. He, A.D. White, S. Jiang, Difference in hydration between carboxybetaine and sulfobetaine, J. Phys. Chem. B 114 (49) (2010) 16625–16631.
[194] Q. Shao, S. Jiang, Molecular understanding and design of zwitterionic materials, Adv. Mater. 27 (1) (2015) 15–26.
[195] J. Wu, W. Lin, Z. Wang, S. Chen, Y. Chang, Investigation of the hydration of nonfouling material poly (sulfobetaine methacrylate) by low-field nuclear magnetic resonance, Langmuir 28 (19) (2012) 7436–7441.
[196] J.B. Schlenoff, Zwitteration: coating surfaces with zwitterionic functionality to reduce nonspecific adsorption, Langmuir 30 (32) (2014) 9625–9636.
[197] C. Zhang, G.A. Parada, X. Zhao, Z. Chen, Probing surface hydration and molecular structure of zwitterionic and polyacrylamide hydrogels, Langmuir 35 (41) (2019) 13292–13300.
[198] J. Zheng, Y. He, S. Chen, L. Li, M.T. Bernards, S. Jiang, Molecular simulation studies of the structure of phosphorylcholine self-assembled monolayers, J. Chem. Phys. 125 (17) (2006), 174714.
[199] M. Kikuchi, Y. Terayama, T. Ishikawa, T. Hoshino, M. Kobayashi, H. Ogawa, H. Masunaga, J.-i. Koike, M. Horigome, K. Ishihara, Chain dimension of polyampholytes in solution and immobilized brush states, Polym. J. 44 (1) (2012) 121–130.
[200] M. Kobayashi, K. Ishihara, A. Takahara, Neutron reflectivity study of the swollen structure of polyzwitterion and polyeletrolyte brushes in aqueous solution, J. Biomater. Sci. Polym. Ed. 25 (14–15) (2014) 1673–1686.
[201] K. Ishihara, M. Mu, T. Konno, Y. Inoue, K. Fukazawa, The unique hydration state of poly (2-methacryloyloxyethyl phosphorylcholine), J. Biomater. Sci. Polym. Ed. 28 (10–12) (2017) 884–899.
[202] P.-F. Ren, H.-C. Yang, H.-Q. Liang, X.-L. Xu, L.-S. Wan, Z.-K. Xu, Highly stable, protein-resistant surfaces via the layer-by-layer assembly of poly (sulfobetaine methacrylate) and tannic acid, Langmuir 31 (21) (2015) 5851–5858.
[203] J.G. Weers, J.F. Rathman, F.U. Axe, C.A. Crichlow, L.D. Foland, D.R. Scheuing, R. J. Wiersema, A.G. Zielske, Effect of the intramolecular charge separation distance on the solution properties of betaines and sulfobetaines, Langmuir 7 (5) (1991) 854–867.
[204] K.L. Willes, J.R. Genchev, W.F. Paxton, Hybrid lipid-polymer bilayers: pH-mediated interactions between hybrid vesicles and glass, Polymers 12 (4) (2020) 745.
[205] S. Paschke, K. Lienkamp, Polyzwitterions: from surface properties and bioactivity profiles to biomedical applications, ACS Appl. Polym. Mater. 2 (2) (2020) 129–151.
[206] Q. Shao, L. Mi, X. Han, T. Bai, S. Liu, Y. Li, S. Jiang, Differences in cationic and anionic charge densities dictate zwitterionic associations and stimuli responses, J. Phys. Chem. B 118 (24) (2014) 6956–6962.
[207] Q. Shao, S. Jiang, Effect of carbon spacer length on zwitterionic carboxybetaines, J. Phys. Chem. B 117 (5) (2013) 1357–1366.
[208] L. Mi, M.M. Giarmarco, Q. Shao, S. Jiang, Divalent cation-mediated polysaccharide interactions with zwitterionic surfaces, Biomaterials 33 (7) (2012) 2001–2006.
[209] X. Peng, H. Liu, Q. Yin, J. Wu, P. Chen, G. Zhang, G. Liu, C. Wu, Y. Xie, A zwitterionic gel electrolyte for efficient solid-state supercapacitors, Nat. Commun. 7 (1) (2016) 1–8.
[210] C. Tiyapiboonchaiya, J.M. Pringle, J. Sun, N. Byrne, P.C. Howlett, D. R. MacFarlane, M. Forsyth, The zwitterion effect in high-conductivity polyelectrolyte materials, Nat. Mater. 3 (1) (2004) 29–32.
[211] L. Rebollar, M.J. Panzer, Zwitterionic copolymer-supported ionogel electrolytes: impacts of varying the zwitterionic group and ionic liquid identities, Chemelectrochem 6 (9) (2019) 2482–2488.

[212] W. Mei, A.J. Rothenberger, J.E. Bostwick, J.M. Rinehart, R.J. Hickey, R.H. Colby, Zwitterions raise the dielectric constant of soft materials, Phys. Rev. Lett. 127 (22) (2021), 228001.
[213] H. Xu, L. Huang, W. Li, S. Gu, D. Zeng, Y. Zhang, Y. Sun, H. Cheng, Shielding the electrostatic attraction by design of zwitterionic single ion conducting polymer electrolyte with high dielectric constant, J. Membr. Sci. (2022), 120452.
[214] M.T. Nguyen, Q. Shao, Effects of zwitterionic molecules on ionic association in ethylene oxide-based electrolytes, Fluid Phase Equil. 515 (2020), 112572.
[215] J. Yang, Z. Xu, J. Wang, L. Gai, X. Ji, H. Jiang, L. Liu, Antifreezing zwitterionic hydrogel electrolyte with high conductivity of 12.6 mS cm− 1 at− 40 C through hydrated lithium ion hopping migration, Adv. Funct. Mater. 31 (18) (2021), 2009438.
[216] E. Stavrinidou, P. Leleux, H. Rajaona, D. Khodagholy, J. Rivnay, M. Lindau, S. Sanaur, G.G. Malliaras, Direct measurement of ion mobility in a conducting polymer, Adv. Mater. 25 (32) (2013) 4488–4493.
[217] F. Makhlooghiazad, L.A. O'Dell, L. Porcarelli, C. Forsyth, N. Quazi, M. Asadi, O. Hutt, D. Mecerreyes, M. Forsyth, J.M. Pringle, Zwitterionic materials with disorder and plasticity and their application as non-volatile solid or liquid electrolytes, Nat. Mater. 21 (2) (2022) 228–236.
[218] Y. Wu, Y. Liu, T. Emrick, T.P. Russell, Polymer design to promote low work function surfaces in organic electronics, Prog. Polym. Sci. 103 (2020), 101222.
[219] Y. Liu, T.P. Russell, Electroactive ionenes: efficient interlayer materials in organic photovoltaics, Acc. Chem. Res. 55 (8) (2022) 1097–1108.
[220] Y. Liu, V.V. Duzhko, Z.A. Page, T. Emrick, T.P. Russell, Conjugated polymer zwitterions: efficient interlayer materials in organic electronics, Acc. Chem. Res. 49 (11) (2016) 2478–2488.
[221] Z.A. Page, V.V. Duzhko, T. Emrick, Conjugated thiophene-containing polymer zwitterions: direct synthesis and thin film electronic properties, Macromolecules 46 (2) (2013) 344–351.
[222] F. Liu, Z.A. Page, V.V. Duzhko, T.P. Russell, T. Emrick, Conjugated polymeric zwitterions as efficient interlayers in organic solar cells, Adv. Mater. 25 (47) (2013) 6868–6873.
[223] J. Fang, B.H. Wallikewitz, F. Gao, G. Tu, C. Muller, G. Pace, R.H. Friend, W. T. Huck, Conjugated zwitterionic polyelectrolyte as the charge injection layer for high-performance polymer light-emitting diodes, J. Am. Chem. Soc. 133 (4) (2011) 683–685.
[224] B.H. Lee, I.H. Jung, H.Y. Woo, H.K. Shim, G. Kim, K. Lee, Multi-charged conjugated polyelectrolytes as a versatile work function modifier for organic electronic devices, Adv. Funct. Mater. 24 (8) (2014) 1100–1108.
[225] H. Lee, J.C. Stephenson, L.J. Richter, C.R. McNeill, E. Gann, L. Thomsen, S. Park, J. Jeong, Y. Yi, D.M. DeLongchamp, The structural origin of Electron injection enhancements with fulleropyrrolidine interlayers, Adv. Mater. Interfac. 3 (10) (2016), 1500852.
[226] S. van Reenen, S. Kouijzer, R.A. Janssen, M.M. Wienk, M. Kemerink, Origin of work function modification by ionic and amine-based interface layers, Adv. Mater. Interfac. 1 (8) (2014), 1400189.
[227] L. Yang, H. Wu, Y. Liu, Q. Xia, Y. Yang, N. Chen, M. Yang, R. Luo, G. Liu, Y. Wang, A robust mussel-inspired zwitterionic coating on biodegradable poly (L-lactide) stent with enhanced anticoagulant, anti-inflammatory, and anti-hyperplasia properties, Chem. Eng. J. 427 (2022), 130910.
[228] V. Yesilyurt, O. Veiseh, J.C. Doloff, J. Li, S. Bose, X. Xie, A.R. Bader, M. Chen, M. J. Webber, A.J. Vegas, A facile and versatile method to endow biomaterial devices with zwitterionic surface coatings, Adv. Healthc. Mater. 6 (4) (2017), 1601091.
[229] X. Xie, J.C. Doloff, V. Yesilyurt, A. Sadraei, J.J. McGarrigle, M. Omami, O. Veiseh, S. Farah, D. Isa, S. Ghani, Reduction of measurement noise in a continuous glucose monitor by coating the sensor with a zwitterionic polymer, Nat. Biomed. Eng. 2 (12) (2018) 894–906.
[230] A. Golabchi, B. Wu, B. Cao, C.J. Bettinger, X.T. Cui, Zwitterionic polymer/polydopamine coating reduce acute inflammatory tissue responses to neural implants, Biomaterials 225 (2019), 119519.
[231] T. Feng, W. Ji, Y. Zhang, F. Wu, Q. Tang, H. Wei, L. Mao, M. Zhang, Zwitterionic polydopamine engineered interface for in vivo sensing with high biocompatibility, Angew. Chem., Int. Ed. 59 (52) (2020) 23445–23449.
[232] A. Chen, D. Chen, K. Lv, G. Li, J. Pan, D. Ma, J. Tang, H. Zhang, Zwitterionic polymer/polydopamine coating of electrode arrays reduces fibrosis and residual hearing loss after cochlear implantation, Adv. Healthc. Mater. (2022), 2200807.
[233] D.M. Bennion, R. Horne, A. Peel, P. Reineke, A. Henslee, C. Kaufmann, C. A. Guymon, M.R. Hansen, Zwitterionic photografted coatings of cochlear implant biomaterials reduce friction and insertion forces, Otol. Neurotol. 42 (10) (2021) 1476–1483.
[234] H. Wu, C.-J. Lee, H. Wang, Y. Hu, M. Young, Y. Han, F.-J. Xu, H. Cong, G. Cheng, Highly sensitive and stable zwitterionic poly (sulfobetaine-3, 4-ethylenedioxy-thiophene)(PSBEDOT) glucose biosensor, Chem. Sci. 9 (9) (2018) 2540–2546.
[235] T. Sorrentino, M. Côté, E. Eter, M.-L. Laborde, N. Cochard, O. Deguine, B. Fraysse, Cochlear reimplantations: technical and surgical failures, Acta Otolaryngol. 129 (4) (2009) 380–384.
[236] C.-S. Kim, D.-K. Kim, M.-W. Suh, S.H. Oh, S.O. Chang, Clinical outcomes of cochlear reimplantation due to device failure, Clinical and Experimental Otorhinolaryngology 1 (1) (2008) 10.
[237] A. Williamson, M. Ferro, P. Leleux, E. Ismailova, A. Kaszas, T. Doublet, P. Quilichini, J. Rivnay, B. Rózsa, G. Katona, Localized neuron stimulation with organic electrochemical transistors on delaminating depth probes, Adv. Mater. 27 (30) (2015) 4405–4410.
[238] X. Strakosas, M. Seitanidou, K. Tybrandt, M. Berggren, D.T. Simon, An electronic proton-trapping ion pump for selective drug delivery, Sci. Adv. 7 (5) (2021), eabd8738.
[239] C. Cea, G.D. Spyropoulos, P. Jastrzebska-Perfect, J.J. Ferrero, D. Khodagholy, Enhancement-mode ion-based transistor as a comprehensive interface and real-time processing unit for in vivo electrophysiology, Nat. Mater. 19 (6) (2020) 679–686.
[240] C. Pitsalidis, A.-M. Pappa, A.J. Boys, Y. Fu, C.-M. Moysidou, D. van Niekerk, J. Saez, A. Savva, D. Iandolo, R.M. Owens, Organic bioelectronics for in vitro systems, Chem. Rev. 122 (4) (2021) 4700–4790.